USGS
science for a changing world

Prepared in cooperation with the Upper Loup and Lower Loup Natural Resources Districts and the Nebraska Environmental Trust

Age and Water-Quality Characteristics of Groundwater Discharge to the South Loup River, Nebraska, 2019

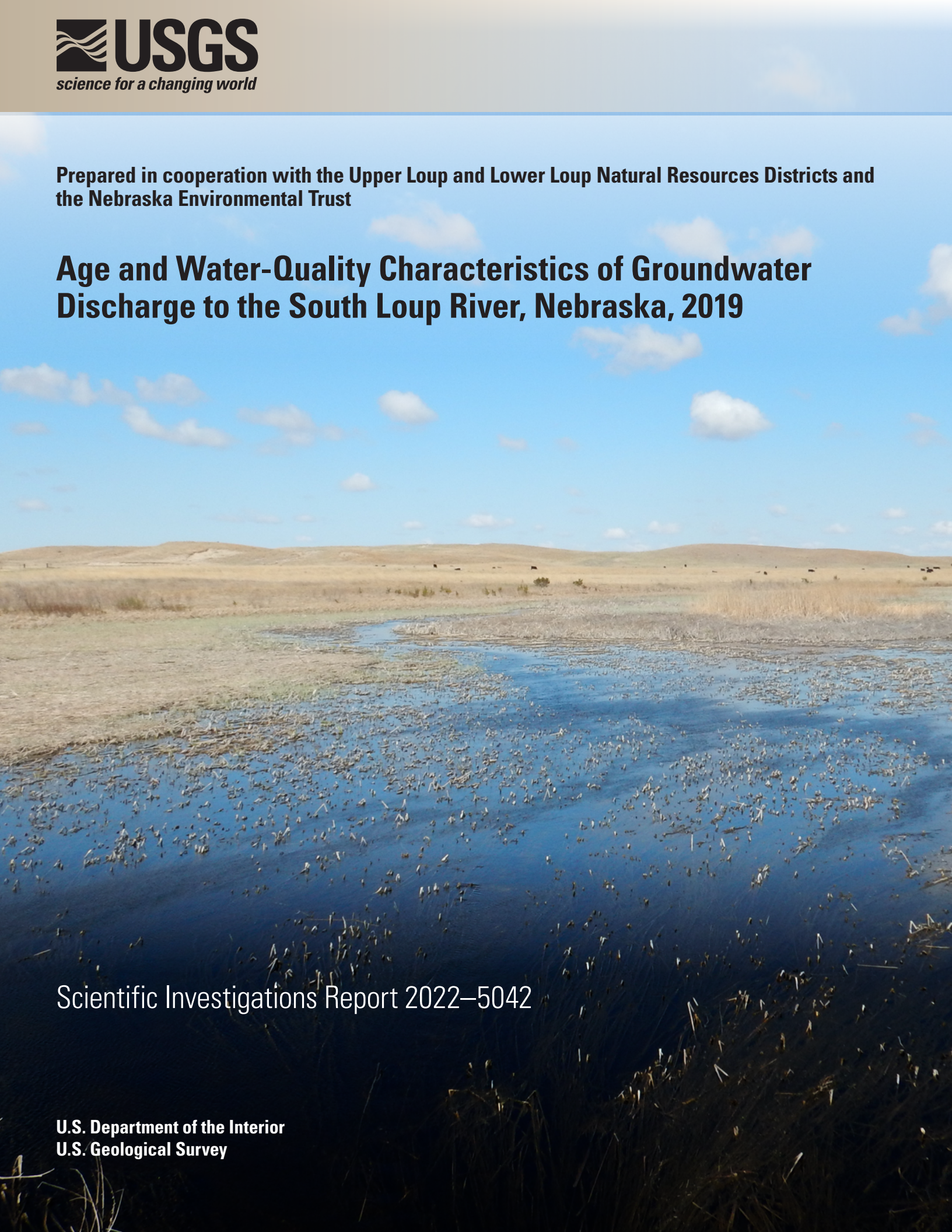

Scientific Investigations Report 2022–5042

U.S. Department of the Interior
U.S. Geological Survey

Front cover: The North Fork South Loup River, Logan County, Nebraska, May 2019. Photograph by Chris Hobza, U.S. Geological Survey.

Back cover:

Top: U.S. Geological Survey personnel recording field readings while sampling groundwater discharge from Pliocene-age sand and gravel deposits, Custer County, Nebraska, August 2019. Photograph by Chris Hobza, U.S. Geological Survey.

Bottom: U.S. Geological Survey personnel sampling groundwater from paired monitoring wells, Custer County, Nebraska, September 2019. Photograph by Chris Hobza, U.S. Geological Survey.

Age and Water-Quality Characteristics of Groundwater Discharge to the South Loup River, Nebraska, 2019

By Christopher M. Hobza and John E. Solder

Prepared in cooperation with the Upper Loup and Lower Loup Natural Resources Districts and the Nebraska Environmental Trust

Scientific Investigations Report 2022–5042

U.S. Geological Survey, Reston, Virginia: 2022

Suggested citation:
Hobza, C.M., and Solder, J.E., 2022, Age and water-quality characteristics of groundwater discharge to the South Loup River, Nebraska, 2019: U.S. Geological Survey Scientific Investigations Report 2022–5042, 57 p., https://doi.org/10.3133/sir20225042.

Associated data for this publication:
Solder, J.E., 2021, Lumped parameter models of groundwater age, South Loup River, Nebraska: U.S. Geological Survey data release, https://doi.org/10.5066/P9L6B4XE.

ISSN 2328-0328 (online)

Acknowledgments

The authors would like to thank Anna Baum with the Upper Loup Natural Resources District and Tylr Naprstek with the Lower Loup Natural Resources District for their financial, administrative, and logistical support during this project. The authors would like to thank Kyle Charron, Shane Young, and Bryan Kolar for their assistance with data collection and field support. The authors thank landowners for allowing access to their property for data collection activities.

Groundwater discharging from Pliocene-age sand and gravel deposits, Custer County Nebraska, May 2019. Photograph by Chris Hobza, U.S. Geological Survey

Contents

Figures

Tables

Conversion Factors

U.S. customary units to International System of Units

Multiply	By	To obtain
	Length	
inch (in.)	2.54	centimeter (cm)
inch (in.)	25.4	millimeter (mm)
foot (ft)	0.3048	meter (m)
mile (mi)	1.609	kilometer (km)
	Flow rate	
cubic foot per second (ft^3/s)	0.02832	cubic meter per second (m^3/s)
	Precipitation rate	
inches per year (in/yr)	2.54	centimeters per year (cm/yr)
	Volume	
gallon (gal)	3.785	liter (L)
gallon (gal)	3,785	milliliters (mL)
	Gradient	
feet per mile (ft/mi)	0.1894	meters per kilometer (m/km)

Temperature in degrees Celsius (°C) may be converted to degrees Fahrenheit (°F) as follows:
°F = (1.8 × °C) + 32.

Temperature in degrees Fahrenheit (°F) may be converted to degrees Celsius (°C) as follows:
°C = (°F – 32) / 1.8.

Datum

Vertical coordinate information is referenced to the North American Vertical Datum of 1988 (NAVD 88).

Horizontal coordinate information is referenced to the North American Datum of 1983 (NAD 83).

Elevation, as used in this report, refers to distance above the vertical datum.

Supplemental Information

Specific conductance is given in microsiemens per centimeter at 25 degrees Celsius (µS/cm at 25 °C).

Concentrations of chemical constituents in water are given in either milligrams per liter (mg/L) or micrograms per liter (µg/L).

Activities for radioactive constituents in water are given in picocuries per liter (pCi/L).

Results for measurements of stable isotopes of an element (with symbol E) in water, solids, and dissolved constituents commonly are expressed as the relative difference in the ratio of the number of the less abundant isotope (iE) to the number of the more abundant isotope of a sample with respect to a measurement standard.

Abbreviations

‰	per mil
$\delta^{13}C$	carbon-13-to-carbon-12 isotopic ratio or delta carbon-13 of water
$\delta^{2}H$	hydrogen-2-to-hydrogen-1 isotopic ratio or delta deuterium of water
$\delta^{18}O$	oxygen-18-to-oxygen-16 isotopic ratio or delta oxygen-18 of water
^{12}C	carbon-12
^{13}C	carbon-13
^{14}C	carbon-14
^{1}H	hydrogen-1
^{2}H	deuterium
^{3}H	tritium
^{16}O	oxygen-16
^{18}O	oxygen-18
Ar	argon
BMM	binary mixing model
CDF	cumulative distribution function
CH_4	methane
CO_2	carbon dioxide
DIC	dissolved inorganic carbon
DM	dispersion model
DO	dissolved oxygen
DP	dispersion parameter
EA	excess air
EMM	exponential mixing model
EPA	U.S. Environmental Protection Agency
GMWL	global meteoric water line
LC-excess	line conditioned excess
LMWL	local meteoric water line
LPM	lumped parameter model
N	nitrogen
NRD	Natural Resources District
NWIS	National Water Information System
O	oxygen
pmC	percent modern carbon
redox	oxidation reduction

SF_6	sulfur hexafluoride
SI	susceptibility index
SO_4	sulfate
TDS	total dissolved solids
TU	tritium unit
USGS	U.S. Geological Survey
VSMOW	Vienna Standard Mean Ocean Water
WMA	Wildlife Management Area

Age and Water-Quality Characteristics of Groundwater Discharge to the South Loup River, Nebraska, 2019

By Christopher M. Hobza and John E. Solder

Abstract

Streams in the Loup River Basin are sensitive to groundwater withdrawals because of the close hydrologic connection between groundwater and surface water. The U.S. Geological Survey, in cooperation with the Upper Loup and Lower Loup Natural Resources Districts, and the Nebraska Environmental Trust, studied the age and water-quality characteristics of groundwater near the South Loup River to assess the possible effects of a multiyear drought on streamflow.

Groundwater sampled in wells screened in Quaternary-age deposits displayed a wide range of mean ages (27 to 2,100 years), fraction modern, and susceptibility index values. Groundwater with higher concentrations of chloride and higher specific conductance was indicative of younger groundwater with a narrower age distribution and is more sensitive to climatic disturbances such as short-term drought conditions, based on the calculated susceptibility index. Groundwater samples from wells and springs in Pliocene-age deposits were categorized into two groups with different geochemical and age characteristics. One sample group of springs and wells, called the Western Pliocene, had higher concentrations of chloride and nitrate with young mean ages (18 to 77 years) and narrow age distributions. Groundwater in the Western Pliocene sample group is susceptible to short-term drought. In contrast, the other sample group from Pliocene-age deposits to the east (called Pliocene) had lower concentrations of nitrate, chloride, and mean groundwater ages ranging from 1,900 to 2,900 years old and is less likely to be affected by short-term drought conditions. Groundwater sampled from three wells screened in the Ogallala Formation was shown to have the oldest mean ages ranging from 8,700 to 23,000 years and the lowest calculated susceptibility index values observed in this study. Strong upward hydraulic gradients measured in wells indicated that groundwater from the Ogallala Formation is likely contributing to streamflow of the South Loup River.

Continuously measured gage height and specific conductance data indicated groundwater discharge from Quaternary-age deposits was highly responsive to precipitation events. In contrast, groundwater discharge from Pliocene-age deposits (Pliocene sample group) was far less responsive, indicating groundwater discharge from Pliocene-age deposits is likely more resilient to short-term drought conditions.

Introduction

Streams in the Loup River Basin are sensitive to groundwater withdrawals because of the close hydrologic connection between groundwater and surface water (Flynn and Stanton, 2018). The Upper Loup and Lower Loup Natural Resources Districts (NRDs) have recently approved the South Loup Watershed Management Plan (JEO Consulting Group, Inc., 2017) to guide the implementation of future projects intended to improve water quality and address water sustainability concerns. As part of this plan, additional hydrologic analyses were completed to evaluate the feasibility of capturing streamflow from tributaries (fig. 1) for retiming and augmentation during low-flow periods.

In a previous study, the U.S. Geological Survey (USGS), in cooperation with the Upper Loup and Lower Loup NRDs, and the Nebraska Environmental Trust, collected aerial thermal imagery along the South Loup River to map locations of focused groundwater discharge points (Hobza and Schepers, 2018). Results showed that groundwater discharge from mapped focused points (springs) emanated from different geologic formations within the South Loup River Basin. At the headwaters of the South Loup River, groundwater discharge flows from many small springs within Quaternary-age deposits. The highest concentration of springs was mapped along a 4-mile (mi) reach of the North Fork South Loup River (fig. 1), where groundwater discharge doubled the flow of the South Loup River and provided approximately 40 percent of the flow measured at the USGS streamgage South Loup River at Arnold, Nebraska (USGS station 06781600, referred to hereafter as the "Arnold streamgage"; fig. 1) during the summer months. Further downstream, below the Arnold streamgage, the river incises into Pliocene-age sand and gravel deposits and streamflow increases by a factor of 5 across a 62-mi reach. The additional streamflow for this reach is from a combination of diffuse groundwater discharge through the streambed and large springs.

These mapped springs are important hydrologic features that sustain the flow of the South Loup River and its tributaries. Although their location has been mapped, the ability of these springs to maintain consistent flow during periods of prolonged drought has not yet been studied. In natural groundwater flow systems, the relation between climatic disturbances such as drought and groundwater

discharge to streams can be complex and difficult to characterize. Statistical trend analyses of streamflow and precipitation records are not possible because streamflow records for the downstream part of the critical reach of the South Loup River only date back to 2017 (U.S. Geological Survey, 2021b). An alternative approach is to use environmental tracers with supporting geochemical data in a multitracer approach to identify recharge source(s) and groundwater flow paths to estimate the age of water discharging from springs and nearby wells. Groundwater environmental tracers are natural or anthropogenic compounds that are widely distributed across the Earth. Variations in tracer concentration, or isotopic ratios, can be interpreted to indicate recharge source and groundwater age, defined in this study as the average length of time for groundwater to move from areas of recharge to areas of discharge (springs or streams). Older groundwater, with longer transit times, is generally sourced from larger aquifers with more groundwater storage volumes that can dampen the effect of short-term recharge variations on discharge rates. Conversely, groundwater discharge sustained by springs with shorter transit times and respective smaller storage volumes are more susceptible to short-term recharge variations such as multiyear droughts. Information on the age of groundwater discharge improves understanding of the timing and relative magnitude of streamflow changes in response to prolonged drought conditions.

To assess groundwater interaction and possible effects of a multiyear drought on the streamflow of the South Loup River, the USGS in cooperation with the Upper Loup NRD and Lower Loup NRD, and the Nebraska Environmental Trust, began a study examining the age and water-quality characteristics of groundwater from selected springs and monitoring wells located near the South Loup River. Real-time water-quality, gage height, and discharge data collected at three locations provided additional support and context for age tracer interpretations. The interpretation of data collected from this study will provide water resource managers with information regarding the age of groundwater and groundwater discharge, which is needed for future water resources planning and management.

Purpose and Scope

The purpose of this report is to describe the age and water-quality characteristics of groundwater discharging from Pliocene-age deposits (called Pliocene-age springs) and groundwater from wells completed in Quaternary-age deposits, Pliocene-age deposits, and the Ogallala Formation. This report documents the methods of data collection and analysis, which include the collection of 20 samples from springs and wells in August and September 2019 for major ions, trace elements, nutrients, stable isotopes, dissolved gases, and selected age tracers. Age tracer and supporting geochemical data were interpreted to determine the age distributions for the springs and wells sampled. Continuous water-quality, gage height, and discharge data collected from May to October 2019 at three locations provided additional support and context for age tracer interpretations.

Study Area Description

The study area for this report is the South Loup River Basin upstream from the South Loup River at Pressey WMA (Wildlife Management Area) near Oconto, Nebr., streamgage (referred to hereafter as “South Loup River at Pressey”; USGS station 06781900) and covers parts of Custer and Logan Counties (fig. 1). Physiography and land use characteristics vary from west to east across the study area. The dissected loess plains constitute 68.7 percent of the study area in eastern Logan County and southwestern Custer County (fig. 1; Conservation and Survey Division, University of Nebraska-Lincoln, 2020b). The dissected loess plains are characterized by rolling to steep topography with flat upland tables that support a mix of row crops and rangeland. The Sand Hills, west of the dissected loess plains, cover about 26 percent of the study area (fig. 1; Conservation and Survey Division, University of Nebraska-Lincoln, 2020b) and are characterized by grass-covered eolian dunes that are dominated by undeveloped rangeland primarily used for cattle grazing (Bleed and Flowerday, 1989). The plains cover about 3.5 percent of the study area, and about 1.7 percent of the study area is classified as valleys, which are flat areas generally along rivers and larger tributaries (Conservation and Survey Division, University of Nebraska-Lincoln, 2020b). Valleys are generally well suited for irrigated row-crop agriculture, and corn and soybeans are the principal crop types (Strauch and Linard, 2009).

Land use across the study area is dominated by rangeland, which covers approximately 76 percent of the study area (Center for Advanced Land Management Information Technologies, 2007). Irrigated crops, such as corn, soybeans, and alfalfa, accounted for 11 percent of the study area. Approximately two-thirds of the irrigated land within the study area are within the Lower Loup NRD (fig. 1). Other major aggregated land use categories included dryland crops, 9.6 percent; open water, wetlands, and riparian forest, 2.7 percent; and other categories were less than 1 percent (Center for Advanced Land Management Information Technologies, 2007). Much of the groundwater within the South Loup River Basin is withdrawn for irrigation downstream from the study area. Based on 2000 countywide estimates, the highest amount of groundwater pumpage within the South Loup River Basin is in Buffalo County (Hutson and others, 2004; not shown on any maps), which is east of Custer County.

The climate in the study area is typical of continental midlatitude locations (Peel and others, 2007), characterized by cold winters and warm summers. Precipitation within the study area increases from west to east. The average annual precipitation from 1981 to 2010 near Arnold, Nebr., (fig. 1) was 23 inches per year (in/yr; National Centers for Environmental Information, 2021). Potential evapotranspiration, similar to precipitation, is greatest during the crop-growing season of April through September. Potential evapotranspiration generally is highest in July and often exceeds precipitation in this time period (Dugan and Zelt, 2000). Most of the annual groundwater recharge occurs

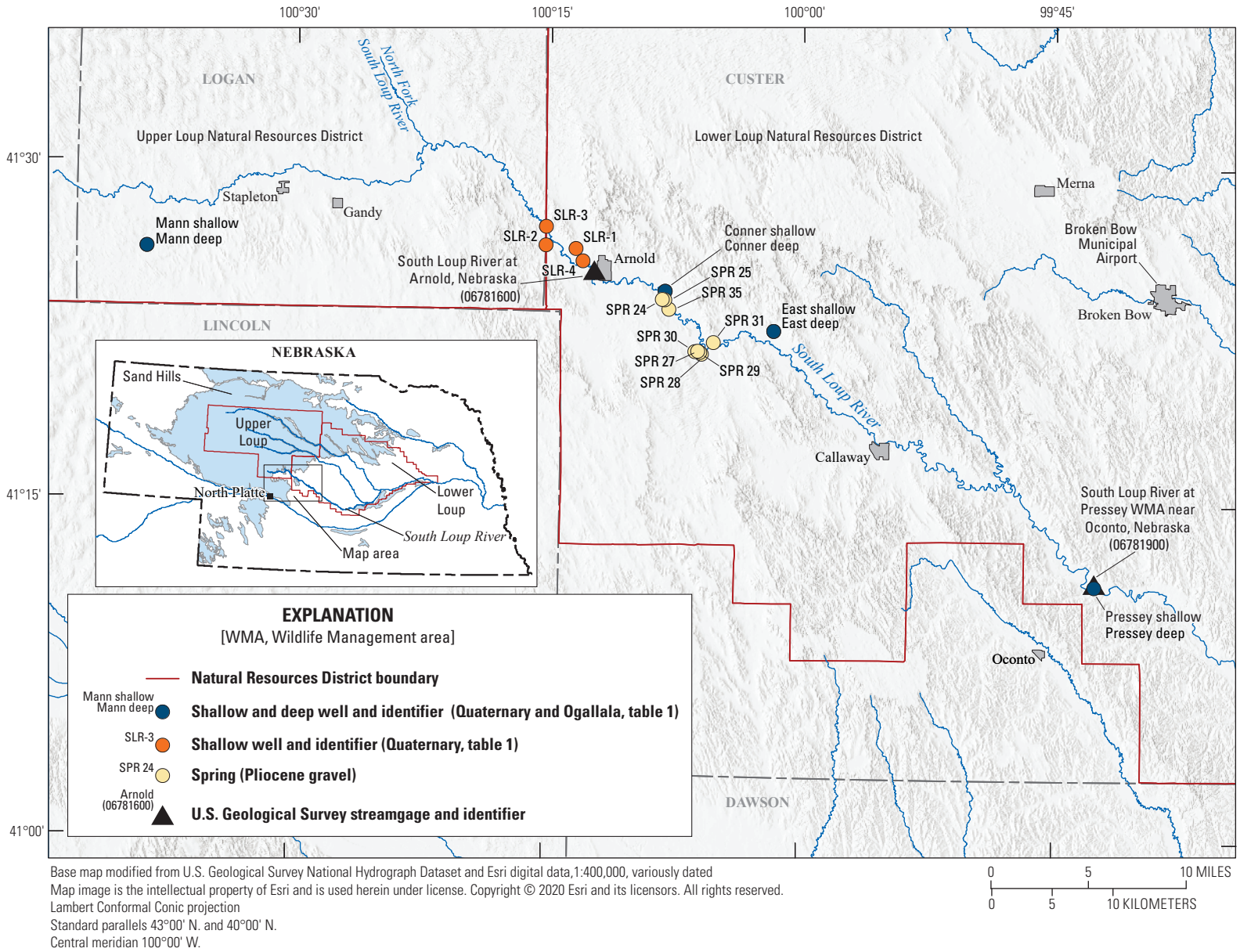

Base map modified from U.S. Geological Survey National Hydrograph Dataset and Esri digital data,1:400,000, variously dated

Lambert Conformal Conic projection
Standard parallels 43°00' N. and 40°00' N.
Central meridian 100°00' W.

Figure 1. Map of study area, sampled springs and wells, and U.S. Geological Survey streamgages, South Loup River Basin, Nebraska.

during winter and early spring when precipitation is greater than evapotranspiration. Mean annual evapotranspiration in the study area is approximately 17 inches (in.; Dugan and Zelt, 2000).

The Sand Hills are located at the headwaters of the South Loup and North Fork South Loup River in the western and northwestern parts of the study area (fig. 1). Unique physical characteristics of the Sand Hills resulted in a substantial amount of meteoric water being stored in the groundwater system (Stanton and others, 2011; McGuire and others, 2012). Highly permeable soils allow water to infiltrate even during heavy precipitation, resulting in higher recharge rates when compared to the dissected loess plains to the east and fewer runoff-induced high-flow events. Based on a soil-water balance model approach, Stanton and others (2011) estimated annual recharge rates for the Sand Hills at 2.3 in/yr, or approximately 10 percent of the annual precipitation measured at Arnold, Nebr. (National Centers for Environmental Information, 2021). Recharge in the area to the east of the Sand Hills is variable; in areas where the dissected loess plains dominate, recharge generally decreases to 0.5 in/yr or less because of the low permeability of loess deposits (Stanton and others, 2011).

As streams flow out of the Sand Hills, groundwater discharge to streams, also known as base flow, ranges from about 80 to 95 percent of total streamflow (Szilagyi and others, 2003; Stanton and others, 2010). To the east, the percentage of drainage basin area covered by the Sand Hills decreases and the percentage of irrigated cropland increases because soils developed in the dissected loess plains and valleys are more conducive to row-crop production. Increased groundwater withdrawals, particularly during the growing season, reduce the amount of groundwater discharge received by streams (Peterson and others, 2008; Stanton and others, 2010; Flynn and Stanton, 2018). As the streams cross the dissected and loess-covered plains to the south and east, surface runoff constitutes a larger portion of streamflow, and groundwater contributions drop to between about 60 and 80 percent (Stanton and others, 2010; Szilagyi and others, 2003).

Geologic Setting

The study area overlies the High Plains aquifer system, where saturated thicknesses can exceed 600 feet (ft; McGuire and others, 2012). The High Plains aquifer system is considered to be inclusive of all hydrologically connected Tertiary- and Quaternary-age units. According to Gutentag and others (1984), the Tertiary-age units include the fractured part of the Oligocene-age Brule Formation of the White River Group, the Miocene-age Arikaree Group, and the Miocene-age Ogallala Formation (fig. 2). The Pliocene-age, Pleistocene-age, and Quaternary-age units include alluvial and eolian deposits (fig. 2). In areas where the Brule Formation is not present, the Cretaceous Pierre Shale forms the base of aquifer. The base of aquifer surface generally dips 8 feet per mile to the east and contains paleovalleys that also drain eastward (Peterson and others, 2008).

The geologic history relevant to this study begins about 70 million years ago with the deposition of Cretaceous-age sediments. During the Cretaceous period, much of the study area was covered by a shallow inland sea, where marine sediments were deposited to form the Dakota Sandstone, Carlile Shale of the Colorado Group, the Niobrara Formation of the Colorado Group, and Pierre Shale. After regression of the Cretaceous sea, uplift resulted in the formation of the Chadron and Cambridge arches trending from northwest to southeast across the study area (Swinehart and others, 1985). Subsequent fluvial erosion removed as much as 1,800 ft of the Cretaceous section and created a topographic low over the previously uplifted region.

For most of the study area, the unfractured Brule forms the base of aquifer. The Brule is a massive siltstone consisting of primarily eolian silt but also containing some alluvium. Deposits of volcaniclastic sediments and some ash derived from volcanic complexes from the Western United States make up most of its volume in some localities (Souders, 2000). When unfractured, the Brule is impermeable relative to the overlying units.

Overlying the Brule Formation is the Arikaree Group, which is a massive, very fine- to fine-grained sandstone with localized beds of volcanic ash, silty sand, and sandy clay (Darton, 1903; Condra and Reed, 1943; Souders, 2000). The Arikaree Group is considered part of the High Plains aquifer system; however, it does not yield large quantities of water to wells (Gutentag and others, 1984). Within the study area, the Arikaree Group typically is not used as a water source.

The Ogallala Formation is the principal geologic unit in the High Plains aquifer system and reaches a thickness of 500 ft beneath the study area (Diffendal, 1991). The Ogallala Formation consists of a poorly sorted mixture of sand, silt, clay, and gravel (Condra and Reed, 1943). The Ogallala Formation is generally unconsolidated or weakly consolidated but can contain layers of sandstone cemented by calcium carbonate or limestone. Because of the difficulty correlating these units in the subsurface, the Ogallala Formation has not been subdivided into stratigraphic units recognized in other areas (Swinehart and others, 1985). The Ogallala Formation was deposited by aggrading streams that filled paleovalleys that were eroded into pre-Ogallala Formation rocks (Swinehart and others, 1985). The base of the Ogallala Formation is a complex surface formed from multiple episodes of erosion. Paleovalleys in the Ogallala Formation have been suggested by previous researchers (Swinehart and others, 1985; Swinehart and Diffendal, 1989), but these may represent only a fraction of the drainage network that existed during Miocene time. Much of the deposition was restricted to valleys along drainage systems originating from mountains in Wyoming and Colorado (Swinehart and others, 1985), but deposition may have also been on broad low-relief plains (Swinehart and Diffendal, 1989).

<table>
<tr><th>Period</th><th>Epoch</th><th colspan="3">Stratigraphy</th><th>Lithology</th><th>Hydrostratigraphy</th></tr>
<tr><td rowspan="2">Quaternary</td><td>Holocene</td><td colspan="3">Alluvium and eolian deposits</td><td rowspan="2">Gravel, sand, silt, and clay</td><td rowspan="5">High Plains aquifer</td></tr>
<tr><td>Pleistocene</td><td colspan="3">Long Pine Formation and undifferentiated alluvial and eolian deposits</td></tr>
<tr><td rowspan="5">Tertiary</td><td>Pliocene</td><td colspan="3">Broadwater Formation</td><td>Gravel and sand</td></tr>
<tr><td rowspan="2">Miocene</td><td colspan="3">Ogallala Group</td><td>Gravel, sand, silt, and clay</td></tr>
<tr><td colspan="3">Arikaree Group</td><td>Very fine- to fine-grained sandstone</td></tr>
<tr><td rowspan="2">Oligocene</td><td rowspan="2">Brule Formation</td><td>Upper</td><td>Siltstone and sandstone</td><td rowspan="4">Confining unit(s)</td></tr>
<tr><td>Lower</td><td>Siltstone and claystone</td></tr>
<tr><td>Eocene</td><td colspan="3">Chadron Formation[1]</td><td>Siltstone and claystone</td></tr>
<tr><td>Cretaceous</td><td>Upper</td><td colspan="3">Pierre Shale</td><td>Shale</td></tr>
</table>

Modified from Gutentag and others, 1984; Korus and Joeckel, 2011; Souders, 2000; and Swinehart and Diffendal, 1989
[1]Recognized as the Chamberlain Pass Formation by the University of Nebraska Conservation and Survey Division (Korus and Joeckel, 2011).

Figure 2. Description of geologic and hydrostratigraphic units, South Loup River Basin, Nebraska.

An unconformable time period, owing to erosion or nondeposition, of at least 1.5 million years separates the Ogallala Formation from the Pliocene-age Broadwater Formation and the Pleistocene-age Long Pine Formation (Swinehart and Diffendal, 1989). The Pleistocene Long Pine Formation unit name is used by the University of Nebraska-Lincoln, Conservation and Survey Division, but is not formally recognized by the USGS. These fluvial sediments, eroded from central Wyoming and northern Colorado (Stanley and Wayne, 1972), are unevenly deposited and preserved, contain coarse sand and gravel separated by finer grained deposits, and cover the Ogallala Formation through much of the study area. In the study area, Pliocene-age fluvial deposits can be as thick as 300 ft (Swinehart and Diffendal, 1989; Souders, 2000; Conservation and Survey Division, University of Nebraska-Lincoln, 2020a), and are hydrologically connected with the underlying Ogallala. The Broadwater and Long Pine Formations, as parts of the High Plains aquifer system, are used as a water source where present (Hobza and others, 2012).

Quaternary-age deposits that consist of eolian sand, wind-deposited silt, clay, and fine-grained sand (together called loess) and alluvial deposits of sand and gravel cover much of the study area. Quaternary-age alluvial sand and gravel are in modern stream valleys and often are used as a water source (Peterson and others, 2008). Quaternary-age deposits typically are 150–300 ft thick across the study area but can be nearly 500 ft thick near the northern and southern edges of the study area in Custer County (Souders, 2000; Conservation and Survey Division, University of Nebraska-Lincoln, 2020a). Researchers have documented the radiocarbon ages of organic material within eolian deposits to reconstruct dune activity in the Sand Hills during the Holocene (Ahlbrandt and others, 1983; Loope and Swinehart, 2000). Results indicated a complex history of deposition within streams and valleys and documented major periods of dune mobilization and activity 6,000 and 3,000 years before present (2021).

Study Methods

This section of the report describes the methods of data collection and analysis used to improve the understanding of the age and water-quality characteristics of groundwater and groundwater discharge to the South Loup River. The methods used are divided into two sections. The first subsection describes the groundwater sampling methods and analysis procedures, quality assurance and quality control, and geochemical modeling to determine groundwater age distributions. The next subsection describes the collection of real-time water-quality data at three locations to provide additional support to the groundwater-age tracer interpretations. Site selection, data collection procedures, and data analysis and approval of the collected real-time water-quality and gage height data are also discussed.

Water-Quality and Age Tracer Sampling

This section describes the study design and methods used to collect groundwater quality and age tracer samples and the analytical approaches used to describe and interpret these data. Samples from 20 springs and wells were analyzed for major ions, trace elements, nutrients, stable isotopes, dissolved gases, and selected age tracers. Age tracer and supporting geochemical data were interpreted to determine the age distributions for the springs and wells sampled. Quality assurance and quality control sampling and analyses are described in the last subsection of this report.

Spring and Well Selection and Identification

Spring sampling locations were chosen from the mapped focused groundwater discharge locations interpreted by Hobza and Schepers (2018). The spring sampling locations are in an area of groundwater discharge from Pliocene-age sand and gravel deposits along a 62-mi reach of the South Loup River downstream from the Arnold streamgage (fig. 1). Along this reach, groundwater discharge to the South Loup River is dominated by discharge at focused points (Hobza and Schepers, 2018). Monitoring wells were selected for sampling based on their proximity to the South Loup River. Eight of the monitoring wells were clustered monitoring wells where a shallow and deep well are screened in two different geologic units at one location (fig. 1; table 1). Samples also were collected from a group of four shallow monitoring wells screened in Quaternary-age deposits upstream from the Arnold streamgage.

This report uses three different methods of site identification. The first method uses the USGS station number, which is a 15-digit number such as 412340100074901 (table 1). The 15-digit USGS station number is particularly useful for accessing historic water-quality or water-level data for a given well in the USGS National Water Information System (NWIS; U.S. Geological Survey, 2021b). The next identification method is the USGS station identification. This station identification name uses the legal description of the well or spring location and a local well or spring name, such as 17N 24W31C1 SLoup Spr 35. The last method of site identification is the field name, which is the local spring or well name typically used by participating NRDs, such as SPR 35 or SLR-2 (table 1).

Sample Collection

Samples were collected from 12 wells and 8 springs in the South Loup River Basin in Logan and Custer Counties in August and September 2019 (fig. 1; table 1) using the guidelines and protocols described in the USGS National Field Manual (U.S. Geological Survey, variously dated). Groundwater samples were collected from monitoring wells and springs using a stainless-steel submersible pump. All samples were collected in-line, where Tygon tubing was connected to the discharge port of the stainless-steel submersible pump to ensure groundwater samples were not exposed to the atmosphere before collection. Before sampling monitoring wells, the water level was measured using methods described in Cunningham and Schalk (2011). The well casing volume and flow rate were calculated to determine the length of time needed to purge at least three well volumes before samples were collected. Groundwater sampled from springs and wells was pumped into a flow-through chamber to facilitate the monitoring of the physical properties of the water to ensure the collection of a representative sample. Specific conductance, pH, water temperature, and dissolved oxygen (DO) were measured in the field at 3-minute intervals by a multiparameter sonde (Xylem Analytics, 2020). Representative groundwater samples were collected after sequential readings stabilized within limits described by the USGS National Water Quality Field Manual (U.S. Geological Survey, variously dated) and for monitoring wells after three well volumes had been pumped from the well.

Groundwater samples were collected from springs by creating a temporary sampling point emplaced within unconsolidated sediments. Samples were collected by first determining the location where the groundwater discharge was greatest within the exposed sand and gravel. At this location, a 2.5-in. diameter column of sediment was removed using a streambed sediment coring tube. Immediately after removing the column of sediment, a 2.5-in. diameter polyvinyl chloride well screen and casing with a solid endpoint was manually pushed into the sand and gravel deposits to create a temporary sampling point. The temporary sampling point was pushed to a minimum depth of 2 ft, ensuring that the screened interval was beneath the sediment-water interface. Following emplacement of the temporary sampling point, sediments were allowed to collapse against the screen and casing. The water level within the temporary sampling point rose higher than the water level outside the spring, indicating a higher hydraulic head within the sediments of the spring. In some cases, groundwater readily flowed out of the temporary sampling point effectively

Table 1. Wells and springs sampled in the South Loup River Basin, Nebraska, 2019.

[USGS, U.S. Geological Survey; ID, identification; MM, month; DD, day; YYYY, year; NAD 83, North American Datum of 1983; NAVD 88, North American Vertical Datum of 1988; NA, not applicable; Pliocene, undifferentiated Pliocene-age deposits; Quaternary, undifferentiated Quaternary-age deposits; Ogallala, Ogallala Formation]

USGS station	Station ID[1]	Field name	Sample type	Date sampled (MM/DD/YYYY)	Latitude, in decimal degrees (NAD 83)	Longitude, in decimal degrees (NAD 83)	Elevation, in feet above NAVD 88	Screen interval, in feet below land surface	Unit sampled	Measured water level, in feet below land surface[2]	Hydraulic gradient
412340100074901	17N 24W31C1 SLoup Spr 35	SPR 35	Spring	8/12/2019	41.43885278	−100.1302778	2,661	NA	Pliocene	NA	NA
412406100080401	17N 24W31B2 SLoup Spr 25	SPR 25	Spring	8/12/2019	41.43638056	−100.1344444	2,665	NA	Pliocene	NA	NA
412407100080501	17N 24W31B1 SLoup Spr 24	SPR 24	Spring	8/12/2019	41.44109444	−100.1347222	2,676	NA	Pliocene	NA	NA
412146100055701	16N 24W17B3 SLoup Spr 30	SPR 30	Spring	8/13/2019	41.19041667	−100.0991667	2,660	NA	Pliocene	NA	NA
412145100055601	16N 24W17B1 SLoup Spr 27	SPR 27	Spring	8/13/2019	41.37888889	−100.0988889	2,661	NA	Pliocene	NA	NA
412148100061501	16N 24W18A1 SLoup Spr 29	SPR 29	Spring	8/13/2019	41.37888889	−100.1041667	2,658	NA	Pliocene	NA	NA
412213100051001	16N 24W 8D1 SLoup Spr 31	SPR 31	Spring	8/14/2019	41.19041667	−100.0861111	2,621	NA	Pliocene	NA	NA
412149100060401	16N 24W17B2 SLoup Spr 28	SPR 28	Spring	8/14/2019	41.40805556	−100.1011111	2,654	NA	Pliocene	NA	NA
412429100080302	17N 24W30CCDD2	Conner shallow	Monitoring well	9/9/2019	41.36277778	−100.1341667	2,662	80–90	Pliocene	12.24	0.00272
412429100080303	17N 24W30CCDD3	Conner deep	Monitoring well	9/9/2019	41.3633333	−100.1341667	2,662	205–215	Ogallala	11.9	0.00272
412611100384402	17N 29W22ABBB2	Mann deep	Monitoring well	9/10/2019	41.3636111	−100.6456667	3,036.31	184.7–189.5	Pliocene	84.94	−0.04639
412611100384401	17N 29W22ABBB1	Mann shallow	Monitoring well	9/10/2019	41.4298222	−100.6456667	3,036.31	124.6–144.5	Quaternary	82.5	−0.04639
411126099422502	14N 21W 15AB 02 Pressey 2	Pressey shallow	Monitoring well	9/11/2019	41.4548333	−99.7069722	2,398	70–80	Pliocene	2.53	0.00407
411126099422501	14N 21W 15AB Pressey	Pressey deep	Monitoring well	9/11/2019	41.40805556	−99.7069722	2,395.52	360–370	Ogallala	1.23	0.00407
412244100013501	16N 24W 2DDDD1	East shallow	Monitoring well	9/11/2019	41.43638056	−100.0263889	2,644	95–105	Quaternary	27.96	−0.01316
412244100013502	16N 24W 2DDDD2	East deep	Monitoring well	9/11/2019	41.3625	−100.0263889	2,644	190–200	Ogallala	29.21	−0.01316

Table 1. Wells and springs sampled in the South Loup River Basin, Nebraska, 2019.—Continued

[USGS, U.S. Geological Survey; ID, identification; MM, month; DD, day; YYYY, year; NAD 83, North American Datum of 1983; NAVD 88, North American Vertical Datum of 1988; NA, not applicable; Pliocene, undifferentiated Pliocene-age deposits; Quaternary, undifferentiated Quaternary-age deposits; Ogallala, Ogallala Formation]

USGS station	Station ID[1]	Field name	Sample type	Date sampled (MM/DD/YYYY)	Latitude, in decimal degrees (NAD 83)	Longitude, in decimal degrees (NAD 83)	Elevation, in feet above NAVD 88	Screen interval, in feet below land surface	Unit sampled	Measured water level, in feet below land surface[2]	Hydraulic gradient
412628100150701	17N 25W 18CB (SLR-2)	SLR-2	Monitoring well	9/9/2019	41.39444444	−100.25195	2,746	19.5–29.5	Quaternary	7.62	NA
412717100150701	17N 25W 7CC (SLR-3)	SLR-3	Monitoring well	9/9/2019	41.40166667	−100.2518806	2,741	13–23	Quaternary	5.29	NA
412620100132101	17N 25W 17DC (SLR-1)	SLR-1	Monitoring well	9/12/2019	41.43888889	−100.2225111	2,738	30–40	Quaternary	24.51	NA
412547100125601	17N 25W 20DA (SLR-4)	SLR-4	Monitoring well	9/12/2019	41.40194444	−100.2154944	2,704	10–20	Quaternary	2.95	NA

[1]Legal description: ABCD, codes for the quarter section, as A, B, C, and D, respectively from largest to smallest quarter, where A is northeast, B is northwest, C is southwest, and D is southeast quarter of the next larger unit, and (optional) field name for the well.

[2]Water level measured during sample collection.

creating an artesian well. As with samples collected from monitoring wells, spring samples were collected using a stainless-steel submersible pump. The stainless-steel submersible pump was used in part to develop the temporary sampling point and ensure the sampled groundwater was free of fine-grained sediments. All samples were collected in-line, where Tygon tubing was connected to the discharge port of the stainless-steel submersible pump to ensure groundwater samples were not exposed to the atmosphere prior to collection. When groundwater samples were collected from springs, the flow rate of the submersible pump was adjusted so that the water level inside the casing of the temporary sampling point remained above the level of the sediment water interface to avoid entraining air into the sample or pumping water that had already been exposed to the atmosphere.

Dissolved gas and age tracer samples were collected with specific protocols to ensure representative samples. Dissolved gas samples were collected in septum stopper glass bottles using methods described in U.S. Geological Survey (2020a). Samples were analyzed by the USGS Reston Groundwater Dating Lab in Reston, Virginia, for argon (Ar), nitrogen (N_2), oxygen (O_2), carbon dioxide (CO_2), and methane (CH_4) as described in U.S. Geological Survey (2020a). Stoppered N_2/Ar bottles were chilled to halt biological activity after sampling, but continued gas transformation could not be assured. Unfiltered samples for tritium (^3H) were collected in 1-liter (L) polyethylene bottles, sealed with no air space in the container, and analyzed by the USGS Tritium Laboratory in Menlo Park, California, by electrolytic enrichment (U.S. Geological Survey, 2020b). Samples for sulfur hexafluoride (SF_6) were collected unfiltered in duplicate 1-L amber glass bottles with polyseal cone-lined caps. The samples were collected by submerging the bottle and using a short section of copper tubing to fill from the bottom of the bottle to minimize exposure to the atmosphere. Each sample was allowed to overflow for at least three bottle volumes in order to rinse the bottles while minimizing contact with the air. Samples were analyzed by the USGS Age Dating Laboratory in Reston, Va., according to methods described by Busenberg and Plummer (2000). The USGS Age Dating Laboratory reported that analytical precision of the water samples is about 20 percent at the detection limit of less than (<) 0.01 fentamol per liter (fmol/L) and about 3 percent or better at concentrations from 0.2 fmol/L to a maximum reporting level of 20 fmol/L. Samples of carbon-14 (^{14}C) and stable isotopes of carbon (delta carbon-13 [$\delta^{13}C$]) were filtered with a capsule filter (poresize 0.45 micron) and collected in 1-L glass bottles. The bottles were filled from the bottom and allowed to overflow for several volumes in order to rinse the bottles while minimizing contact with the air, sealed with polyseal caps, and analyzed at the National Ocean Sciences Accelerator Mass Spectrometry Facility at the Woods Hole Oceanographic Institution in Woods Hole, Massachusetts, by accelerator mass spectrometry (Woods Hole Oceanographic Institution, 2020). Analyses of ^{14}C are reported as percent modern carbon (pmC) with "modern" carbon being defined as 95 percent of the activity of Nation Bureau of Standards oxalic acid from 1950 (Stuiver and Polach, 1977) and converted to non-normalized values following Mook and van der Plicht (1999). Delta carbon-13 ($\delta^{13}C$) refers to the abundance of ^{13}C to carbon-12 (^{12}C) in the sample relative to the standard Vienna Pee Dee Belemite (Coplen and others, 2006) and analysis results are reported as per mil. Analytical error for ^{14}C was less than 0.5 pmC; for $\delta^{13}C$, it was greater than or equal to 0.3 per mil (‰) (Woods Hole Oceanographic Institution, 2020).

Except for an initial equipment blank, all environmental and quality control samples were collected and processed on site. Samples that required filtration (major ions, trace elements, nutrients, and ^{14}C) were filtered using a disposable 0.45-micron filter. Field equipment was cleaned immediately following sample collection according to procedures described in the USGS National Water Quality Field Manual (U.S. Geological Survey, variously dated). Samples were sent to analytical laboratories within 3 days of sample collection. Samples that were preserved by cooling (nutrients, dissolved gases, and ^{14}C) were packed on ice to ensure the sample temperature did not exceed 4 degrees Celsius (°C) prior to delivery to the analytical laboratory. Other samples were placed into coolers without ice and delivered to the appropriate analytical laboratories.

Water-Quality Sample Analysis and Reporting

Water samples from all sites were analyzed for major ions, trace elements, nutrients, stable isotopes, dissolved gases, and selected age tracers (^3H, SF_6, and ^{14}C). The analytes, analyzing laboratories, references to methods used, and field preservation procedures are provided in table 2. Sampling results from all analyses are available online from the USGS NWIS (U.S. Geological Survey, 2021b).

For this report, conventional nomenclature was used to describe analyses of water samples for stable isotopes. The composition of stable isotopes of low mass (light) of O and H commonly are reported as "δ" (del) values, which indicate parts per thousand or per mil (‰). The reported value is compared to the isotopic ratio of the Vienna Standard Mean Ocean Water (VSMOW; Clark and Fritz, 1997). The general expression for the δ value is calculated by the following equation (Clark and Fritz, 1997):

Table 2. Laboratory analytical methods and field preservation procedures for water-quality constituents collected from groundwater in the South Loup River Basin, 2019.

[µm, micrometer; °C, degree Celsius; USGS, U.S. Geological Survey; NWQL, National Water Quality Laboratory, Denver, Colo.; <, less than; RSIL, Reston Stable Isotope Laboratory, Reston, Va.; MPTL, Menlo Park Tritium Laboratory; WHOI, Woods Hole Oceanographic Institution]

Analyte(s)	Analyzing laboratory	Analytical methods	References	Field preservation procedures
Physical properties	Analyzed onsite	Various methods	U.S. Geological Survey, variously dated	None
Carbonate alkalinity	Analyzed onsite	Inflection point titration	U.S. Geological Survey, variously dated	Filter through 0.45-µm filter
Nutrients	USGS NWQL	Various methods	Fishman, 1993	Filter through 0.45-µm filter, chill, and maintain at 4°C
Major ions	USGS NWQL	Inductively coupled plasma	Fishman and Friedman, 1989; Fishman, 1993	Anions: filter through 0.45-µm filter, cations: filter through 0.45-µm filter, acidify sample to pH <2 with nitric acid (HNO3)
Trace elements	USGS NWQL	Inductively coupled plasma, atomic absorption spectrometry	Fishman and Friedman, 1989; Fishman, 1993; Garbarino, 1999; Struzeski and others, 1996; Garbarino and Damrau, 2001; Garbarino and others, 2006	Filter through 0.45-µm filter, acidify sample to pH <2 with nitric acid (HNO3)
Stable isotopes	USGS RSIL	Mass spectrometry	U.S. Geological Survey, 2020c	Fill bottle two-thirds full
Dissolved gases	USGS Groundwater Dating Laboratory	Gas chromatograph with thermal conductivity detector and flame ionization detector	U.S. Geological Survey, 2020a	Fill 2-4 liter plastic container with sample water, bottom fill sample bottle with water, with discharge line still in bottle submerge at bottom of larger container, cap with rubber septum, check for bubbles, repeat with second bottle
Tritium	USGS MPTL	Electrolytic enrichment and liquid scintillation	U.S. Geological Survey, 2020b	Fill bottle to top, seal with cap and wrap with electrical tape
Sulfur hexafluoride	USGS Groundwater Dating Laboratory	Electron capture detector	Busenberg and Plummer, 2000	Bottom fill sample bottle until approximately 3 liters of water have been flushed, slowly remove discharge tube, cap sample and tape cap, repeat for second bottle
Carbon-14	WHOI	Accelerator mass spectrometry	Woods Hole Oceanographic Institution, 2020	Filter through 0.45-µm filter, bottom fill bottle flushing two volumes before capping and sealing with electrical tape, chill and maintain at 4°C

$$\delta \text{ (in per mil)} = \left[\frac{Rx}{Rs} - 1\right] * 1,000 \quad (1)$$

where

Rx is the ratio of the heavy to light isotope of the sample; and

Rs is the ratio of the heavy to light isotope of the standard (VSMOW).

A negative δ value indicates that the sample is depleted of the rare isotope relative to the standard; that is, the sample is isotopically "light." A positive δ value indicates that the sample is enriched in the rare isotope relative to the standard; that is, the sample is isotopically "heavy." Understanding and interpreting the stable isotopic composition of groundwater samples are aided by understanding hydrologic processes that can affect isotopic ratios. Isotopic fractionation occurs where the isotopic composition is altered by chemical, biological, or physical processes that may result in the preferential enrichment or depletion of one isotope over another. This fractionation process partitions isotopes as a function of the differences in the masses of the isotopes. Because the heavier isotope has a stronger molecular bond (deuterium [^{2}H] has a stronger molecular bond than hydrogen-1 [^{1}H], and oxygen-18 [^{18}O] has a stronger molecular bond than oxygen-16 [^{16}O]), the liquid phase of water generally is "heavier" than the gaseous phase (Kendall and Caldwell, 1998). As a result, evaporation is a major fractionation process in which the lighter isotope is concentrated in water vapor, whereas the heavier isotope enriches the aqueous phase. Additional information on isotopes and their presence in the environment can be found in Clark and Fritz (1997).

Water-Quality Data Analysis Procedures

Data-analysis procedures include general statistical analyses, creation of Piper diagrams (Piper, 1944), scatter plots, statistical testing, and summary tables. This report only contains selected plots and tables necessary to support the interpretations and conclusions presented. Analyses of stable isotope data and age tracer results, including radiocarbon dating procedures, are also described in this section of the report.

Correlation coefficients were calculated to determine the strength of correlation between two constituents or physical parameters for a set of samples or sample group. Measures of correlation are dimensionless values and range from −1 and 1 where values close to −1 or 1 show a very strong inverse and direct correlations, respectively, and a value of zero indicates no correlation (Helsel and others, 2020). Monotonic correlation occurs when one variable increases or decreases as another variable increases. A scatterplot is a useful diagnostic tool that can indicate if data are correlated linearly or nonlinearly. One type of monotonic correlation is linear correlation where a scatterplot of the two variables will produce a linear pattern (Helsel and others, 2020).

The strength of correlations of different variables or constituents was examined in this study. Pearson's r test (Helsel and others, 2020) was used to measure the strength of linear correlation and Spearman's rho (ρ) test (Helsel and others, 2020) was used the measure the strength of nonlinear, monotonic correlation. Pearson's r is not resistant to outliers because it is computed using means and standard deviations, which are nonresistant measures. If the data lie precisely along a straight line with a positive slope, then r=1, and if the line has a negative slope then r=−1. A low value for Pearson's r may be calculated even though the two variables are highly correlated because of skewness or outliers. The null hypothesis for this test is that r is not significantly different from zero, which is to say no correlation. The alternative hypothesis is that r is significantly different from zero and the variables are linearly correlated (Helsel and others, 2020). Spearman's ρ is a rank-based correlation coefficient that depends on the ranks of the data rather than the observed values. Spearman's ρ is resistant to outliers and is particularly useful for examining water-quality data where concentrations are known to be less than the detection limit. The statistical significance of ρ is tested under the null hypothesis that ρ is not significantly different from zero, or there is no correlation, and the alternate hypothesis is that the test statistic is significantly different from zero (Helsel and others, 2020).

The Wilcoxon rank-sum test (Helsel and others, 2020) was used to determine if differences between distributions of the selected values from the two subsets of samples collected from Pliocene deposits were significant. Water samples collected from the Pliocene-age deposits were divided into two groups based on geographic location and water-quality characteristics. The null hypothesis for the test was that the distributions for the two groups are identical, and the alternative hypothesis was that the distributions between the two groups are different (Helsel and others, 2020). The null hypothesis was accepted when the calculated *p*-value was less than an alpha value (α) of 0.05, which indicates a 95-percent confidence level that the probability value from the statistical test generated an accurate representation of the populations being tested (Helsel and others, 2020). A *p*-value is defined as the measure of the probability that an observed difference occurred by random chance (Helsel and others, 2020). If a calculated *p*-value is less than 0.05, then it can be inferred there is a significant difference between the medians of the sample groups with 95-percent confidence.

Stable Isotopes

In terrestrial waters, the ratio of the two most common isotopes of H and O (δ^{2}H and δ^{18}O) are covariant and vary by a factor of 2 and 5 percent, respectively (Coplen and Kendall, 2000). Craig (1961) determined that for fresh water, isotopic composition of precipitation worldwide could be correlated on a global scale and could be described using the global meteoric water line (GMWL), which is given as $\delta^{2}H=8\ \delta^{18}O+10$. The GMWL is the average of many local or

regional meteoric water lines, which differ in slope and delta deuterium (δ^2H) intercept (Clark and Fritz, 1997). Variations in the slope and deuterium intercept for local and regional meteoric water lines are affected by water vapor source, seasonal precipitation patterns, and climate. For a given area, precipitation during cold seasons is depleted in ^2H and ^{18}O, whereas precipitation in warm seasons is typically isotopically enriched (Clark and Fritz, 1997).

This report uses a local meteoric water line (LMWL) established by Harvey and Welker (2000) from analysis of precipitation samples collected at North Platte, Nebr. (fig. 1). Harvey and Welker (2000) reported the LMWL as $\delta^2H=7.66\ \delta^{18}O+4.96$. North Platte is roughly 20 mi south of the most upstream sample and 55 mi west of the farthest downstream sample. Although North Platte (fig. 1) is located outside the study area, the LMWL is assumed to adequately represent precipitation within the study area. Line-conditioned excess was examined in samples to determine local deviations from the LMWL. Line-conditioned excess was first described by Landwehr and Coplen (2006) as a means to compare major river basins with local precipitation and describe relevant hydrologic processes. Deviations in δ^2H and $\delta^{18}O$ from the LMWL may indicate hydrologic processes, such as additional evaporation or a depleted recharge source relative to local precipitation.

The distinct seasonality of isotopes in precipitation is reflected in groundwater such that δ^2H and $\delta^{18}O$ in groundwater can be used to estimate the relative seasonal precipitation contributions to recharge. The fraction of recharge sourced from winter precipitation (fraction winter [F_{win}]) for a given groundwater sample was calculated using an isotopic mass balance model described by Jasechko and others (2014) as

$$F_{win} = \frac{\delta_{gw} - \delta_s}{\delta_w - \delta_s} \quad (2)$$

where

F_{win} is the fraction of recharge sourced from winter (October to March) precipitation,

δ_{gw} is the measured isotopic ratio in groundwater,

δ_s is the precipitation volume-weighted mean isotopic ratio of summer precipitation or surface water, and

δ_w is the precipitation volume-weighted mean isotopic ratio of winter precipitation.

F_{win} was calculated for $\delta^{18}O$ only because it is less sensitive to fractionation such that the observed precipitation datasets are more likely to be representative of actual recharge. Uncertainty in F_{win} was calculated following Phillips and Gregg (2001) as

$$\sigma_{F_{win}} = \sqrt{\frac{1}{(\delta_w - \delta_s)^2}\left(\sigma^2_{\delta_{gw}} + F_{win}{}^2\sigma^2_{\delta_w} + (1 - F_{win})^2\sigma^2_{\delta_s}\right)} \quad (3)$$

where

σ is the respective standard deviation for each component.

The σ of groundwater is taken to be the analytical uncertainty (0.2 ‰ for $\delta^{18}O$; Révész and Coplen, 2008a, 2008b). The σ of seasonal end members (δ_s and δ_w) were calculated as the pooled standard deviation derived from the observed precipitation data.

Seasons were defined as April through September for summer and October through March for winter. An arithmetic mean and standard deviation were calculated for each of the seasons from $\delta^{18}O$ data (n=215) compiled from Water Isotope System for Data Analysis, Visualization and Electronic Retrieval database (International Atomic Energy Agency and World Meteorological Organization, 2021). The seasonal datasets used to calculate the end members for the F_{win} analysis were evaluated for statistically significant difference by nonparametric Wilcoxon test (Helsel and others, 2020) at the 95-percent confidence interval.

PHREEQC

Geochemical software PHREEQC (Parkhurst and Appelo, 1999) and default thermodynamic database (phreeqc.dat) was used to calculate mineral saturation indices from the observed groundwater chemistry. The evaluation of mineral saturation indices can be useful in understanding groundwater flow paths, residence time, and mixing. Saturation index of zero indicates chemical equilibrium between the solution and a given mineral phase. Saturation indices greater than zero indicate conditions favorable for mineral precipitation, and values less than zero indicate conditions favorable for dissolution.

Oxidation Reduction

Oxidation-reduction (redox) reactions describe the transfer of electrons and chemical potential energy between ions. The redox conditions of groundwater can strongly affect the persistence and mobility of many contaminants and are important for understanding geochemical processes in the groundwater system (McMahon and Chapelle, 2008). The redox condition of each sample was categorized as "oxic" if concentrations of DO were greater than or equal to 0.5 milligram per liter (mg/L) or "anoxic" if concentrations of DO were less than 0.5 mg/L (McMahon and Chapelle, 2008; Jurgens and others, 2009). During dissolved gas analysis, anoxic or mixed conditions were used as indicators for the possibility of excess nitrogen gas (N_2) resulting from denitrification; anoxic or mixed conditions were also used as indicators during ^{14}C geochemical corrections for the possible influence of organic carbon geochemistry.

Dissolved Gas

Dissolved concentrations of N_2 and Ar gases were used in this study to estimate recharge temperature at the water table, excess N_2 concentrations, and dissolved gas in excess of atmospheric solubility (excess air [EA]) in groundwater samples. Equilibrium solubility concentrations of atmospheric gases are dictated according to Henry's law (Faure, 1998)

as a function of recharge conditions such as elevation (a proxy for barometric pressure), temperature, and salinity. Measured gas concentrations can be fit by solubility gas models such that recharge conditions and excess N_2 of a sample can be estimated following Vogel and others (1981). Additional N_2 in excess of atmospheric solubility, possibly from denitrification, was estimated at four sites based on redox conditions and reasonability of modeled recharge conditions. Recharge parameters for these four sites are less certain as a result of model sensitivity to estimates of excess N_2. The closed-equilibrium model (Aeschbach-Hertig and others, 1999) was used to calculate solubility equilibrium gas concentrations based on modeled recharge parameters for comparison to measured concentrations of O_2, CO_2, and CH_4.

Groundwater Age Tracers

Estimating the age of groundwater is an increasingly common approach to inform water resource management strategies. Groundwater age is often used to estimate groundwater recharge rates, examine the sustainability of groundwater resources, and assist in groundwater model calibration (Kazemi and others, 2006). For this report, ^3H, SF_6, and ^{14}C samples were collected from selected wells and springs. Data analysis procedures including radiocarbon adjustments of ^{14}C data are discussed below.

Tritium and Sulfur Hexafluoride

Tritium (^3H) is a radioactive isotope of hydrogen, present in water as part of the water molecule with a half-life of 12.32 years (Lucas and Unterweger, 2000) and is typically used to estimate the age of younger waters (Lindsey and others, 2019). ^3H is produced naturally in the upper atmosphere by cosmic-ray spallation. During the 1950s and 1960s, large amounts of ^3H were released into the atmosphere and introduced into the hydrologic cycle by aboveground thermonuclear weapons testing. As a result, ^3H concentrations in precipitation in the northern hemisphere during 1963–64 peaked at three orders of magnitude above natural concentrations (Michel, 1989). The detection limit of ^3H was reported to be 0.1 tritium unit (TU) and the analytical precision was generally better than 0.2 TU but could be as high as 0.6 TU (U.S. Geological Survey, 2020b).

Atmospheric SF_6 was used to evaluate the age of modern (post-mid-1950s recharge) groundwater or identify a component of modern water in a mixed signal. SF_6 can occur naturally but is primarily an anthropogenic input to the atmosphere. In the 1960s there was substantial production of SF_6 in the manufacturing of high-voltage electrical switches (Busenberg and Plummer, 2000). Age dating groundwater using SF_6 has been possible since around 1970; however, SF_6 is particularly useful in dating groundwater recharged after 1990 (Steele and others, 2007). Concentrations of SF_6 in groundwater are subject to potential anthropogenic and natural contamination and degradation. For example, SF_6 is produced naturally in fluorite deposits and volcanic or hydrothermal environments (Busenberg and Plummer, 2000). SF_6 concentrations were corrected for EA using the calculated value from dissolved gas modeling as described previously and were not corrected for the potential unsaturated-zone time lag (Cook and Solomon, 1995).

Carbon-14

Carbon-14 (^{14}C) is a naturally occurring radioactive isotope that is useful for dating groundwater ranging from several hundred to more than 30,000 years old. Wang and others (1998) reported the natural production of ^{14}C in the atmosphere by the interaction of cosmic ray produced neutrons with N (Kalin, 2000). Once produced, ^{14}C mixes with CO_2 and is assimilated into the hydrosphere. Consequently, the half-life of ^{14}C (5,730 years) and the ubiquity of carbon make it an ideal tracer to date groundwater that can be several hundred to more than 30,000 years old (Kalin, 2000). ^{14}C analyses are typically reported in percent modern Carbon. The method of ^{14}C dating is based on determining the initial ^{14}C concentration and the predictable rate of radioactive decay of ^{14}C. Kalin (2000) and Han and Plummer (2016) provided comprehensive reviews of the radiocarbon groundwater dating method.

Use of ^{14}C for groundwater age dating often requires geochemical correction for nonatmospheric dissolved inorganic carbon (DIC) contributions. In aquifers with little to no subsurface carbon sources, such as in the South Loup River study area, it may be possible to use measured ^{14}C directly for age determinations. Investigation of major ion chemistry, mineral saturation indices, and tracer concentrations were used to confirm the absence of nonatmospheric inorganic carbon. Regardless, major ion chemistry in this study did not clearly indicate similar processes, such as pyrite oxidation, which would necessitate the geochemical modeling complexity used in McMahon and others (2007).

Lumped Parameter Modeling

Groundwater age is described in this study by the estimated mean age and the age distribution. In most cases, a groundwater sample is a mixture of flow paths with varying ages, and the age distribution represents the probability of a water parcel with a given estimated age occurring in the sample. Narrow age distributions indicate a narrow range of groundwater ages captured in the sample mixture, whereas a broad distribution indicates a wide range of captured ages. Mean ages, age distributions, and the susceptibility index (SI; described in the "Susceptibility Index and Fraction Modern" section of this report) were determined by calibrating lumped parameter models (LPMs) to the measured tracer concentrations. Tracers used for age determination are assumed to be conservative or have a predictable decay rate. The LPMs simulate tracer concentrations in accordance with the model's distribution type and parameters (Jurgens and others, 2012). In groundwater studies, fitted distributions are

interpreted to represent the aquifer dimensions, mean age, and extent of flow path mixing. The LPMs are optimized by minimizing the misfit between measured and LPM-calculated tracer concentrations. A modified version of the USGS program TracerLPM (Jurgens and others, 2012) was used for calibration of LPMs. The approach for LPM selection and interpretation was dictated by the measured tracer concentrations and the conceptual hydrogeology. Estimated age distributions describe the advective age of groundwater and provide a maximum estimate of the response time to hydraulic perturbations (for example, the propagation of pressure driven by changing water levels); that is, groundwater levels at wells and discharge at springs will respond to changes in aquifer hydraulic conditions over time scales less than the mean age.

The LPMs used in this study were the dispersion model (DM), the exponential mixing model (EMM), and the binary mixing model (BMM; Jurgens and others, 2012). The DM is a solution to the advection-dispersion equation and describes the amount of mixing along and between flow paths being captured in a sample. The DM is parametrized by the mean age and the dispersion parameter (DP), which is the inverse of the Peclet number (Gelhar and others, 1992). Based on field scale studies of dispersion in groundwater (Gelhar and others, 1992), the DP varies between 0.001, which approximates a piston-flow model with very little mixing and a narrow age distribution, to 3, which approximates the EMM with a broad age distribution. The EMM is used to represent groundwater age distribution in a sample capturing flow paths across the full depth of an aquifer receiving areally distributed recharge. Exponentially mixed samples capture the full range of groundwater flow paths and respective varying ages with the relative contributions of the flow paths determined by the mean age, which is the single fitting parameter of the EMM. The BMM describes mixtures of two distinct water sources. The two components of the BMMs, the young and old components, were modeled by two DMs parameterized based on results from other samples in this study and a previous study of groundwater mixing parameters (for example, Bexfield and others, 2012; Eberts and others, 2012; Stackelberg and others, 2018; Solder and others, 2020). The dispersion parameter and mean age for the young component DM was estimated from fully constrained LPM solutions for nearby samples. For the old component DM, a dispersion parameter of 0.1 was assumed, consistent with kilometer scale longitudinal dispersion (Gelhar and others, 1992). Measured tracer concentrations were fit by varying the mean age of the old component DM and the mixing fraction of the two BMM components. Full description of the LPMs used in this study are provided by Jurgens and others (2012).

Susceptibility Index and Fraction Modern

The SI and fraction modern metrics are used in this study as complimentary measures of groundwater susceptibility to changing hydrologic conditions, such as drought, during somewhat short time periods. The SI is most sensitive to relative contributions of very young water less than 10 years old. Conversely, the fraction modern is more sensitive than the SI to contributions of groundwater that are greater than about 20 years old (Solder and others, 2020). Combined, the two metrics provide a useful means of summarizing the groundwater age distribution.

The SI provides a quantitative estimate of susceptibility of a well to land surface contamination. More specifically, it is a relative measure of how soon a conservative contaminant in the recharge area would arrive at the well by groundwater transport and does not include unsaturated zone travel time. The SI is calculated as the normalized difference between the LPM-derived cumulative distribution function (CDF) of age and a reference CDF (Solder and others, 2020) as described by the following equations:

$$SI = \frac{1}{1 + D_H} \tag{4}$$

where

D_H is the Hellinger distance, which is calculated as

$$D_H = \frac{\sqrt{\sum_{i=1}^{k} \left(\sqrt{P(\mathrm{i})} - \sqrt{Q(\mathrm{i})}\right)^2}}{\sqrt{2}} \tag{5}$$

where

$P(i)$ is the cumulative probability of the age distribution of interest for a given time step;

$Q(i)$ is the cumulative probability of the reference age distribution for a given time step;

i is the time step of the cumulative distribution function, in years; and

k is the age corresponding to the last time step, in years.

The reference CDF was defined as a piston-flow model with a mean age of 1 year. The value of the SI is unitless and ranges between one (indicating young ages and a narrow age distribution) and approaching zero (indicating older ages and a broad age distribution).

The SI was initially conceptualized to examine the movement of contaminants from the land surface; however, in this study it was used as a proxy for determining the susceptibility to short-term drought. Groundwater discharging from a spring or sampled from a well with an SI close to 1 indicates relatively young groundwater with a narrow age distribution. Groundwater in this scenario is sourced from recent recharge and would likely be affected by short-term

drought conditions. In contrast, groundwater samples with an SI that approaches zero indicates old groundwater with a broad age distribution. Groundwater in this scenario is not as reliant on recent recharge and is likely more resilient to short-term drought conditions. The SI is a relative measure for comparison between sites in the same study area under the assumption of similar aquifer properties, such as transmissivity and porosity, that control the hydraulic response to changing hydrologic conditions such as drought.

The LPM fraction modern describes the relative contribution of recharge post-1950 to the full LPM estimated age distribution. The fraction modern is a standardized measure to understand the relative contribution of modern recharge to a sample and for comparison between samples. The calculated value of the fraction modern is extracted directly from the LPM-estimated cumulative age distribution as the cumulative fraction of water recharged after 1950.

Quality Assurance and Quality Control

Quality control samples were collected for this study and included an equipment blank, field blanks, and field replicates. Quality control samples were collected to evaluate and determine if samples have been contaminated or if the data were biased by the sampling equipment, collection, processing, storage, or laboratory analysis. For this report, one equipment blank, two field blanks, and two field replicate samples were collected (table 3). One field blank and one replicate were collected during each of the two field campaigns (August and September 2019). Equipment blanks were collected in the laboratory before sampling to determine if the samples were biased by the sampling equipment and cleaning procedures. Field blank samples were collected to determine the occurrence and magnitude of sample contamination from collection, processing, storage, and analysis. Blank samples were collected using water that has been certified to be free of inorganic constituents.

Blank samples were analyzed for major ions, trace elements, and nutrients. Relatively few concentrations were greater than the reporting limit in the field blanks. Most of the concentrations were within the range of environmental samples for specific constituents (table 3); however, there were some notable exceptions. Concentrations of copper were an order of magnitude greater than the reporting level in the equipment blank and one field blank and were within an order of magnitude with the other field blank (table 3). Manganese had concentrations exceeding an order of magnitude of the lower detection limit for one of the two field blanks (table 3). The source(s) of copper and manganese in blank samples is currently (2021) unknown.

The relative percent difference was calculated for all sample pairs for each constituent using the following formula:

$$relative\ percent\ difference = \frac{\left(sample1 - sample2\right)}{\left(\left(sample1 + sample2\right)/2\right)} \times 100 \quad (6)$$

Where there is no variability between paired analyses, the relative percent is zero percent. The relative percent difference could not be calculated if the paired replicate concentration was less than the laboratory reporting level.

The relative percent differences between replicates for major ions and trace elements were 5 percent or less, with the exception of higher differences of fluoride, chromium, cobalt, and nickel; however, the differences between the replicates and the samples were near the reporting limit (table 3). For one replicate sample (East shallow), the relative percent difference of lithium was nearly 19 percent and the difference in concentration between the environmental sample concentration and the replicate was 2.75 micrograms per liter (µg/L), which is an order of magnitude greater than the reporting limit (table 3). For nutrients, relative percent differences between samples were less than 5 percent. For the East shallow sample, the relative percent difference for ammonia and nitrite were 12 percent and 143 percent, respectively (table 3). Although the relative percent differences between the environmental and replicate samples were large, actual differences in concentration were small; 0.00913 mg/L for ammonia and <0.206 mg/L for nitrite (table 3).

Real-Time Water-Quality Monitoring

This section of the report describes the collection of continuous water temperature, specific conductance, gage height, and discrete discharge data at three locations (fig. 3; table 4) from May 2019 to October 2019 to provide additional support to the groundwater age tracer interpretations. Site selection, data collection, and data processing procedures are discussed.

Monitoring locations were selected to examine the hydrologic responses of springs or streamflow. One monitoring site (South Loup River Spring 0.86 mile west of Arnold, Nebr.; USGS station 412542100125301; referred to hereafter as “Mills Valley) was sited at a spring where groundwater discharged from Quaternary-age deposits and another monitoring location (South Loup River Tributary Spring 1.3 miles Southwest of Finchville, Nebr.; USGS station 412147100055301; referred to hereafter as “Finchville”) was located at a spring where groundwater discharged from Pliocene-age deposits (table 4). The third monitoring site (South Loup River Spring below North Fork South Loup River at Hoagland, Nebr.; USGS station 413054100220201; referred to hereafter as “Hoagland”) was located on the South Loup River, near the headwaters, below the confluence with the North Fork South Loup River. It should be noted that groundwater discharging from the Mills Valley

Table 3. Results and selected statistics of field blank samples and relative percent difference between replicate samples, Nebraska, 2019.

[N, nitrogen, <, less than; NH_3, ammonia; NH_4+, ammonium; N, nitrogen; ND, not detected]

Constituent	Field blank samples				Replicate samples			
					Relative percent difference		Difference in concentration	
	Equipment blank	Station 412244100013501, 16N 24W 2DDDD1 (East shallow)	Station 412145100055601, 16N 24W 2DDDD1 (SPR 27)	Reporting level	Station 412146100055701, 16N 24W17B3 SLoup Spr 30 (SPR 30)	Station 412244100013501, 16N 24W 2DDDD1 (East shallow)	Station 412146100055701, 16N 24W17B3 SLoup Spr 30 (SPR 30)	Station 412244100013501, 16N 24W 2DDDD1 (East shallow)
Physical properties								
Specific conductance, in microsiemens per centimeter	<5	<5	<5	1	0.49	0.30	0.92	1.65
Dissolved solids, filtered, in milligrams per liter	<20	<20	<20	20	3.98	1.27	5.89	4.79
Dissolved solids, filtered, sum of constituents, in milligrams per liter	<3.2	<3.2	<3.2	3.2	0.00	1.04	0	4
Hardness, as calcium carbonate, in milligrams per liter	<0.203	<0.096	<0.155	0.096	0.31	0.22	0.24	0.6
Major ions, in milligrams per liter								
Calcium	[1]0.063	<0.022	[1]0.044	0.022	0.39	0.22	0.1	0.19
Magnesium	<0.011	<0.01	<0.011	0.01	0.06	0.15	0.002	0.02
Potassium	<0.3	<0.3	<0.3	0.3	0.61	0.20	0.029	0.02
Sodium	<0.4	<0.4	<0.4	0.4	0.25	0.32	0	0.001
Alkalinity, as calcium carbonate	<4	<4	<4	4	0.39	0.70	0.31	1.8
Chloride	<0.02	<0.02	<0.02	0.02	1.33	0.97	0.021	0.016
Fluoride	<0.01	<0.01	<0.01	0.01	[1]5.94	1.45	0.012	0.003
Silica	<0.05	<0.05	<0.05	0.05	0.25	0.47	0.12	0.27
Sulfate	<0.02	<0.02	<0.02	0.02	0.48	1.96	0.023	0.78
Nutrients, in milligrams per liter								
Ammonia (NH_3 + NH_4+) as nitrogen	<0.01	<0.01	<0.01	0.01	ND	[1]12.06	<0.0129	0.00913
Nitrate plus nitrite as N	<0.04	<0.04	<0.04	0.04	0.08	4.27	0.00182	0.02087
Nitrate as N	<0.0400	<0.0400	<0.0400	0.04	0.08	4.91	0.002	0.0239
Nitrite as N	<0.0033	<0.001	<0.001	0.001	ND	[1]143.00	<0.001	<0.206

Table 3. Results and selected statistics of field blank samples and relative percent difference between replicate samples, Nebraska, 2019.—Continued

[N, nitrogen, <, less than; NH_3, ammonia; NH_4+, ammonium; N, nitrogen; ND, not detected]

Constituent	Field blank samples				Replicate samples			
					Relative percent difference		Difference in concentration	
	Equipment blank	Station 412244100013501, 16N 24W 2DDDD1 (East shallow)	Station 412145100055601, 16N 24W 2DDDD1 (SPR 27)	Reporting level	Station 412146100055701, 16N 24W17B3 SLoup Spr 30 (SPR 30)	Station 412244100013501, 16N 24W 2DDDD1 (East shallow)	Station 412146100055701, 16N 24W17B3 SLoup Spr 30 (SPR 30)	Station 412244100013501, 16N 24W 2DDDD1 (East shallow)
Nutrients, in milligrams per liter—Continued								
Orthophosphate as phosphorus	<0.004	<0.004	<0.004	0.004	4.15	0.36	0.00595	0.00089
Orthophosphate as phosphate	<0.0123	<0.0123	<0.0123	0.0123	4.14	0.36	0.0182	0.0027
Trace elements, in micrograms per liter								
Aluminum	<3	<3	<3	3	ND	ND	<3	<3
Barium	[1]0.1263	[1]0.2472	<0.1	0.1	ND	ND	0.9039	3.2814
Beryllium	<0.01	<0.01	<0.01	0.01	ND	ND	<0.01	<0.01
Cadmium	<0.03	<0.03	<0.03	0.03	ND	4.20	<0.03	0.0021
Chromium	<1	<1	<1	1	[1]20.64	[1]19.37	0.749	0.48
Cobalt	<0.03	<0.03	<0.03	0.03	ND	[1]12.74	<0.0076	0.0176
Copper	[1]2.0935	[1]2.3827	[1]0.726	0.2	ND	ND	<0.2	<0.2
Iron	<10	<10	<10	10	ND	ND	<10	<10
Lead	<0.02	<0.02	<0.02	0.02	ND	ND	<0.02	<0.02
Lithium	<0.15	<0.15	<0.15	0.15	1.44	[1]18.58	0.1314	2.7508
Manganese	<0.4	[1]1.2245	<0.4	0.4	ND	2.40	<0.4	0.9469
Molybdenum	<0.05	<0.05	<0.05	0.05	2.58	2.51	0.0371	0.1982
Nickel	<0.2	<0.2	<0.2	0.2	ND	[1]10.67	<0.2	0.0537
Silver	<1	<1	<1	1	ND	ND	<1	<1
Strontium	<0.5	<0.5	<0.5	0.5	0.81	0.11	1.0387	0.3725
Vanadium	<0.1	[1]0.1319	<0.1	0.1	2.98	3.63	0.2539	0.25
Zinc	<2	<2	<2	2	ND	ND	<2	<2
Arsenic	<0.1	<0.1	<0.1	0.1	3.58	1.66	0.141	0.1453
Boron	[1]2.198	<2	<2	2	0.47	2.65	0.08	0.91
Selenium	<0.05	<0.05	<0.05	0.05	0.55	1.31	0.0052	0.0089
Uranium	<0.03	<0.03	<0.03	0.03	0.79	1.11	0.0031	0.1595

[1]Detections for blank samples and where the relative percent difference exceeds 5 percent for replicate samples.

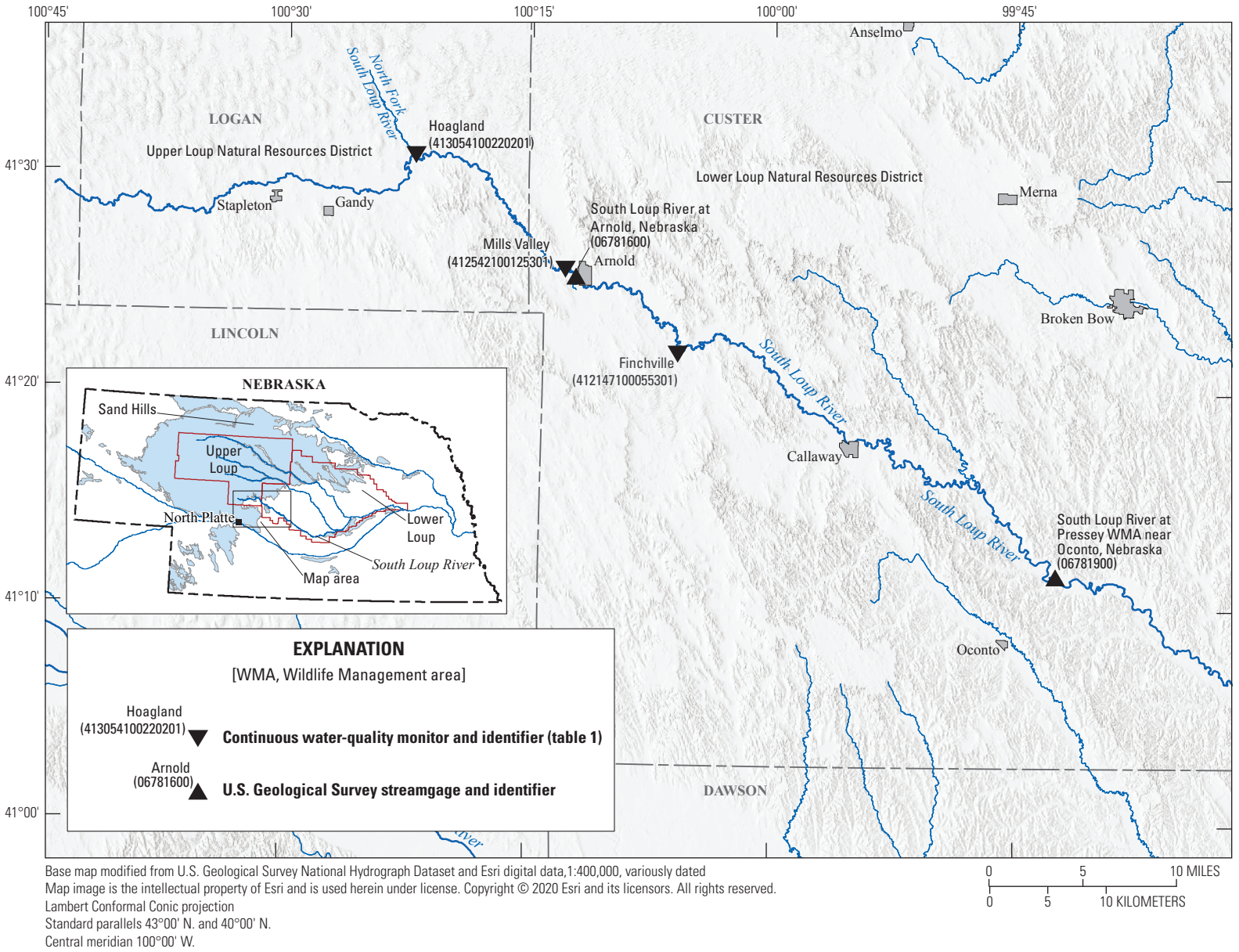

Figure 3. Map of real-time monitoring sites, South Loup River Basin, Nebraska, 2019.

Table 4. U.S. Geological Survey station number, station identification, location, and data collection period of real-time monitoring sites, South Loup River Basin, Nebraska, 2019.

[USGS, U.S. Geological Survey; ID, identification; NAVD 88, North American Vertical Datum of 1988]

USGS station	Station ID	Field name	Latitude (decimal degrees)	Longitude (decimal degrees)	Land surface elevation (feet above NAVD 88)	Data collection period
413054100220201	South Loup River Spring below North Fork South Loup River at Hoagland, Nebraska	Hoagland	41.515044	−100.367112	2,813	5/20/2019–10/23/2019
412542100125301	South Loup River Spring 0.86 mile west of Arnold, Nebraska	Mills Valley	41.428777	−100.214556	2,701	5/14/2019–10/22/2019
412147100055301	South Loup River Tributary Spring 1.3 miles Southwest of Finchville, Nebraska	Finchville	41.362958	−100.098325	2,642	5/14/2019–10/23/2019

monitoring site was not sampled because the discharge was too low to maintain water levels within the temporary sampling point, which is needed to avoid atmospheric contamination in age tracer samples. In contrast, groundwater was sampled at the two main discharge points (SPR30 and SPR27) immediately upstream from the Finchville monitoring site because each discharge point provided adequate flow to collect representative age tracer samples.

A continuous water-quality monitor and a pressure transducer were deployed at each monitoring site to measure water temperature, specific conductance, and gage height. At each monitoring site, a YSI 6-series sonde (Xylem Analytics, 2020) recorded data at 15-minute intervals and provided a near-continuous record of water temperature and specific conductance. The sondes deployed at the two monitoring sites (Mills Valley and Finchville) were located within flat lying areas near the South Loup River, and water was impounded behind a weir to ensure that the multiprobe sonde was submerged in flowing water. The sonde at the South Loup River monitoring site (Hoagland) was deployed inside a vertical pipe anchored near the wingwall on the upstream side of a county road bridge. The sondes for all monitoring sites were deployed inside of vertical polyvinyl chloride pipes with holes drilled to ensure adequate water flow. Gage height was measured with a KPSI 355 vented transducer (TE Connectivity, 2020). Gage height data were collected, processed, and published using the methods and guidelines described in Sauer and Turnipseed (2010) and Turnipseed and Sauer (2010). All recorded data were transmitted through satellite telemetry and are available on the USGS NWIS web page (U.S. Geological Survey, 2021b).

Water-quality monitors were operated and maintained in accordance with the standard procedures described in Wagner and others (2006). Field maintenance quality protocols routinely evaluated error associated with sensor fouling (from sedimentation, for example) and with calibration drift. Based on the error evaluation, the data were adjusted accordingly or, if the error magnitude was too large, deleted to produce a final water-quality record. Data adjustments and final records were thoroughly checked and reviewed before publication on the USGS NWIS web page (U.S. Geological Survey, 2021b).

Specific conductance is the ability of water to conduct an electric current and is a function of the amount of dissolved ions in water (Hem, 1985). Typically, these ion concentrations—and the resulting specific conductance values—are lowest in precipitation and greatest in groundwater owing to interaction with minerals in the subsurface. As a result, specific conductance can indicate rainfall runoff in streams and can be used to examine the recovery time associated with a return to prestorm conditions following rainfall runoff. Water temperature plays an important role in the chemistry of freshwater ecosystems by affecting the solubility of dissolved constituents, specific conductance, biological activity, and rates of biogeochemical reactions (U.S. Geological Survey, variously dated). Water temperature can also be used as a tracer of water source. Groundwater temperature is typically equal to mean annual air temperature. Surface water temperatures are affected by diurnal air temperature variations and direct solar radiation. The relative stability and response of water temperature to climatic conditions can provide information on the source and relative contributions of groundwater to streamflow.

Discharge was measured at selected locations using a handheld acoustic Doppler velocimeter at the time the water-quality monitors were being cleaned and calibrated. Discharge measurements were collected in accordance with the guidelines and recommendations stated in Turnipseed and Sauer (2010) and the U.S. Geological Survey (2004). Discharge measurements are provided in table 5 and stored in NWIS (U.S. Geological Survey, 2021b). Because of backwater conditions at the mouth of the North Fork South Loup River (North Fork South Loup River at Hoagland, Nebr., USGS station 413055100221101, referred to hereafter as “North Fork South Loup”), discharge was estimated by calculating

Table 5. Discharge measurements collected in South Loup River Basin, Nebraska, 2015 and 2019.

[USGS, U.S. Geological Survey; ID, identification; MM, month; DD, day; YYYY, year; ft^3/s, cubic feet per second; ADV, acoustic doppler velocimeter; NA, not applicable; NR, not recorded]

USGS station	Station ID	Field name	Date (MM/DD/YYYY)	Time	Discharge (ft^3/s)	Gage height (ft)	Measurement rating	Measurement method
413054100220201	South Loup River Spring below North Fork at Hoagland	Hoagland	5/14/2019	12:19	31.3	2.81	Good	ADV
			6/13/2019	11:54	27.6	2.87	Good	ADV
			7/11/2019	11:49	57.1	4.60	Good	ADV
			8/2/2019	9:14	20.5	2.52	Good	ADV
			9/5/2019	10:18	25	3.03	Good	ADV
			10/3/2019	10:31	28.8	3.17	Good	ADV
			10/23/2019	14:44	24.4	2.99	Good	ADV
413053100221401	South Loup River above North Fork South Loup River at Hoagland, Nebraska	Upper South Loup	8/27/2015	10:43	3.26	NA	Fair	ADV
			5/14/2019	13:09	21.3	NA	Good	ADV
			6/13/2019	12:23	22.7	NA	Good	ADV
			7/11/2019	11:15	27	NA	Fair	ADV
			8/2/2019	9:56	9.4	NA	Good	ADV
			9/5/2019	11:15	14.1	NA	Fair	ADV
			10/3/2019	11:33	13	NA	Good	ADV
			10/23/2019	13:31	14.6	NA	Good	ADV
413055100221101	North Fork South Loup River at Hoagland, Nebraska	North Fork South Loup	8/27/2015	12:00	7.14	NA	Fair	Difference
			5/14/2019	12:23	9.95	NA	Fair	Difference
			6/13/2019	11:50	4.91	NA	Fair	Difference
			7/11/2019	12:21	30.2	NA	Fair	Difference
			8/2/2019	10:10	11.1	NA	Good	Difference
			9/5/2019	11:18	11	NA	Fair	Difference
			10/3/2019	12:18	15.9	NA	Good	Difference
			10/23/2019	15:28	10	NA	Good	Difference
413055100220901	South Loup River below North Fork South Loup River at Hoagland, Nebraska		8/27/2015	12:02	10.4	NA	Good	ADV
412542100125301	South Loup River Spring 0.86 mile west of Arnold	Mills Valley	5/14/2019	8:26	0.04	NR	Poor	ADV
			6/13/2019	9:01	0.01	2.65	Good	flume
			7/11/2019	14:56	0.07	2.95	Fair	ADV
			8/1/2019	15:28	0.01	2.61	Good	flume
			9/4/2019	9:26	0.01	2.41	Fair	flume
			10/3/2019	15:15	0.01	2.60	Fair	flume
			10/22/2019	10:14	0.01	2.68	Excellent	flume
412147100055301	South Loup River Tributary Spring 1.3 miles Southwest of Finchville, Nebraska	Finchville	5/14/2019	15:09	0.85	NR	Fair	ADV
			6/13/2019	14:34	0.89	3.69	Poor	ADV
			7/12/2019	6:51	0.92	3.32	Poor	ADV
			8/1/2019	12:13	1.12	3.59	Poor	ADV
			9/4/2019	10:46	0.85	3.64	Poor	ADV
			10/3/2019	13:50	0.84	3.57	Poor	ADV
			10/23/2019	8:09	0.94	3.54	Poor	ADV

the difference in discharge immediately upstream (South Loup River above North Fork South Loup River at Hoagland, Nebr.; USGS station 413053100221401, referred to hereafter as "Upper South Loup") and downstream from the confluence (Hoagland) with the South Loup River (fig. 4; table 5).

Intense and frequent precipitation events occurred throughout the data collection period (May to October 2019), which caused sedimentation and precluded the ability to develop a gage height-discharge relation at the three monitoring sites. Exposed sand and gravel deposits at the Finchville monitoring site were eroded and deposited behind the weir, affecting the performance. As a result, small changes in gage height (less than 0.1 ft) throughout the deployment period cannot be confidently associated with changes in discharge. A 1-week gap in the measured data occurred in early July when sand covered much of the specific conductance probe, affecting the performance of the sensor. The proximity of the Mills Valley monitoring site to the active channel of the South Loup River created some challenges in data collection. The weir at the monitoring site likely experienced backwater conditions when the gage height of the Arnold streamgage exceeded approximately 5.5 ft, affecting the gage height-discharge relationship. Backwater conditions likely occurred for prolonged periods of time from May 20 to June 7; July 8 to July 18; and during storm events on August 3, 16, and 21. Gage height data were not used from August 3 to 9 when silty sediments around the weir structure were eroded, allowing flow to bypass the weir.

Figure 4. Map of South Loup River discharge measurement locations near the confluence with the North Fork South Loup River.

Water Quality, Groundwater Age, and Streamflow in the South Loup River Basin

This section of the report describes the water-quality, groundwater age, and streamflow characteristics in the South Loup River Basin. A description of the results of the groundwater sampling of 20 wells and springs is presented in the "Water-Quality and Groundwater Age Characteristics" subsection. Groundwater age characteristics and interpretations for 20 samples are also provided. The discharge, gage height, specific conductance, and water temperature data collected at the three monitoring sites are described in the "Discharge and Continuous Monitoring of Spring Complexes and the South Loup River" subsection. Comparisons of computed streamflow from streamgages and discrete discharge measurements are described in the "Reach-Scale Streamflow Comparisons" subsection. A discussion of drought resilience of groundwater discharge is discussed in the final subsection.

Water-Quality and Groundwater Age Characteristics

Water-Quality Characteristics

In general, groundwater sampled from wells and springs in the South Loup River Basin in 2019 was relatively fresh, with total dissolved solids (TDS) generally less than about 500 mg/L (table 6) and generally calcium-bicarbonate type (fig. 5). Spring sites from Pliocene-age units had a higher relative proportion of sulfate (SO_4), whereas SLR-1 and two wells in Logan County (Mann shallow and Mann deep) had a higher relative proportion of sodium and potassium. The difference in dissolved ions indicates differing flow paths and subsequent geochemical evolution of groundwater or differences in groundwater recharge chemistry. Groundwater samples are oxic for 15 of the 20 sites, with measured DO greater than or equal to 0.5 mg/L (table 6). Oxic conditions are consistent with very low amounts of dissolved iron and aluminum in solution for most of the samples (table 6).

Local land use appears to be a dominant control on nitrate concentrations within the study area. Nitrate concentrations of samples are below the background concentration of 2 mg/L (Mueller and Helsel, 1996) for 10 of the 20 samples and below 3 mg/L for 17 of the 20 samples. The U.S. Environmental Protection Agency (EPA) maximum contaminant level of 10 mg/L (U.S. Environmental Protection Agency, 2018) was exceeded in two samples (SPR 25 and SPR 35). Elevated nitrate concentrations in groundwater indicate a portion of the sample collected contains groundwater recharged within the past 50 years, approximately the time when commercial fertilizers were widely available. An anthropogenic source of nitrate is supported by generally higher nitrate concentrations in samples with higher ^3H and ^{14}C, suggestive of younger water, as discussed in the "Groundwater Age Tracers" section of this report. The effects of land use on groundwater quality are evident when examining nitrate concentrations from springs and wells in Pliocene deposits. The nitrate concentrations of springs SPR 24, SPR 25, and SPR 35 were the highest for this study with nitrate concentrations of 6.51, 14.3, and 16.5 mg/L, respectively. The chloride concentrations for these samples were among the highest for the 20 samples collected (table 6). The nitrate concentration of Connor shallow well was below the background concentration of 2 mg/L; however, the DO concentration was 0.2 mg/L, indicating anoxic conditions and possible denitrification. The four samples (SPR 24, SPR 25, SPR 35, and Connor shallow) are located approximately 3.5 mi downstream from the Arnold streamgage and downgradient from groundwater-irrigated row crops (fig. 6). The general groundwater flow direction in this area is northeast, towards the South Loup River (Summerside and others, 2001). Other springs in Pliocene-age deposits (SPR 27, SPR 28, SPR 29, SPR 30, and SPR 31) sampled 7 mi downstream are downgradient from rangeland and appear to be unaffected by agricultural activities (fig. 6). Nitrate concentrations for Pliocene-age samples downgradient of rangeland were less than 3 mg/L and chloride concentrations were all less than 3 mg/L (table 6). Because of the differences in groundwater chemistry, sites in Pliocene-age deposits have been subdivided into two groups: Western Pliocene (SPR 24, SPR 25, SPR 35, and Connor shallow) and Pliocene (SPR 27, SPR 28, SPR 29, SPR 30, SPR 31).

Groundwater Age Characteristics

This section of the report describes the groundwater age and recharge characteristics of 20 springs and wells sampled in August and September 2019. Isotopic ratios, dissolved gas concentrations, and tracer concentrations were used to examine groundwater recharge sources, characterize recharge conditions and seasonality, and estimate groundwater ages. The "Isotope Tracers" subsection compares the concentrations of isotope tracers to concentrations of other sampled constituents to assist with hydrogeologic conceptualization. The interpretation of stable isotope data is also presented in the "Isotope Tracers" subsection. The "Dissolved Gases" subsection discusses concentrations of dissolved gases to estimate groundwater recharge temperature, assess denitrification, and support interpretations of age tracer data. The "Lumped Parameter Models and Groundwater Age Metrics" subsection discusses the age metrics estimated by calibration of LPMs to concentrations of ^3H and ^{14}C.

Isotope Tracers

Isotope and age tracer data indicate a wide range of possible groundwater ages with a stable recharge source. Groundwater samples contain ^3H ranging from about zero to 7 TUs and ^{14}C ranging from less than 20 pmC to greater

than 100 pmC (table 7), which is indicative of the presence of premodern and modern waters. In general, groundwater with concentrations of ^{3}H greater than 3 TUs is likely modern. Conversely, the stable isotopes $\delta^{2}H$ and $\delta^{18}O$ are consistent with local precipitation (fig. 7*A*) and relatively invariant across the sample sites, with the notable exception of SLR-1, indicating a temporally stable recharge source across the sites. Carbon-13 isotopic ratios ($\delta^{13}C$) are relatively invariable and range from about −11 and −6 ‰ with no clear consistent relation between $\delta^{13}C$ and ^{14}C.

Values of $\delta^{2}H$ and $\delta^{18}O$ plotted near the LMWL (fig. 7*A*, *B*). Line conditioned excess (LC-excess; Landwehr and Coplen, 2006) ranges from −1.3 to about 2, indicating local deviations from the LMWL. The most negative values of LC-excess, indicating additional evaporation prior to recharge, occur along the central portion of the study reach, with the lowest values of LC-excess north of the South Loup River (East deep, SPR 31). The highest values of LC-excess, indicating a more depleted recharge source relative to local precipitation, are located south of the South Loup River (Pressey shallow, SPR 30, SPR 35, SLR-3, SLR-2, Mann shallow, Mann deep).

Precipitation-weighted seasonal $\delta^{18}O$ end members (winter and summer) in precipitation are statistically different with a high level of confidence (*p*-value much less than 0.001) based on the Wilcoxon rank-sum test. Calculated fraction of winter precipitation from $\delta^{18}O$ data ranged from 0.3 to 0.47 (excluding the result from SLR-1 of 0.75), indicating that summer precipitation is the dominant source of recharge (table 7). These results are consistent with 30-year (1981–2010) average precipitation records from Broken Bow Municipal Airport (fig. 1), which show 76 percent of annual precipitation falls between April and September (National Centers for Environmental Information, 2021). At the time this report was written (2021), it is unknown why sample SLR-1 is heavily biased towards wintertime recharge. Samples collected from springs in the Western Pliocene sample group (SPR 24, SPR 25, and SPR 35) are more isotopically enriched and have lower fractions of winter recharge compared to the rest of the springs sampled (table 7). This difference indicates that a larger proportion of recharge to these springs occurs during summer months and is likely caused by the recharge of groundwater applied to row crops or irrigation return flow. This interpretation is supported by the elevated concentrations of nitrate and chloride in these samples (table 6).

Relevant to the use of ^{14}C for age dating, the youngest groundwaters (^{3}H greater than about 3 TUs) are near equilibrium with calcite (saturation indices close to zero; table 6) based on PHREEQC model results, which is suggestive of a solid carbonate phase in the unsaturated zone and shallow aquifer. The shallow carbonate and soil zone CO_2 in isotopic equilibrium with the atmosphere and soil zone sources (plant and microbial respiration) are likely the primary sources of DIC in groundwater. Values of measured $\delta^{13}C$ in groundwater reflect the mixture of C3 and C4 photosynthetic pathways of vegetation in the Sand Hills with a bias in DIC $\delta^{13}C$ toward C4 (warm season) plant activity, which results in soil gas CO_2 $\delta^{13}C$ of about −10 ‰ relative to C3 (cool season) plants which have a $\delta^{13}C$ signature of about −25 ‰ (Cerling, 1984). The DIC $\delta^{13}C$ bias toward C4 plants could be a result of C4 plants preference to more sandy soil, which allows faster infiltration and higher relative recharge; generally lower rates of transpiration from C4 plants, resulting in more relative recharge; and deeper rooting depths of C4 plants, which may result in greater influence on soil CO_2 near the water table (Barnes and Harrison, 1982). Accumulation of groundwater DIC in the unsaturated zone from a single isotopic source is supported by the relative invariance of $\delta^{13}C$ between samples; a lack of clear relation between $\delta^{13}C$ and age tracers (^{3}H and ^{14}C); and the bulk aquifer mineralogy, which does not contain a major carbonate source. For these reasons, the uncorrected ^{14}C is likely a reasonable tracer of groundwater age for the older samples.

Dissolved Gases

Dissolved gas concentrations (table 8) are consistent with gas sourced from the atmosphere (Ar and N_2) and biologic activity resulting in the production of excess N_2 (at select sites) and CO_2, as well as depletion of O_2 relative to atmospheric equilibrium solubility. Laboratory-measured O_2 was lower than field-measured DO values, which is suggestive of microbial activity in sample bottles after collection. Similarly, as a possible product of microbial activity, measured CO_2 is unlikely to represent field conditions. Relative percent difference on duplicate measurements of CO_2 and O_2 was less than 10 percent for 30 of the 38 measurements (one duplicate bottle was not analyzed). Outlier O_2 concentrations were removed from the calculated mean value for sites SPR 30 and SPR 28 reported in table 8. Data for Ar and N_2 are high quality, with less than 1.6 percent error between duplicate sample bottles. Measured concentrations of Ar and N_2 were well captured by equilibrium solubility models, indicating concentrations were not significantly altered, except in situations where excess N_2 was indicated. Concentrations of Ar and N_2 for four samples (Conner shallow, SLR-2, East shallow, East deep) were better fit by solubility models with the addition of excess N_2 gas ranging from 0.5 to 5.5 mg/L, which is indicative of excess N_2 production from nitrate reduction. Field-measured DO and reasonability of solubility modeled recharge temperature and EA were used to guide estimations of excess N_2. Modeled recharge temperatures ranged from 11.6 to 13.7 °C, and EA values ranged from 1.4 to 7.1 mg/L at standard temperature and pressure (table 8). Modeled recharge temperatures were slightly warmer than the 30-year (1981–2010) average air temperature of 9.4 °C at Broken Bow Municipal Airport (National Centers for Environmental Information, 2021), which is consistent with observed seasonal precipitation bias toward summer at the same weather station (National Centers for Environmental Information, 2021) and calculated $\delta^{18}O$ F_{win} values (table 7).

Table 6. Field-measured water-quality parameters, dissolved-ion concentrations, and mineral saturation indices of groundwater samples in South Loup River Basin, Nebraska, 2019.

[USGS, U.S. Geological Survey; ID, identification; °C, degree Celsius; µS/cm, microsiemen per centimeter at 25 degrees Celsius; mg/L, milligram per liter; HCO_3^-, bicarbonate; µg/L, microgram per liter; N, nitrogen; PO_4, phosphate; --, no data]

USGS station	Station ID	Field name	Water temperature (°C)	Specific conductance (µS/cm)	Dissolved oxygen (field, mg/L)	pH (standard units)	Bicarbonate (mg/L) as HCO_3^-	Calcium (mg/L)	Magnesium (mg/L)
412611100384401	17N 29W22ABBB1	Mann shallow	15.5	241	8.7	7.2	144	31.1	2.99
412611100384402	17N 29W22ABBB2	Mann deep	15.4	254	8.5	7.5	175	34.7	3.45
412620100132101	17N 25W 17DC (SLR-1)	SLR-1	12.7	743	--	7.1	476	88.3	13.2
412628100150701	17N 25W 18CB (SLR-2)	SLR-2	15.8	538	0.3	7.1	374	82.2	12.9
412717100150701	17N 25W 7CC (SLR-3)	SLR-3	14.9	212	3	7	132	30	3.76
412547100125601	17N 25W 20DA (SLR-4)	SLR-4	12	284	--	6.84	172	41.1	5.27
411126099422501	14N 21W 15AB Pressey	Pressey deep	15.5	429	0.8	7.2	262	61.7	8.96
412146100055701	16N 24W17B3 SLoup Spr 30	SPR 30	13.6	185	8.8	7.4	52	25.9	3.09
412213100051001	16N 24W 8D1 SLoup Spr 31	SPR 31	12.6	299	5.8	7.1	80.6	42.2	6.16
412145100055601	16N 24W17B1 SLoup Spr 27	SPR 27	13	214	8.6	7.4	31	30.2	3.82
412148100061501	16N 24W18A1 SLoup Spr 29	SPR 29	12.6	227	7.9	7.3	55.7	32.2	3.94
412149100060401	16N 24W17B2 SLoup Spr 28	SPR 28	12.3	186	8.7	7.3	59.4	26.1	3.12
412340100074901	17N 24W31C1 SLoup Spr 35	SPR 35	12.2	700	7.9	6.8	264	103	14.4
412406100080401	17N 24W31B2 SLoup Spr 25	SPR 25	12.8	682	7.1	7.2	286	102	14.3
412407100080501	17N 24W31B1 SLoup Spr 24	SPR 24	13.9	436	6.4	7.3	176	64.7	8.33
411126099422502	14N 21W 15AB 02 Pressey 2	Pressey shallow	14	409	4.5	7.2	255	65.9	8.61
412244100013501	16N 24W 2DDDD1	East shallow	14	539	0.5	7.2	330	85.2	13.2
412244100013502	16N 24W 2DDDD2	East deep	13.9	223	3.2	7.1	135	31.2	4.19
412429100080302	17N 24W30CCDD2	Conner shallow	14.1	449	0.2	6.9	276	67.6	10.1
412429100080303	17N 24W30CCDD3	Conner deep	14.6	321	0.3	7.5	200	45.1	5.77

Sodium (mg/L)	Potassium (mg/L)	Chloride (mg/L)	Sulfate (mg/L)	Fluoride (mg/L)	Silica (mg/L)	Iron (µg/L)	Aluminum (µg/L)	Total dissolved solids (mg/L)	Calcite saturation index	Nitrate (mg/L) as N	Phosphate (mg/L) as PO_4
13.5	6.94	1.98	1.7	0.16	45.5	<10.0	<3	183	−0.68	1.56	0.78
13.9	5.25	1.35	1.16	0.13	44.8	<10.0	<3	193	−0.25	0.424	0.34
57.1	17.9	8.3	22.4	0.48	50.9	11.7	7	505	0.05	2.55	0.40
14.5	11.4	4.08	10.7	0.18	55	<10.0	<3	383	−0.02	1.38	0.60
7.12	5.88	1.18	3.24	0.24	53.1	<10.0	<3	177	−0.93	1.53	0.55
8.9	6.91	1.48	4.29	0.26	52.5	<10.0	7	219	−0.91	2.87	0.43
15.5	8.93	1.25	25.3	0.25	68.8	<10.0	<3	327	−0.17	1.43	0.102
5.89	4.72	1.59	4.79	0.21	47.5	<10.0	<3	130	−0.74	2.37	0.43
9.31	6.97	2.63	7.37	0.26	53.3	<10.0	<3	181	−0.64	2.65	0.55
6.68	5.1	1.78	3.67	0.22	46.5	<10.0	<3	125	−0.61	2.59	0.38
7.79	5.1	1.76	6.67	0.2	45.3	<10.0	<3	140	−0.67	1.95	0.38
5.95	4.68	1.5	4.61	0.2	47.2	<10.0	<3	133	−0.85	2.21	0.42
18.8	12.2	9.07	40.1	0.22	50.3	<10.0	<3	453	−0.36	16.5	0.67
19.1	9.9	10.7	27.3	0.21	49.1	<10.0	<3	438	0.07	14.3	0.26
12.5	7.67	3.77	11	0.22	48.5	<10.0	<3	273	−0.12	6.51	0.25
7.61	7.02	2.01	16.4	0.2	61.4	<10.0	<3	305	−0.18	2.19	0.12
12.5	10.2	1.65	39.4	0.21	56.8	<10.0	<3	386	0.02	0.475	0.75
7.83	6.01	0.78	7.26	0.21	57.1	<10.0	<3	186	−0.82	0.894	0.58
13	9.04	5.53	10.9	0.21	56.5	<10.0	<3	312	−0.44	0.643	0.32
13.3	7.17	1.26	15.3	0.26	65	<10.0	<3	254	−0.11	0.256	0.13

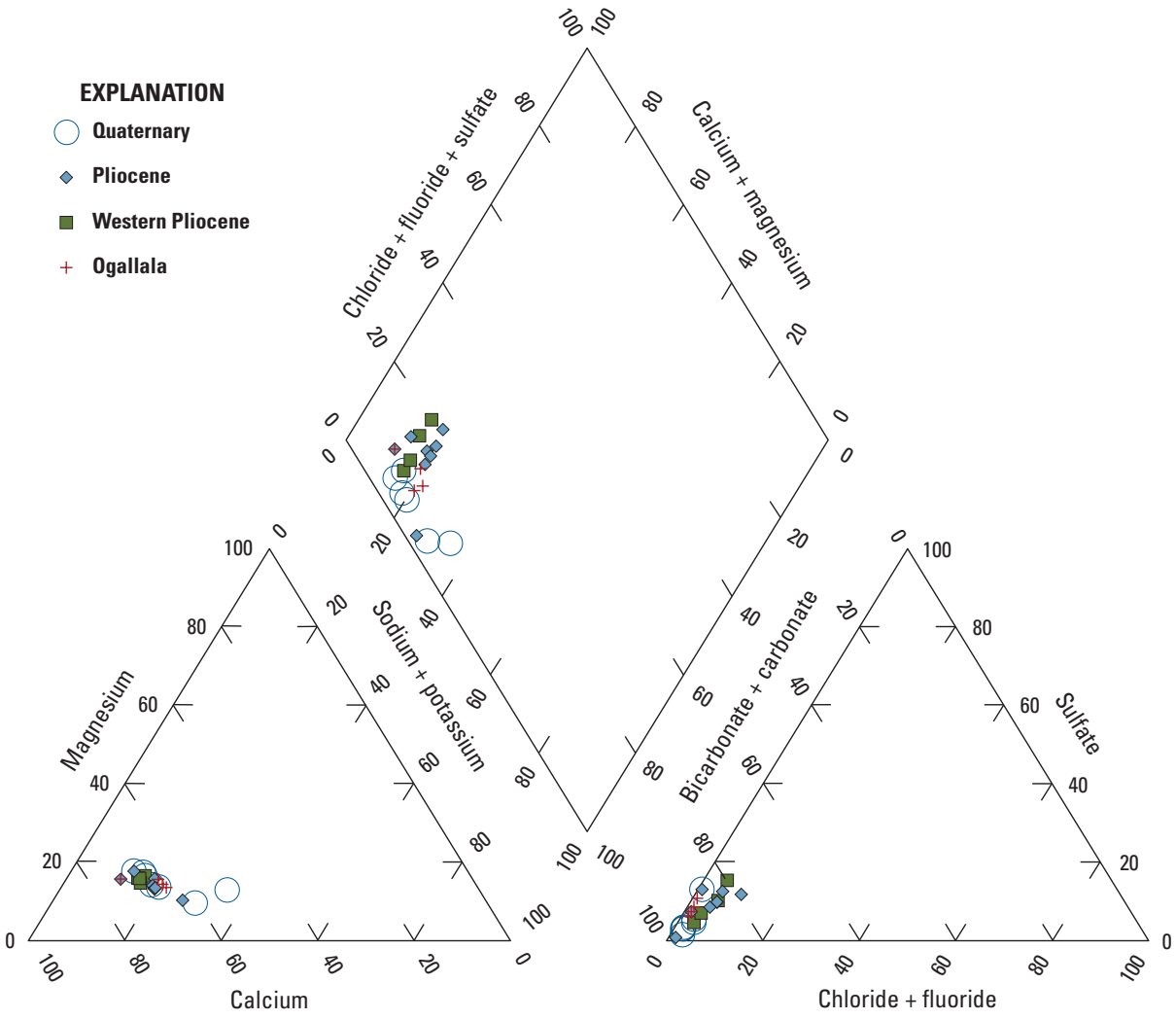

Figure 5. Piper diagram showing ionic composition of groundwater from Quaternary deposits, Pliocene deposits, and Ogallala Formation, Nebraska, 2019.

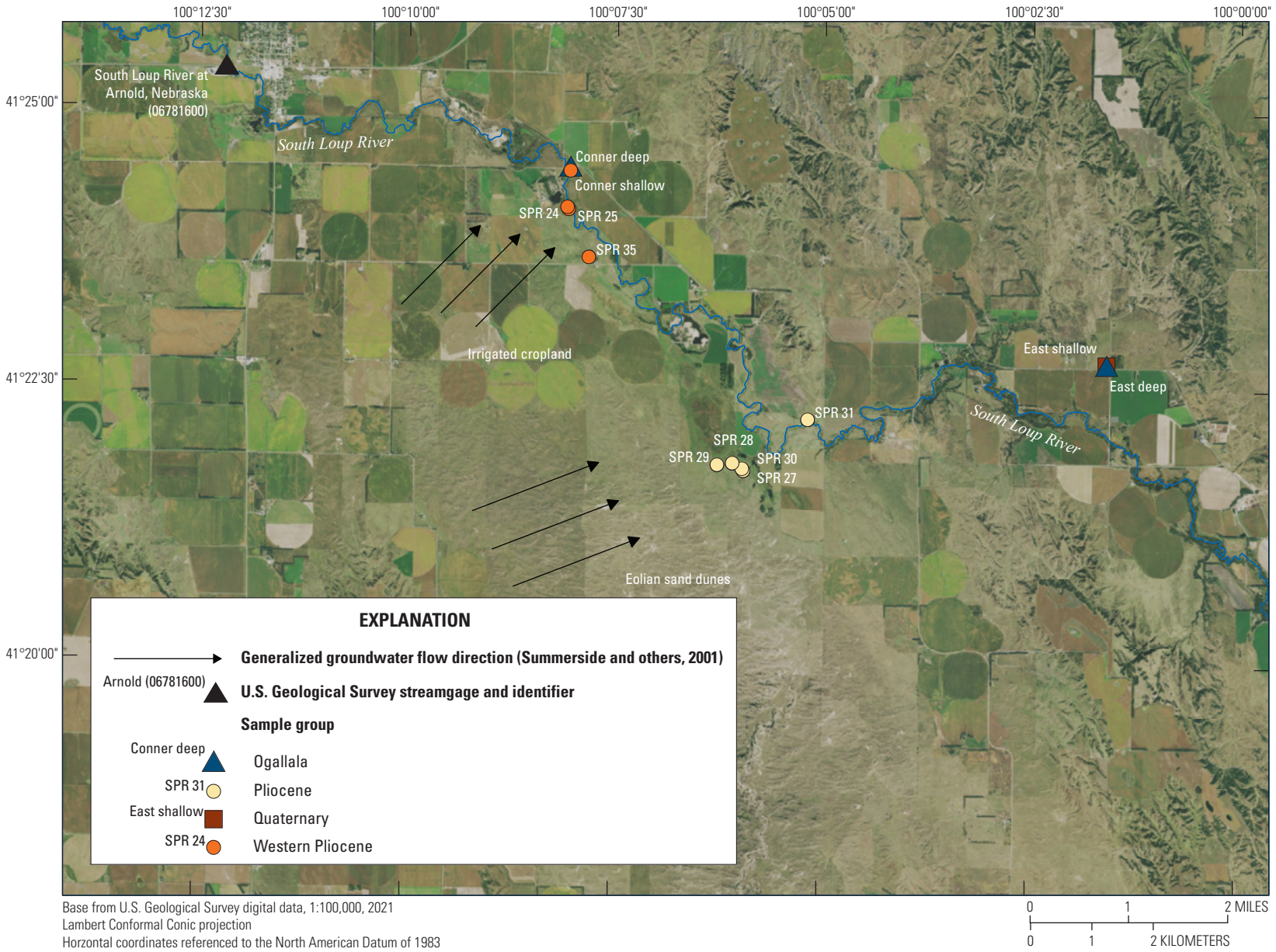

Figure 6. Aerial imagery showing selected sampling locations from the Western Pliocene and Pliocene sample groups downstream from the South Loup River at Arnold, Nebraska, streamgage (U.S. Geological Survey station 06781600). Row crops irrigated with groundwater applied from center pivots appear as circles in the aerial imagery.

Table 7. Tracer concentrations, modeled seasonal precipitation recharge contributions, and modeled age metrics for groundwater sampled in the South Loup River Basin, Nebraska, 2019.

[USGS, U.S. Geological Survey; ID, identification; MM, month; DD, day; YYYY, year; $\delta^{18}O$, ratio of ratio of oxygen-18 to oxygen-16 in sample to ratio of oxygen-18 to oxygen-16 in reference; per mil, parts per thousand; δD, ratio of ratio of deuterium or hydrogen-2 to hydrogen-1 in sample to ratio of deuterium or hydrogen-2 to hydrogen-1 in reference; LC, line conditioned; TU, tritium units; $\delta^{13}C$, ratio of ratio of carbon-13 to carbon-12 in sample to ratio of carbon-13 to carbon-12 in reference; pmC, percent modern carbon; SF_6, sulfur hexafluoride; pptv, parts per trillion, volume; LPM, lumped parameter model; $\chi 2$, chi-squared; BMM, binary mixing model modeled with young and old components each modeled with a dispersion model; ~, approximately; ^3H, tritium; ^{14}C, carbon-14; <, less than; DM, dispersion model; EMM, exponential mixing model]

USGS station	Station ID	Field name	Sample group	Sample date (MM/DD/YYYY)	$\delta^{18}O$ (per mil)	δD (per mil)	LC-excess (unitless)	Fraction winter recharge (unitless)	Tritium (TU)
411126099422502	14N 21W 15AB 02 Pressey 2	Pressey shallow	Pliocene	9/11/2019	−10.1	−70.85	1.63	0.39	0.33
411126099422501	14N 21W 15AB Pressey	Pressey deep	Ogallala	9/11/2019	−9.65	−69.55	-0.48	0.33	<0.12
412244100013501	16N 24W 2DDDD1	East shallow	Quaternary	9/11/2019	−10.4	−74.29	0.46	0.43	6.96
412244100013502	16N 24W 2DDDD2	East deep	Ogallala	9/11/2019	−9.55	−69.12	-0.81	0.31	<0.15
412213100051001	16N 24W 8D1 Sloup Spr 31	SPR 31	Pliocene	8/14/2019	−9.89	−72.19	-1.3	0.36	1.9
412145100055601	16N 24W17B1 Sloup Spr 27	SPR 27	Pliocene	8/13/2019	−9.77	−70.68	-0.7	0.34	0.96
412149100060401	16N 24W17B2 Sloup Spr 28	SPR 28	Pliocene	8/14/2019	−9.89	−70.94	-0.05	0.36	<0.13
412146100055701	16N 24W17B3 Sloup Spr 30	SPR 30	Pliocene	8/13/2019	−9.87	−69.93	0.81	0.36	1.84
412148100061501	16N 24W18A1 Sloup Spr 29	SPR 29	Pliocene	8/13/2019	−9.83	−70.16	0.28	0.35	1.11
412407100080501	16N 24W31B1 Sloup Spr 24	SPR 24	Western Pliocene	8/12/2019	−9.55	−67.76	0.55	0.31	1.14
412406100080401	16N 24W31B2 Sloup Spr 25	SPR 25	Western Pliocene	8/12/2019	−9.45	−67.22	0.34	0.3	3.02
412340100074901	17N 24W31C1 Sloup Spr 35	SPR 35	Western Pliocene	8/12/2019	−9.48	−66.56	1.22	0.3	3.12
412429100080302	17N 24W30CCDD2	Conner shallow	Western Pliocene	9/9/2019	−9.67	−68.7	0.52	0.33	0.58
412429100080303	17N 24W30CCDD3	Conner deep	Ogallala	9/9/2019	−9.67	−68.68	0.54	0.33	<0.17
412717100150701	17N 25W 7CC (SLR-3)	SLR-3	Quaternary	9/9/2019	−9.95	−70.59	0.75	0.37	<0.15
412620100132101	17N 25W 17DC (SLR-1)	SLR-1	Quaternary	9/12/2019	−12.74	−92.5	-0.03	0.75	2.95
412628100150701	17N 25W 18CB (SLR-2)	SLR-2	Quaternary	9/9/2019	−10.65	−74.62	2.03	0.47	1.44
412547100125601	17N 25W 20DA (SLR-4)	SLR-4	Quaternary	9/12/2019	−9.94	−70.72	0.55	0.37	0.34
412611100384401	17N 29W22ABBB1	Mann shallow	Quaternary	9/10/2019	−9.88	−69.85	0.96	0.36	<0.15
412611100384402	17N 29W22ABBB2	Mann deep	Pliocene	9/10/2019	−9.48	−67.01	0.77	0.3	<0.14

Tritium error (TU)	$\delta^{13}C$ (per mil)	Carbon-14 (pmC)	Carbon-14 error (pmC)	SF_6 (pptv)	LPM name	χ^2	Tracers modeled	Estimated mean age (years)	Susceptibility index (unitless)	Fraction modern
0.1	−8	51	0.23	0.91	BMM	~0	^{3}H, ^{14}C	6,700	0.028	0.04
0.12	−10.18	19.2	0.22	1.07	DM	5.72E-17	^{14}C	18,000	0.014	0
0.14	−8.92	102.6	0.24	1.72	EMM	3.79	^{3}H, ^{14}C	27	0.374	0.93
0.15	−9.63	40.8	0.2	0.78	DM	4.36E-17	^{14}C	8,700	0.02	0
0.14	−8	78.2	0.28	1.22	BMM	5.28E-29	^{3}H, ^{14}C	2,900	0.064	0.23
0.14	−8.4	77.1	0.26	0.98	BMM	1.11E-25	^{3}H, ^{14}C	2,400	0.054	0.12
0.13	−8.45	78.1	0.31	0.95	DM	8.63E-17	^{14}C	2,000	0.041	0
0.11	−8.51	78.8	0.28	1.08	BMM	5.21E-29	^{3}H, ^{14}C	2,700	0.065	0.23
0.16	−9.03	81.1	0.31	1.26	BMM	2.67E-19	^{3}H, ^{14}C	1,900	0.062	0.14
0.13	−7.51	94.6	0.32	2.29	DM	0.18	^{3}H, ^{14}C	74	0.15	0.27
0.15	−7.46	106.5	0.33	5.07	DM	0.01	^{3}H, ^{14}C	18	0.257	1
0.2	−9.21	108.1	0.31	3.66	DM	2.5E-15	^{3}H, ^{14}C	20	0.253	1
0.15	−7.83	86.3	0.23	1.15	DM	1.81	^{3}H, ^{14}C	77	0.148	0.16
0.17	−10.43	13.2	0.2	0.99	DM	4.59E-17	^{14}C	23,000	0.012	0
0.15	−9.11	77.3	0.24	1.47	DM	5.28E-17	^{14}C	2,100	0.04	0
0.12	−11.14	93.8	0.21	6.44	DM	0.66	^{3}H, ^{14}C	70	0.154	0.44
0.16	−9	97	0.24	4.63	DM	0.05	^{3}H, ^{14}C	75	0.151	0.26
0.11	−7.44	79.1	0.24	0.67	BMM	6.91E-18	^{3}H, ^{14}C	1,900	0.05	0.04
0.15	−6.44	89.7	0.26	0.58	DM	8.8E-16	^{14}C	840	0.062	0
0.14	−6.1	85.7	0.25	0.55	DM	2.25E-17	^{14}C	1,200	0.053	0

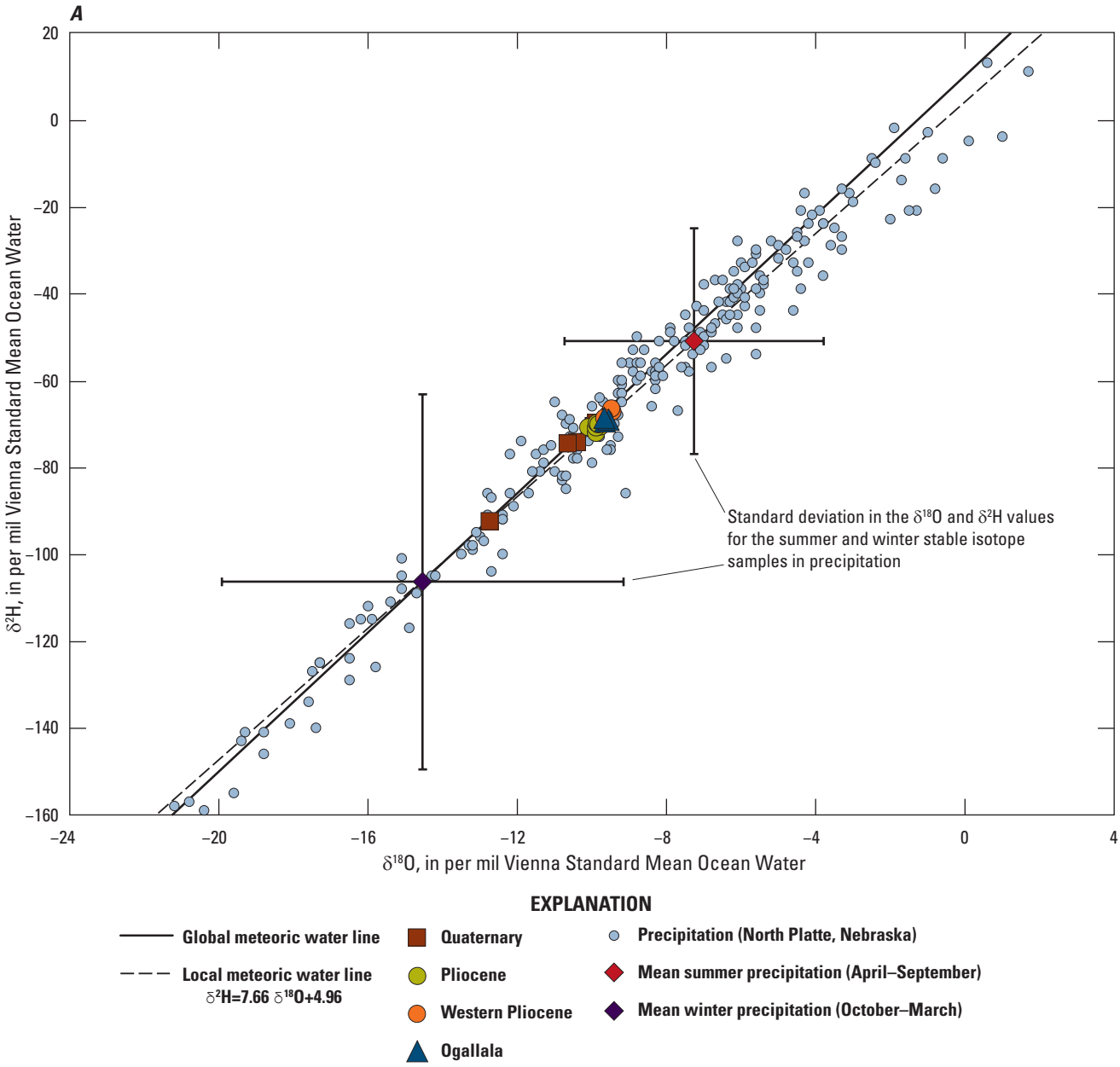

Figure 7. Stable isotope ratios of oxygen ($\delta^{18}O$) and hydrogen ($\delta^{2}H$), Nebraska, 2019. *A,* Precipitation in North Platte, Nebraska (1989–94), and groundwater sampled springs and wells (2019). *B,* Groundwater sampled springs and wells by sample group, Nebraska, 2019.

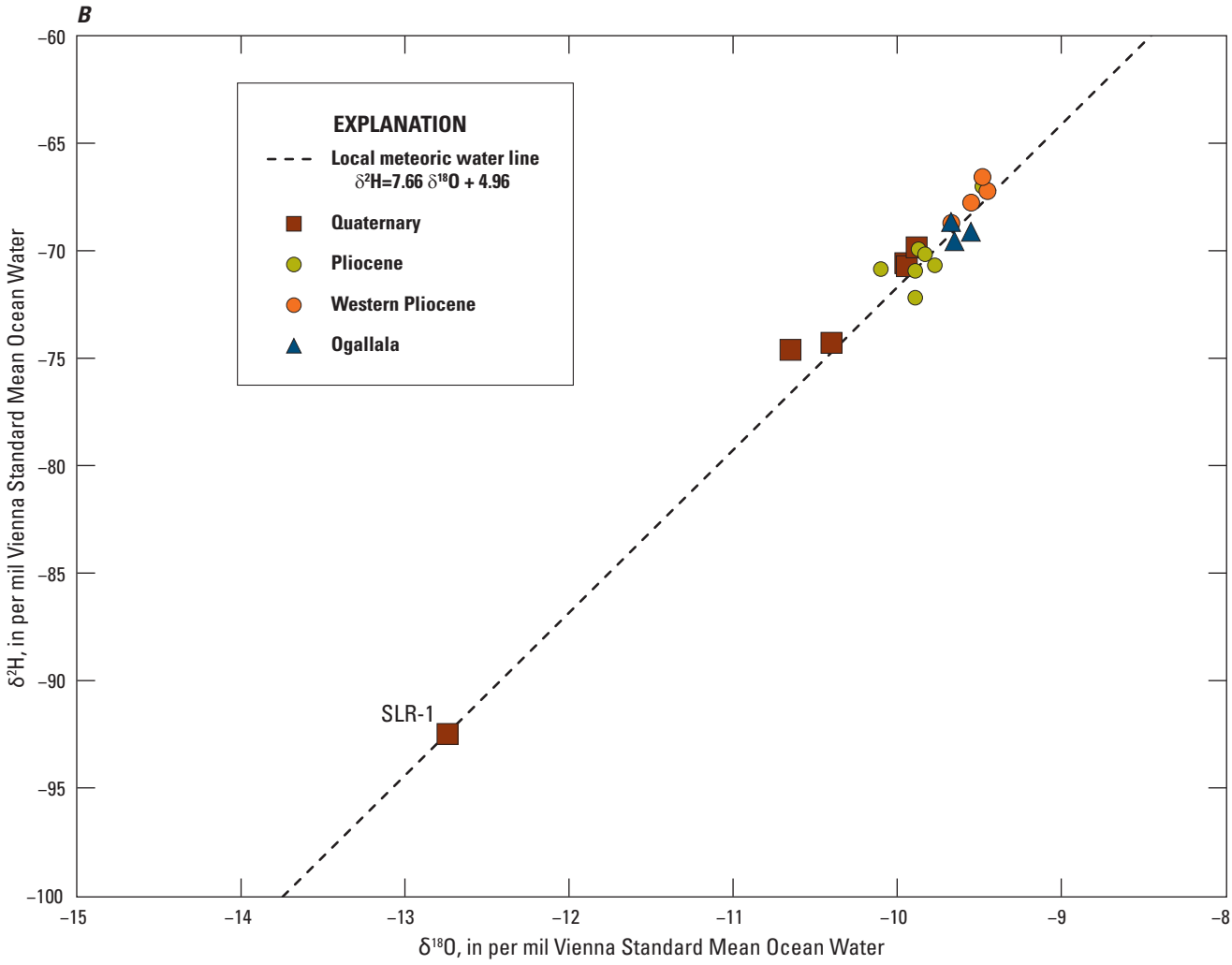

Figure 7.—Continued

Table 8. Dissolved gas concentrations and recharge solubility equilibrium model results for groundwater sampled in the South Loup River Basin, Nebraska, 2019.

[USGS, U.S. Geological Survey; ID, identification; CH_4, methane; mg/L, milligram per liter; CO_2, carbon dioxide; N_2, dissolved nitrogen gas; O_2, dissolved oxygen; Ar, argon; °C, degree Celsius; NA, not applicable]

USGS station	Station ID[1]	Field name	CH_4 (mg/L)	CO_2 (mg/L)	N_2 (mg/L)	O_2 (mg/L)	Ar (mg/L)	Best estimate of excess N_2 (mg/L)	Recharge temperature (°C)	Excess air (mg/L)
412340100074901	17N 24W31C1 Sloup Spr 35	SPR 35	0	28.69	17.6	0.26	0.6296	NA	11.6	1.8
412407100080501	16N 24W31B1 Sloup Spr 24	SPR 24	0	8.44	17.7	0.27	0.618	NA	13.4	2.5
412406100080401	16N 24W31B2 Sloup Spr 25	SPR 25	0	16.26	18.35	0.25	0.642	NA	11.7	2.6
412145100055601	16N 24W17B1 Sloup Spr 27	SPR 27	0	4.86	17.58	0.27	0.620	NA	12.8	2.1
412146100055701	16N 24W17B3 Sloup Spr 30	SPR 30	0	4.07	16.84	0.28	0.606	NA	13.1	1.5
412148100061501	16N 24W18A1 Sloup Spr 29	SPR 29	0	6.62	17.56	0.27	0.623	NA	12.4	2
412149100060401	16N 24W17B2 Sloup Spr 28	SPR 28	0	4.17	16.96	0.25	0.609	NA	12.9	1.6
412213100051001	16N 24W 8D1 Sloup Spr 31	SPR 31	0	6.04	18.87	0.26	0.641	NA	13	3.5
412429100080302	17N 24W30CCDD2	Conner shallow	0.0018	13.05	23.11	0.23	0.635	4.5	13.2	3.4
412429100080303	17N 24W30CCDD3	Conner deep	0	2.34	22.3	0.27	0.699	NA	12.9	7
412628100150701	17N 25W 18CB (SLR-2)	SLR-2	0	10.40	19.52	0.25	0.648	0.5	12.3	3.5
412717100150701	17N 25W 7CC (SLR-3)	SLR-3	0	6.22	18.86	0.24	0.644	NA	12.4	3.4
412611100384402	17N 29W22ABBB2	Mann deep	0	5.51	16.70	0.24	0.603	NA	12.5	1.4
412611100384401	17N 29W22ABBB1	Mann shallow	0	6.21	17.24	0.24	0.608	NA	13.1	2.1
412244100013502	16N 24W 2DDDD2	East deep	0	3.48	21.10	0.25	0.671	1	11.9	4.4
412244100013501	16N 24W 2DDDD1	East shallow	0.0014	8.17	23.48	0.23	0.6204	5.5	13.7	2.9
411126099422501	14N 21W 15AB Pressey	Pressey deep	0	7.89	22.66	0.26	0.711	NA	12.6	7.1
411126099422502	14N 21W 15AB 02 Pressey 2	Pressey shallow	0	9.40	20.72	0.31	0.680	NA	12.4	5.1
412547100125601	17N 25W 20DA (SLR-4)	SLR-4	0	6.44	18.49	0.24	0.629	NA	13.7	3.4
412620100132101	17N 25W 17DC (SLR-1)	SLR-1	0	14.15	18.73	0.25	0.642	NA	12.4	3.3

[1]Legal description: ABCD, codes for the quarter section, as A, B, C, and D, respectively from largest to smallest quarter, where A is northeast, B is northwest, C is southwest, and D is southeast quarter of the next larger unit, and (optional) field name for the well

Measured SF_6 concentrations corrected for recharge EA and temperature are higher than expected relative to observed ^3H (table 7). The ^3H concentrations below the detection limit in samples from Pressey, East deep, SPR 28, Connor deep, Mann shallow, and Mann deep are clear indications of pre-1950 recharge. However, the concentration of SF_6 for these samples ranged from 0.55 to 1.47 parts per trillion by volume. The atmospheric input histories for SF_6 for this range in concentration would suggest recharge from 1977 and 1985, respectively (U.S. Geological Survey, 2021a). Given the disparate concentrations of ^3H and SF_6 and unlikelihood of ^3H contamination, it is likely that SF_6 is anomalously high. The source of elevated SF_6 concentrations is uncertain and prevents the use of SF_6 for determination of groundwater ages. Nonatmospheric SF_6 has been previously reported in groundwater of the High Plains aquifer (Solder, 2019; Tesoriero and others, 2019) and concentrations from these studies are reported here for future research purposes but will not be discussed further.

Lumped Parameter Models and Groundwater Age Metrics

Groundwater age metrics estimated by calibration of LPMs to concentrations of ^3H and ^{14}C are reported in table 7, and the complete model results are available in Solder (2021). Final LPM solutions were selected based on hydrologic reasonability for a given sample and tracer concentrations, based on reasonability in the context of the other samples analyzed, and by minimizing the tracer misfit or chi-squared (χ^2) with values less than 1 considered a very good fit and values less than 3.8 (95-percent confidence, one sided with one degree of freedom) considered to be acceptable. Groundwater ages fall into two distinct groups of mean ages less than 80 years (n=7) and greater than 800 years (n=13), which is suggestive of at least two primary sources of groundwater to the sampled wells and springs. Six samples were best fit by a binary mixture of two age distributions, further supporting the idea of multiple distinct sources of groundwater. Relevant to the understanding of flow paths contributing to the sample sites, fitted dispersion parameters for a single DM were low (less than about 0.006; Solder, 2021) and indicated a limited amount of mixing along and between flow paths. The exception is East shallow, for which the DM indicated a very high amount of mixing (dispersion parameter greater than about 3) and the EMM was selected for the final age estimate, although there is greater relative uncertainty (χ^2) in the LPM solutions for this sample. Calculated metrics of SI and fraction modern from the age distributions indicate which sites are more likely to respond during short time periods (less than about 20 years) to changes in groundwater chemistry and recharge. Samples with high values of the SI (greater than 0.1) and fraction modern (greater than 0.2; table 7) are more likely to respond to system changes during a shorter period of time.

Estimated mean groundwater ages, fraction modern, and SI of sampled wells completed in Quaternary deposits are variable (table 7). Mean groundwater ages ranged from 27 to 2,100 years and varied based on depth of the well screen below the water table and the proximity of the well to the South Loup River. Nearby wells SLR-1 and SLR-2 had mean ages of 70 and 75 years, respectively, whereas wells SLR-3 and SLR-4 had mean ages of 2,100 and 1,900 years, respectively. The difference in mean ages can be attributed to the relative topographic position of each well screen and proximity to the South Loup River where multiple flow paths converge. Wells SLR-1 and SLR-2, which have younger mean ages, are located near the South Loup River but out of the modern flood plain. Groundwater in these locations is likely recent recharge moving downgradient towards the South Loup River. Wells SLR-3 and SLR-4 are located within the modern flood plain of the South Loup River near the active stream channel. The groundwater sampled at these locations is likely a mixture of multiple waters with various ages. The fraction modern for both of the latter wells approaches zero, indicating that a negligible amount of groundwater is recent recharge, and SI was lowest of all sampled wells screened in the Quaternary-age deposits. In these two locations, it is possible that older waters may be upwelling from the deeper Ogallala Formation; however, there is a lack of water-level data to confirm that interpretation at the specific location.

Sample groups Western Pliocene and Pliocene had very different groundwater age distributions (fig. 6, table 7). The Western Pliocene sample group (n=4) had mean ages that were much younger than the seven wells and springs from the Pliocene group. Groundwater discharging from SPR 25 and SPR 35 had the youngest mean ages (18 and 20 years, respectively), the highest modern fraction (1 for both samples), and the highest SI (0.257 and 0.253, respectively) of all samples in this study (table 7). Seven groundwater samples collected from springs or wells characterized as Pliocene had much older mean groundwater ages that ranged from 1,200 to 6,700 years (table 7). With the exception of two samples (SPR 28, Mann deep), the samples were described as binary mixtures of modern and older waters, and the modern fraction for these samples ranged from 0.04 to 0.23 (table 7). The SI for the seven Pliocene samples was less than the Western Pliocene samples (table 7) with high statistical significance (Wilcoxon rank-sum test, p=0.006), indicating that groundwater in these areas is less sensitive to short-term variations in precipitation. A previous study by Hobza and Schepers (2018) identified and described a major groundwater discharge zone along a reach downstream from the Arnold streamgage. Western Pliocene springs with higher fraction of modern groundwater are located along the upstream end of the mapped discharge zone. Regional groundwater contour maps (Summerside and others, 2001) show that springs from the Western Pliocene sample group are downgradient from groundwater-irrigated row crops (fig. 6) consistent with observed high nitrate concentrations in some of the springs (table 6) likely associated with irrigation

return flow. Farther downstream, but still within the mapped major groundwater discharge zone, groundwater flows from southwest to northeast, indicating that recharge for the five downstream Pliocene springs is likely partly sourced from an isolated area covered with eolian sand dunes southwest of the spring locations (fig. 6). This interpretation is based on low concentrations of nitrate, chloride, and TDS, which indicate the recharge area is likely covered by rangeland and not row crops.

The mean groundwater ages for samples collected from wells screened in the Ogallala Formation were the oldest for this study and ranged from 8,700 to 23,000 years (table 7). Each of these samples had fraction modern values of zero and relatively low SI values (table 7). Two of the wells sampled (Pressey deep and Conner deep) are located very close to the South Loup River (fig. 1). Each of these wells is paired with another monitoring well screened in a shallower geologic unit (table 1). Measured water levels in these wells indicate an upward hydraulic gradient (U.S. Geological Survey, 2021b) consistent with previous studies (Hobza and Schepers, 2018), where groundwater from the Ogallala discharges through the overlying Pliocene-age deposits to the stream (Hobza and Schepers, 2018).

Distinct grouping of groundwater ages between less than 80 years and greater than 800 years could be a result of the age tracer gap (that is, there was not a tracer sampled that readily identifies groundwater ages between the two age groups). The tracer gap likely increases uncertainty of estimated ages greater than 100 years and less than about 2,000 years (n=6). Regardless of estimated age certainty of a small number of samples, the overall grouping of ages is still meaningful and indicates multiple water sources. In addition to the required BMM age distribution used to match tracer concentrations for six samples (table 7), mean concentrations of chloride and SO_4 are statistically different (Welch's t-test; Helsel and others, 2020) between the two groups of groundwater ages (p-values equal 0.01 and 0.02, respectively), and mean concentrations of chloride, SO_4, and NO_3 are statistically different between samples with greater than or less than 20 percent modern water (significance values equal 0.03, 0.05, and 0.09, respectively), supporting the distinction of groundwater source based on age metrics.

Overall, groundwater chemistry appears to be largely controlled by flow path geochemical conditions and recharge chemistry rather than contact time with aquifer sediments (that is, groundwater age). Concentrations of TDS are highest in the youngest groundwaters where ^{3}H is greater than about 3 TUs (tables 6 and 7), and TDS are statistically correlated with ^{3}H and ^{14}C (Spearman's ρ of 0.41 and 0.54, respectively, at the 90-percent significance level). The positive correlation noted between TDS and ^{3}H and ^{14}C from samples collected indicates an anthropogenic influence on groundwater quality. Concentrations of nitrate, SO_4, and chloride are statistically related to ^{3}H (Spearman's ρ of 0.53, 0.56, and 0.73, respectively, at the 99-percent significance level), which is suggestive of an increasing influence of human activity on groundwater quality through time. A notable exception to the positive correlation between major ion and tracer concentrations is increasing silica with decreasing ^{14}C (given in pmC; tables 6 and 7). The inverse relation of silica to ^{14}C is well explained by a linear model (Pearson's r of −0.72 at 99-percent significance level) and indicates continued gradual dissolution of low-solubility silica bearing minerals, such as quartz. The gradual increase of dissolved silica along flow paths indicates that typical water-rock chemical reactions continue over the length of the flow paths.

Relations between tracer and major ion concentrations should be interpreted with some caution because it is well understood that there is not necessarily a direct mapping of ^{3}H and ^{14}C tracer concentration to groundwater age. The relative age of a given sample based on ^{3}H or ^{14}C alone is potentially uncertain because a given concentration can be reasonably mapped to multiple ages as a result of elevated atmospheric tracer concentrations from aboveground nuclear testing. The comparison of tracer and major ion concentrations across the dataset in this study is supported by the monotonic relation between ^{3}H and ^{14}C (Spearman's ρ of 0.7 at the 99-percent significance level), which would be affected by bomb-pulse inputs and the large difference in decay rates between the two tracers, comparison of measured to predicted tracer concentrations from LPMs of single mixtures, and observed relations between the tracers and more conservative major ions (for example, silica and ^{14}C). Although the reported relations between tracer and major ion concentrations are likely not useful for prediction of concentrations for a given sample, the relations do provide valuable information on geochemical processes and sources at the aquifer scale.

Discharge and Continuous Monitoring of Spring Complexes and the South Loup River

This section of the report describes the results and interpretations of data collected from three monitoring locations that include two spring monitoring sites that represent spring complexes discharging from Pliocene and Quaternary-age units (Finchville and Mills Valley, respectively) and a stream monitoring site below the confluence of the North Fork South Loup River and the South Loup River (Hoagland; fig. 3). Descriptions and interpretations of discharge, gage height, specific conductance, and water temperature data are provided in this report section. The purpose of the analysis is to describe the hydrologic response of spring complexes discharging from Pliocene and Quaternary-age units. Observed precipitation during the period of study was used as a proxy for short-term climatic variation. The characteristic responses of the three monitoring sites to precipitation events, as well as additional context from the groundwater age and water-quality characteristics, were used to understand potential response of reach-scale streamflow sources to climate variations as described in the "Reach-Scale Streamflow Comparisons" section of this report.

During the data collection period, the climatic conditions can be broadly described as wetter than normal. From May 1 to October 31, 2019, approximately 32.6 in. of precipitation fell near Broken Bow, Nebr., and 35.1 in. near Stapleton, Nebr. (fig. 8), exceeding the 30-year (1981–2010) normals totaled of 23.3 in. and 23.0 in., respectively, for those locations (National Centers for Environmental Information, 2021). Although there was no relatively dry period during data collection, analysis of specific storm events provides useful information on the temporal response and relative contributions of quickflow, such as overland flow and shallow subsurface flow, and deeper groundwater discharge to the stream. A precipitation event from July 18 to July 23, 2019, that resulted in about 0.4 in. of precipitation near Stapleton (National Centers for Environmental Information, 2021) is presented in greater detail to illustrate the difference between monitoring sites. Other larger precipitation events occurred during the study period, but data gaps and potential interference in the continuous gage height records at the Mills Valley monitoring site complicated interpretation of larger events. Data records for the July 18–23 event are of good quality and represent a typical response of the monitoring sites to precipitation events.

Finchville Monitoring Site

The Finchville monitoring site is immediately below the convergence of flow from focused groundwater discharge points within an exposed sheet of Pliocene-age sand and gravel, including SPR 27 and SPR 30 (table 4; fig. 3). Seven discharge measurements were collected at the Finchville monitoring site with a handheld acoustic Doppler velocimeter and ranged from 0.84 to 1.12 cubic feet per second (ft^3/s; table 5). All discharge measurements, except one were rated as poor because the narrow channel only allowed for the collection of eight or fewer stations for a given discharge measurement. The poor measurement rating indicates that the difference between measured and true discharge may exceed 8 percent. The gage height record varied relatively little during the monitoring period (May 2019 to October 2019; fig. 9*A*) and measured specific conductance ranged between 75 and 220 microsiemens per centimeter (µS/cm) during the deployment period (fig. 9*B*). The gage height record shows several sharp upward spikes (typically 0.1–0.2 ft) coincident with sharp downward spikes in specific conductance (about 30–125 µS/cm) during periods of intense precipitation, after which the spring appears to immediately return to approximate baseline conditions after rainfall ceased. Nearly all rapid increases in gage height correspond with a decrease in specific conductance. Pronounced response in gage height and specific conductance to precipitation events is likely explained by capture of overland runoff from an exposed sheet of sand and gravel at the monitoring site. Overland runoff resulted in increased gage height and decreased specific conductance by dilution with low conductance rainwater. The measured data indicate a rapid return to the pre-storm event gage height and specific conductance of 200–220 µS/cm. Water temperature indicates diurnal variations and followed seasonal air temperature patterns (fig. 9*B*), indicating some influence of surface conditions and that observed temperature is not solely representative of groundwater temperature.

Mills Valley Monitoring Site

The Mills Valley monitoring site is located upstream from the Arnold streamgage where groundwater discharges from silty Quaternary-age deposits (fig. 3; table 4). The monitoring site is located within a well-defined topographic draw that captures surface runoff during precipitation events. The seven discharge measurements recorded ranged from 0.01 to 0.07 ft^3/s (table 5, fig. 10*A*). Two measurements were collected with a handheld acoustic Doppler velocimeter, and five measurements were collected with a 3-in. Parshall flume (Turnipseed and Sauer, 2010; table 5). The measurements collected with the handheld acoustic Doppler velocimeter were rated poor to fair, and the measurements collected with the 3-in. Parshall flume were rated as fair to excellent (table 5). The discharge measurement collected on July 11 was at the end of a 10-day period of greater than 3 in. of precipitation recorded at nearby weather stations (National Centers for Environmental Information, 2021). Gage height ranged from 1.8 to 6.05 ft (fig. 10*A*) and specific conductance from 64 to about 560 µS/cm (fig. 10*B*). Water temperature shows diurnal variations and followed seasonal air temperature changes (fig. 10*B*), indicating the influence of surface conditions and that observed temperature is not representative of groundwater temperature.

During precipitation events, the increase in gage height and decrease in specific conductance occurred during a short period of time, which is suggestive of the capture of overland flow at the monitoring site. When changes to gage height were large, changes in specific conductance often persisted several days before returning to the base-flow range of 450–550 µS/cm (figs. 10*B* and 11*B*), which is consistent with discharge of shallow subsurface flow. The frequency and intensity of the largest precipitation events during the period of record made continuous data collection and interpretation difficult. Above average precipitation during the study period resulted in "backwater" conditions at the Mills Valley monitoring site. Elevated river stage resulted in gage height measurements that were likely not representative of upgradient discharge from the monitoring site and created the potential for discharge to bypass the measurement weir, such that discharge could not be reliably quantified from those periods. Observed gage height greater than 5.5 ft at the downstream Arnold streamgage was used to identify potentially affected gage-height data. Based on the discharge measurement collected on July 11, 2019 (table 5), the affected gage-height data from Mills Valley monitoring site likely still does represent an increase in discharge. At the end of a 10-day period of precipitation, during which greater than 3 in. fell (fig. 9*C*), the discharge measured at the Mills Valley monitoring site was the highest discharge measured (table 5).

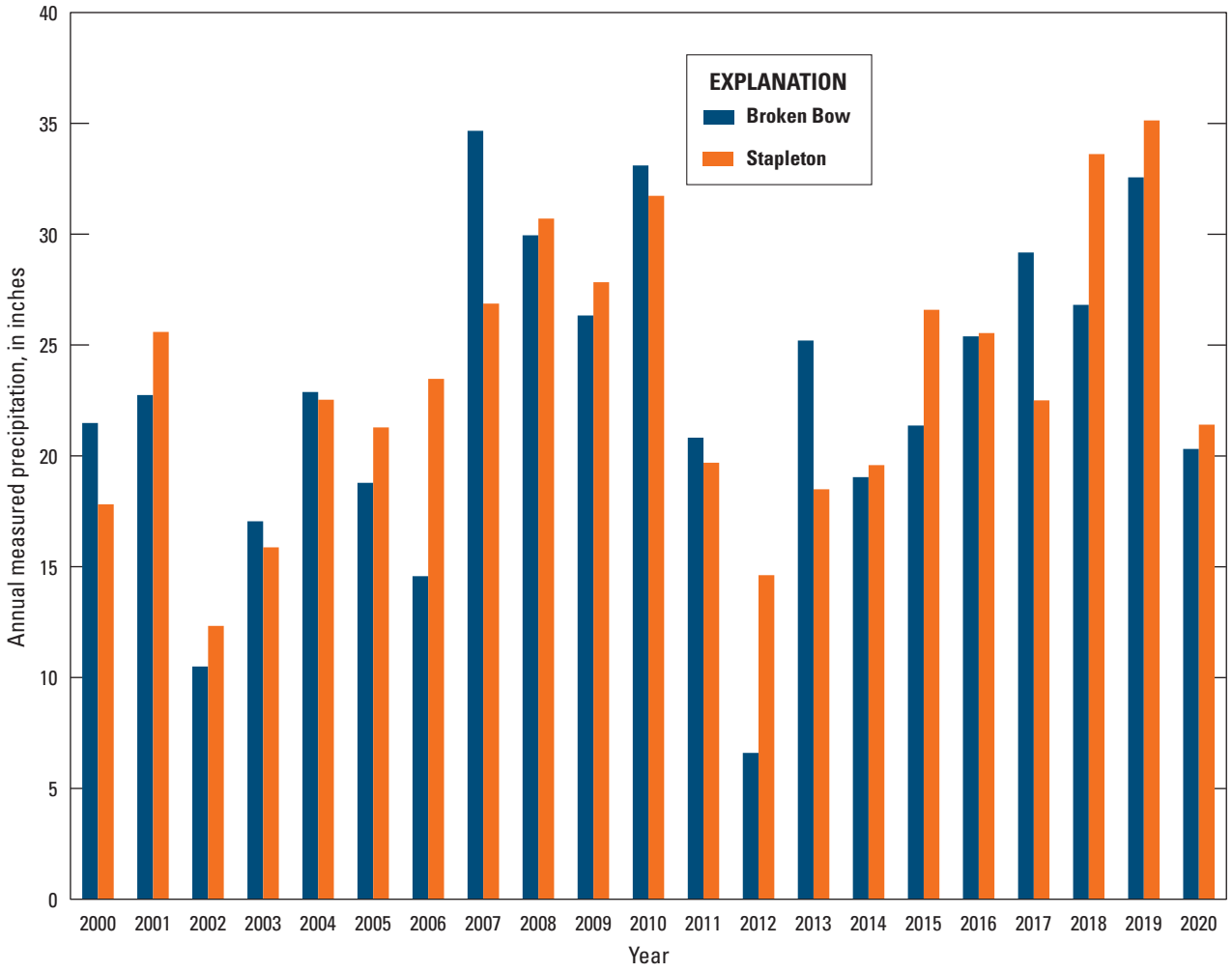

Figure 8. Annual measured precipitation at Broken Bow and Stapleton, Nebraska, 2000 to 2020.

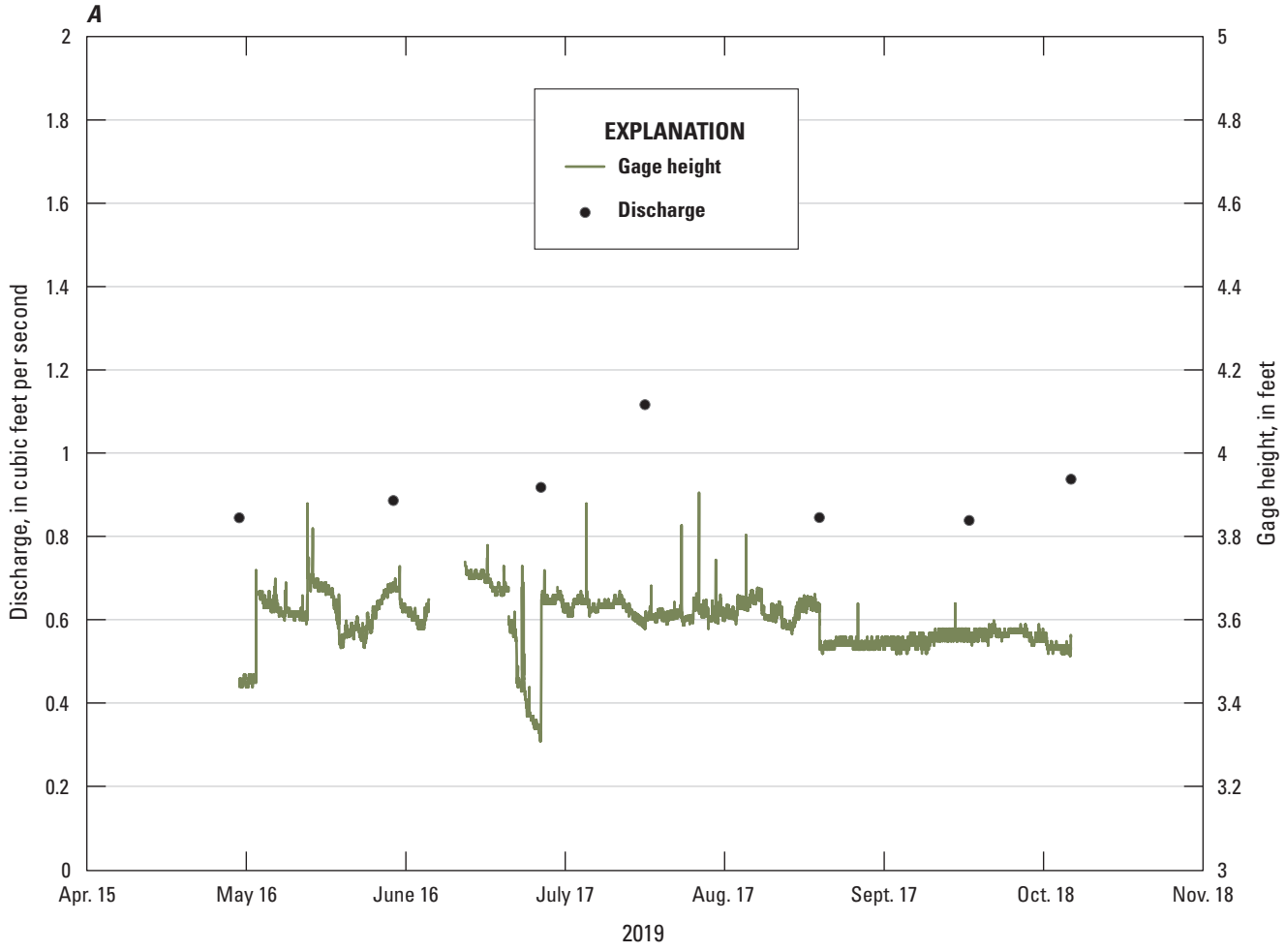

Figure 9. Measured data from South Loup River Tributary Spring 1.3 miles Southwest of Finchville, Nebraska, (Finchville monitoring site; U.S. Geological Survey station 412147100055301), May–October 2019. *A*, Gage height and discrete discharge. *B*, Specific conductance and water temperature. *C*, Daily precipitation measured at Broken Bow Airport.

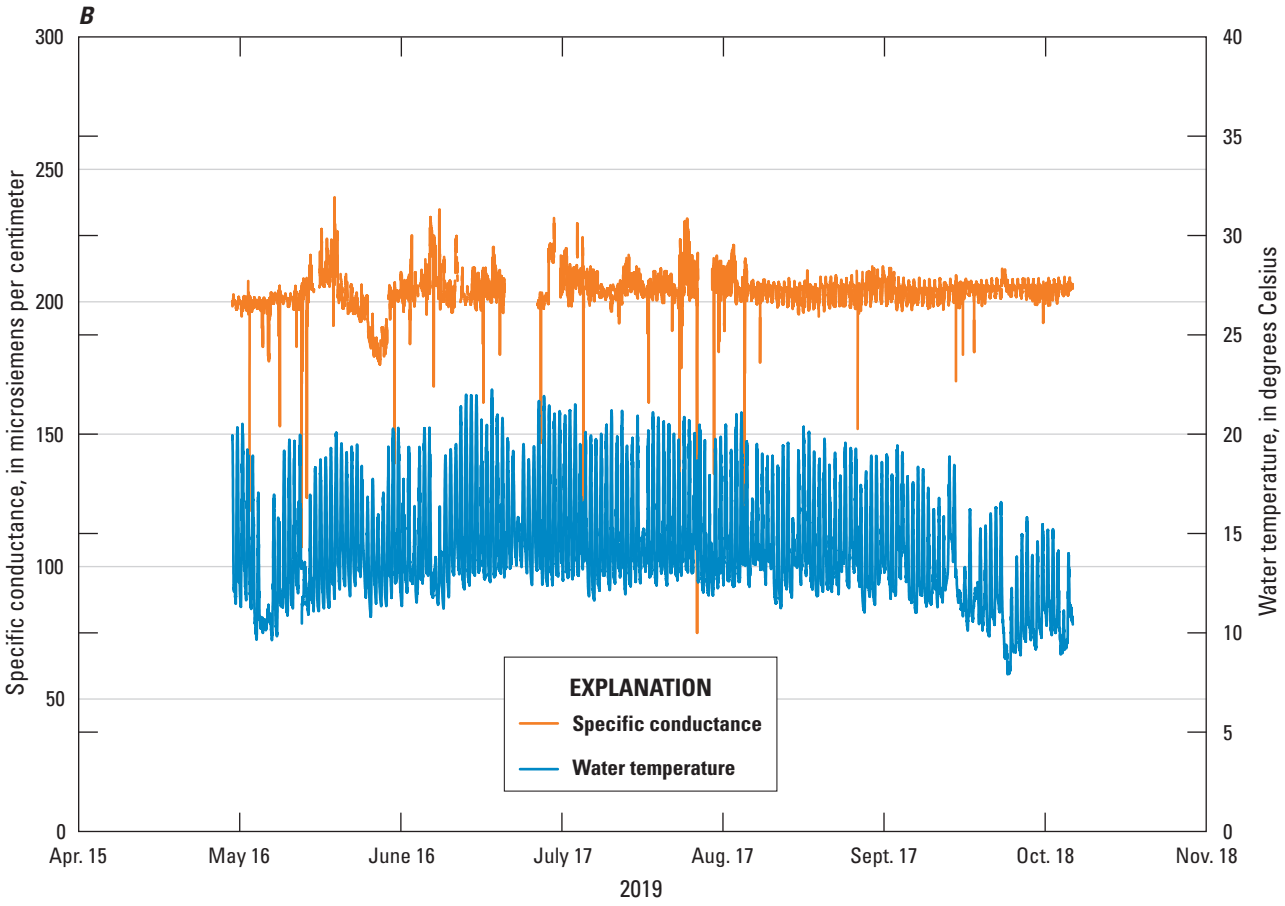

Figure 9.—Continued

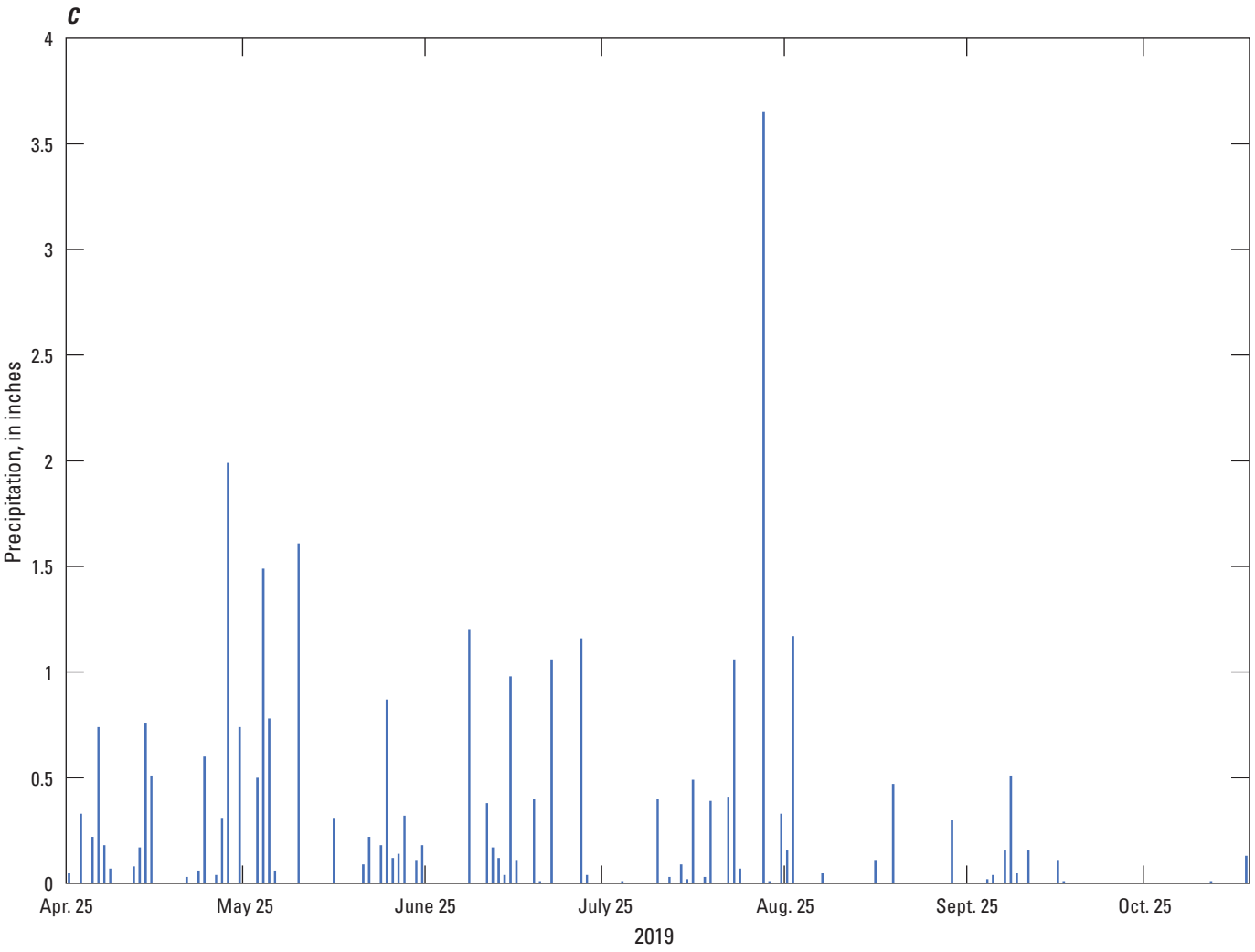

Figure 9.—Continued

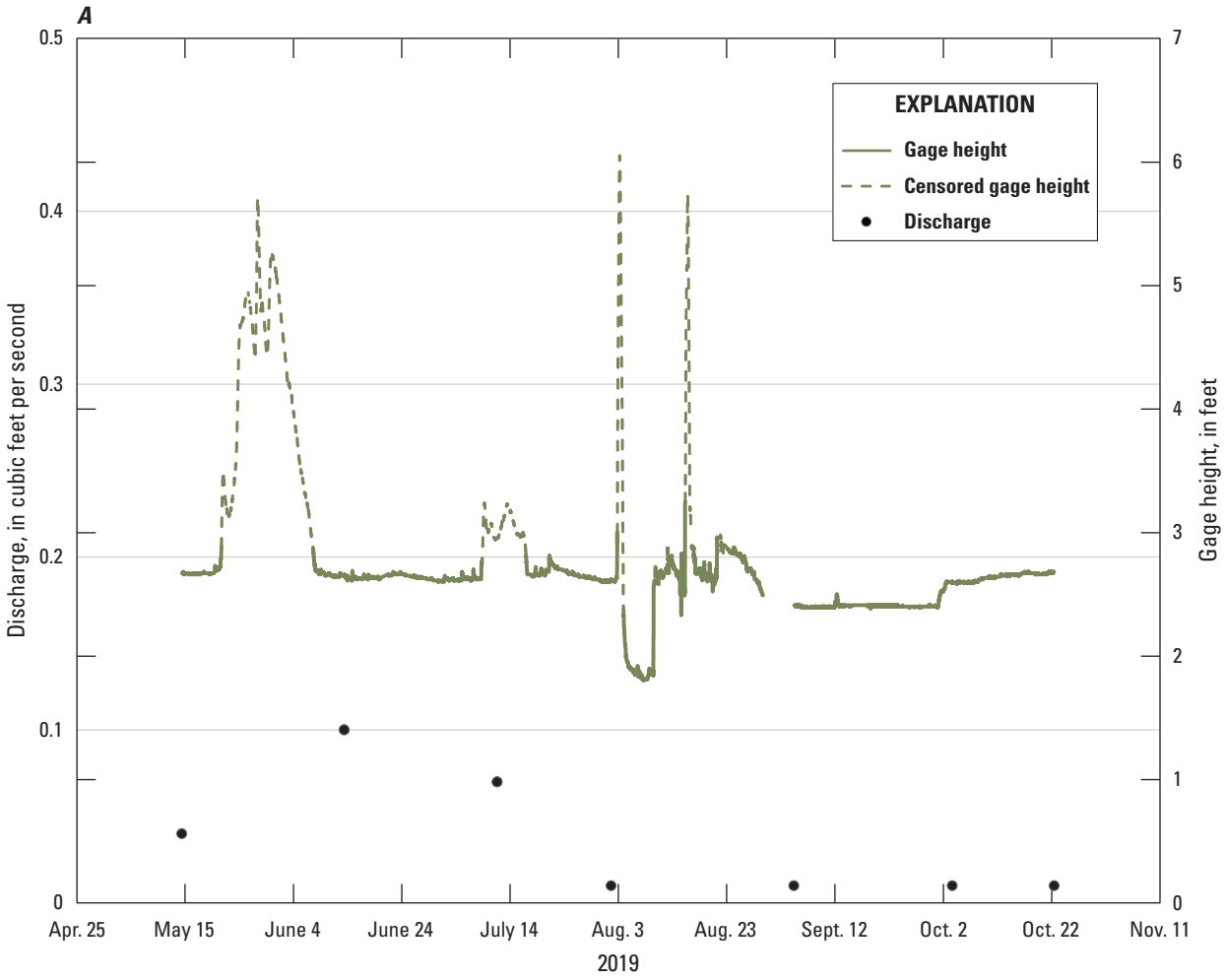

Figure 10. Measured data from South Loup River Spring 0.86 mile west of Arnold, Nebraska, (Mills Valley monitoring site; U.S. Geological Survey station 412542100125301), May–October 2019. *A*, Gage height and discrete discharge measurements. Censored gage height indicates when site was likely experiencing backwater conditions. *B*, Specific conductance and water temperature.

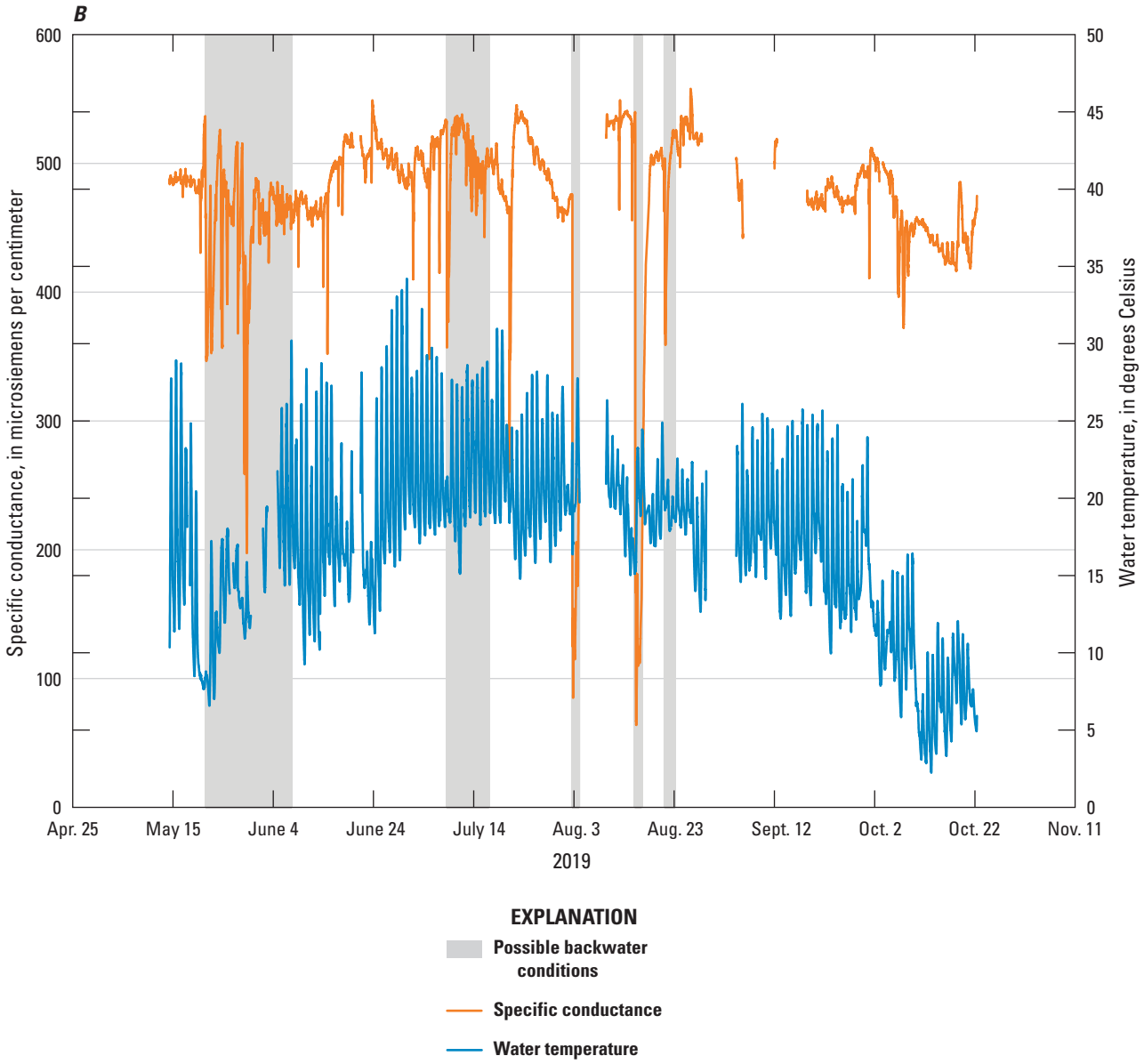

Figure 10.—Continued

The gage height at the Arnold streamgage was stable during the preceding 10-hour period, indicating discharge measured on that day was a reasonable estimate of actual discharge from the monitoring site and not draining of backwater conditions. Further, the monitoring site was positioned such that increases in discharge from the monitoring site could be reliably identified at the onset of the precipitation events before increased river stage resulted in backwater conditions. In regard to water-quality parameters, a comparison of specific conductance and water temperature records from the Mills Valley monitoring site to nearby Hoagland monitoring site during backwater events indicated the continuous water-quality parameters remained a reliable representation of spring complex discharge; that is, elevated river stage altered base levels such that gage height data from the Mills Valley monitoring site was affected, but there was no evidence of mixing of stream water with the spring discharge at the monitoring location.

Comparison of Finchville and Mills Valley

Comparisons of discharge measurements and gage height records from the Finchville and Mills Valley monitoring sites indicate that each monitoring site responds differently to precipitation events. The gage height at the Finchville monitoring site was slower to respond to precipitation events and returned to base-flow (pre-storm event) levels shortly after precipitation ceased, whereas the Mills Valley monitoring site responded more immediately and changes in gage height persisted much longer (figs. 9*A* and 10*A*). The Finchville monitoring site showed a much smaller relative variation in measured discharge compared to the Mills Valley monitoring site during the period of record (May 2019 to October 2019; table 5). Specific conductance records from the two sites show a similar behavior as that of gage height: a delayed response and rapid recovery with overall less variation at the Finchville monitoring site, and rapid response and prolonged recovery with overall greater variation at the Mills Valley monitoring site (figs. 9*B* and 10*B*).

An example of the difference in gage height and specific conductance in response to precipitation events at the two monitoring sites is shown in figure 11. During the period from July 18 to July 23, a total of 0.35 in. of precipitation fell at the Stapleton weather station (National Centers for Environmental Information, 2021). Although larger precipitation events occurred during the period of record, backwater conditions at the Mills Valley monitoring site prevented a direct interpretation of the relative responses between the two monitoring sites for larger precipitation events. Gage height at the Finchville monitoring site was relatively invariant from May to July 21 (fig. 9*A*), whereas gage height at the Mills Valley monitoring site responds to smaller precipitation events before July 21 (fig. 10*A*). The spike in gage height at the Finchville monitoring site lasted approximately 1 hour, whereas the gage height at the Mills Valley monitoring site remained elevated for about 30 hours before returning to base flow (fig. 11*A*). A similar pattern is observed in the specific conductance record (fig. 11*B*), with the Finchville monitoring site showing rapid recovery and the Mills Valley monitoring site showing a prolonged recovery. The rapid response and recovery of the Finchville monitoring site to precipitation events shows overland flow is captured at the monitoring site but overall, the effect is relatively small and short lived. The stability at the Finchville monitoring site indicates that groundwater discharge from Pliocene-age sand and gravel deposits changes little in response to recent precipitation and likely short-term climatic changes. This interpretation is supported by mean groundwater ages of 2,400 and 2,700 years for Pliocene sites SPR 27 and SPR 30, respectively, indicating a larger storage volume that buffers discharge from short-term variations in recharge (table 7). At the Mills Valley monitoring site, the relation between gage height and specific conductance response varied between precipitation events. Gage height increased in response to larger precipitation events, such as July 21, and resulted in decreased specific conductance, consistent with overland flow. Conversely, gage height increased in response to relatively smaller precipitation events, such as those on July 18–19, and resulted in increased specific conductance (fig. 11*B*), which is suggestive of shallow groundwater flow path activation that mobilizes soil salinity. In both cases of response to precipitation, the prolonged recovery of gage height and specific conductance was consistent with capture of a component of shallow subsurface groundwater that is sensitive to short-term precipitation variability. The Quaternary-age deposits attenuated the hydrologic response to precipitation events, manifesting as a prolonged period of increased discharge as the system drained the recent recharge. Capture of shallow groundwater sensitive to short-term precipitation changes is consistent with younger ages observed in Quaternary-age deposits (table 7). Furthermore, during low-flow conditions the range in specific conductance measured at the Mills Valley monitoring site was two times greater than the range at the Finchville monitoring site (figs. 9*B* and 10*B*). Sampling results from this study indicated that groundwater with higher specific conductance generally had higher SI values and fraction modern, and younger estimated mean ages (tables 6 and 7), which further supports the relatively greater vulnerability of groundwater in the Quaternary-age deposits groundwater to short-term changes in precipitation patterns.

The measured water temperature for Mills Valley and Finchville monitoring sites displayed a diurnal temperature signal in response to daytime warming and nighttime cooling (figs. 9*B* and 10*B*). At the Finchville monitoring site, the daily minimum temperature recorded through the summer months was similar to the ambient groundwater temperature measured during sampling, indicating that measured water temperatures are not dominated solely by air temperature (fig. 9*B*; table 6). During the summer months at the Mills Valley monitoring site, the minimum measured water temperatures were much higher than the ambient groundwater temperature recorded in nearby wells, indicating influence of runoff and exposure to warmer ambient air temperatures prior to measurement (fig. 10*B*).

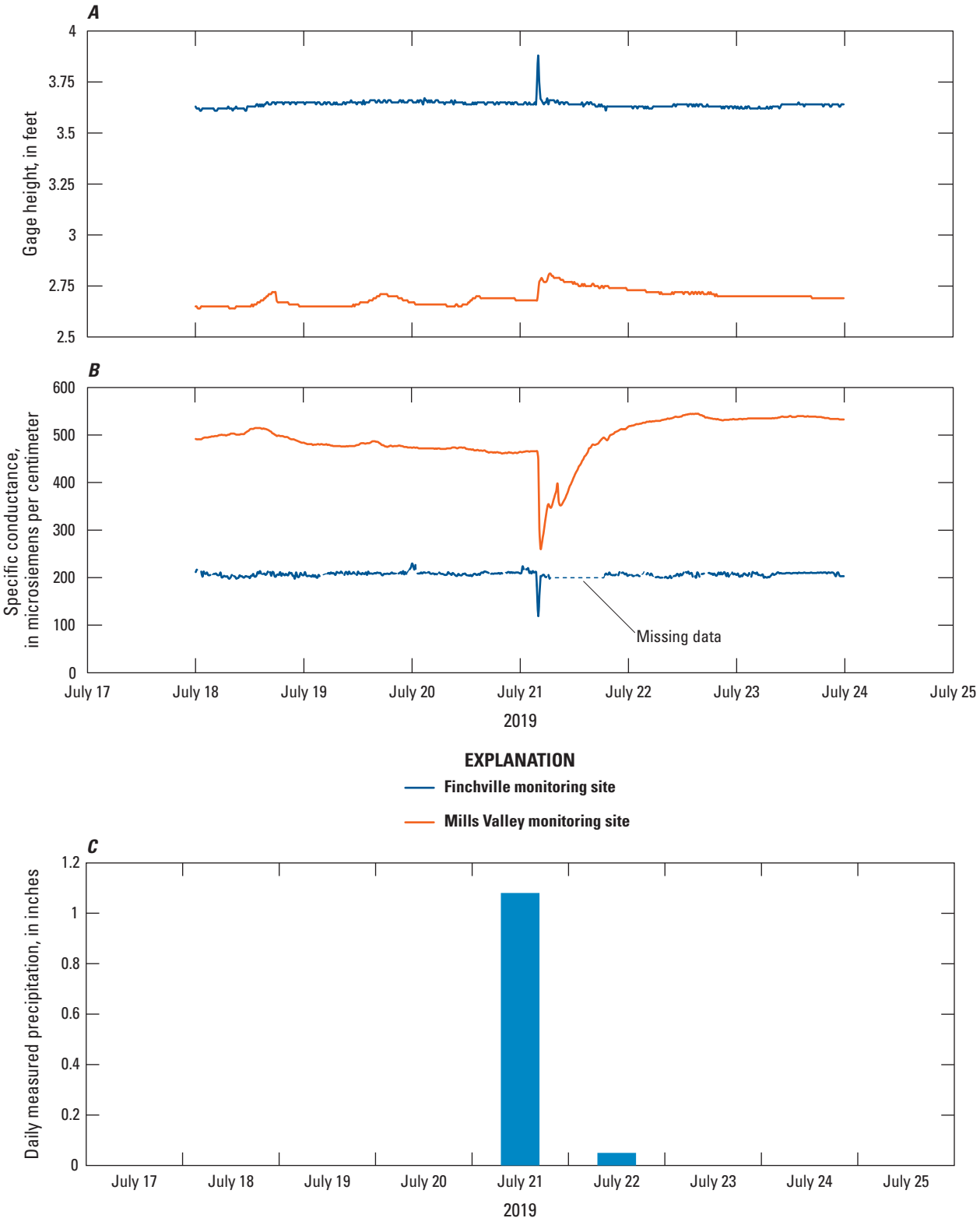

Figure 11. Gage height, specific conductance data showing hydrologic response to July storm events at South Loup River Tributary Spring 1.3 miles Southwest of Finchville, Nebraska, (U.S. Geological Survey station 412147100055301) and South Loup River Spring 0.86 mile west of Arnold, Nebraska, (U.S. Geological Survey station 412542100125301). *A*, Gage height. *B*, Specific conductance. *C,* Daily precipitation data measured at Stapleton, Nebr. (shown in fig. 1).

Hoagland Monitoring Site

The Hoagland monitoring site is located on the main stem of the South Loup, near the headwaters, approximately 750 ft downstream from the confluence with the North Fork South Loup River (figs. 3 and 4). The seven discharge measurements made from May 2019 through October 2019 ranged between 20.5 and 57.1 ft^3/s (table 5, fig. 12*A*). Discharge measurements were generally consistent, with the exception of elevated discharge on July 11 (57.1 ft^3/s; table 5), measured at the end of a 10-day period of greater than 3 in. of precipitation recorded at nearby weather stations (National Centers for Environmental Information, 2021). Discharge was also measured on the South Loup above the confluence with the North Fork South Loup River (413053100221401) and calculated for the North Fork South Loup River (413055100221101) (table 5, fig. 12*A*). At the Hoagland monitoring site, gage height ranged from 2.42 to 5.58 ft and specific conductance ranged from 148 to 329 µS/cm (fig. 12*B*). Water temperature shows diurnal variations and a general trend upward then downward (fig. 12*C*) consistent with seasonal air temperature changes. A low temperature spike recorded in late May is associated with decrease in gage height and was likely a result of increased groundwater contributions with a cooler temperature. Cool temperatures in September and October did not correspond with decreased gage heights and are more likely a result of cooler air temperatures.

The gage height record at the Hoagland monitoring site is highly variable and indicates frequent increases in discharge in response to precipitation events (fig. 12*A*, *B*). The gage height recorded at the Hoagland monitoring site closely resembles the gage height record at the Arnold streamgage with the exception of two sharp increases in gage height at Arnold streamgage in response to two specific intense precipitation events (fig. 12*A*). These precipitation events are recorded as slower gage height increases at the Hoagland monitoring site indicating a slower response to overland runoff, as compared to the Arnold streamgage. Much of the drainage area within the headwaters of the South Loup River represented by the Hoagland monitoring site is nearly flat lying rangeland or grass-covered eolian sand dunes. The topography and high permeability soils likely reduce overland runoff to streams and maximize infiltration and recharge to the shallow groundwater system (Dugan and Zelt, 2000). However, the Hoagland monitoring site does capture overland runoff, as indicated by sharp decreases in specific conductance at the start of a gage height increase (fig. 12*B*). Overall, specific conductance at the Hoagland monitoring site tended to increase with an increase in discharge and gage height (fig. 12*A*, *B*), likely the result of activation of shallow subsurface flow that discharges to the river. Precipitation events and subsequent recharge elevated water tables, resulting in dissolution and mobilization of salts accumulated in the root zone (Steele and others, 2014). Similar capture of shallow subsurface flow and the resulting increase in specific conductance during relatively small precipitation events are observed at the Mills Valley monitoring site (fig. 11*B*). For many runoff events at the Hoagland monitoring site, there is a lag between gage height peaks and specific conductance peaks (fig. 12*B*), which supports the interpretation that rises in groundwater levels trigger increases in shallow groundwater discharge and measured specific conductance in the South Loup River. Prolonged recovery period of gage height and specific conductance (fig. 12*B*) similarly observed at the Mills Valley monitoring site (fig. 11*B*) is consistent with attenuation of the recharge signal in gage height and dropping water table signal and decreasing specific conductance. Recharge to the shallow groundwater system drains to the river during a period of weeks after the precipitation event.

In addition to the sharp short-lived decreases in specific conductance at the start of intense precipitation events, there were decreases in specific conductance near the peak of responses to larger precipitation events. This behavior was most clearly observed during the largest (late May 2019) and a relatively intermediate (late August 2019) response to precipitation events (fig. 12*B*). Decreases in specific conductance were associated with gage height increases, indicating overland flow, but the timing indicates these events were likely caused by a different mechanism of overland flow generation. Overland flow during early periods of the precipitation events was likely generated through infiltration excess, which occurs when precipitation rates exceed the soil infiltration capacity. Partially saturated soils have a lower hydraulic conductivity than fully saturated soil, and thus precipitation falling on relatively dry soil is less likely to infiltrate than precipitation on wet soil. Overland flow during later stages of the precipitation event, when gage height and thus discharge is at a maximum, is likely generated by saturation excess, which occurs when the soil column becomes fully saturated and any additional precipitation becomes runoff. The decreases in specific conductance at the peak gage height is likely caused by saturation excess.

Overall, the specific conductance and gage height data collected at the Hoagland monitoring site indicated capture of overland runoff and contributions of shallow groundwater to streamflow. The relatively similar but more subdued gage height at Hoagland as compared to the Arnold streamgage (fig. 12*A*) indicated that discharge at the Hoagland monitoring site was slightly less dependent on recent precipitation. However, the Hoagland record is more similar to the Mills Valley monitoring site (fig. 10) than the Finchville monitoring site (fig. 9), which suggests relatively young groundwater captured at Hoagland, similar to the Quaternary-age springs complex (table 7).

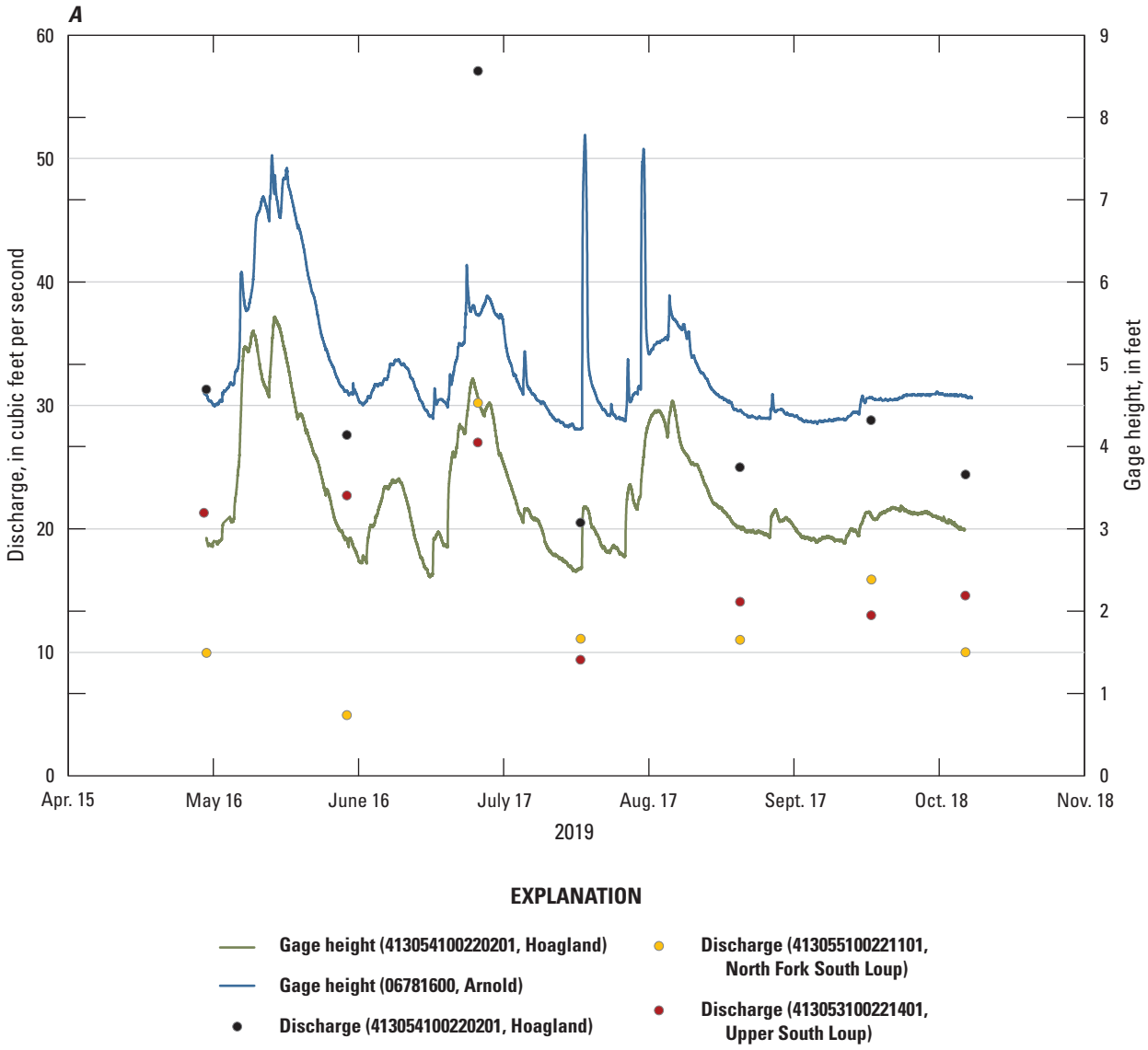

Figure 12. Measured data from South Loup River Spring below North Fork at Hoagland, Nebraska (Hoagland monitoring site; 41305410022201), May–October 2019. *A*, Gage height and discrete discharge measurements, including North Fork South Loup River at Hoagland, Nebr. (413055100221101), South Loup River above North Fork South Loup River at Hoagland, Nebr. (41305410022201), and South Loup River at Arnold, Nebr. (06781600). *B*, Specific conductance and gage height. *C*, Specific conductance and water temperature.

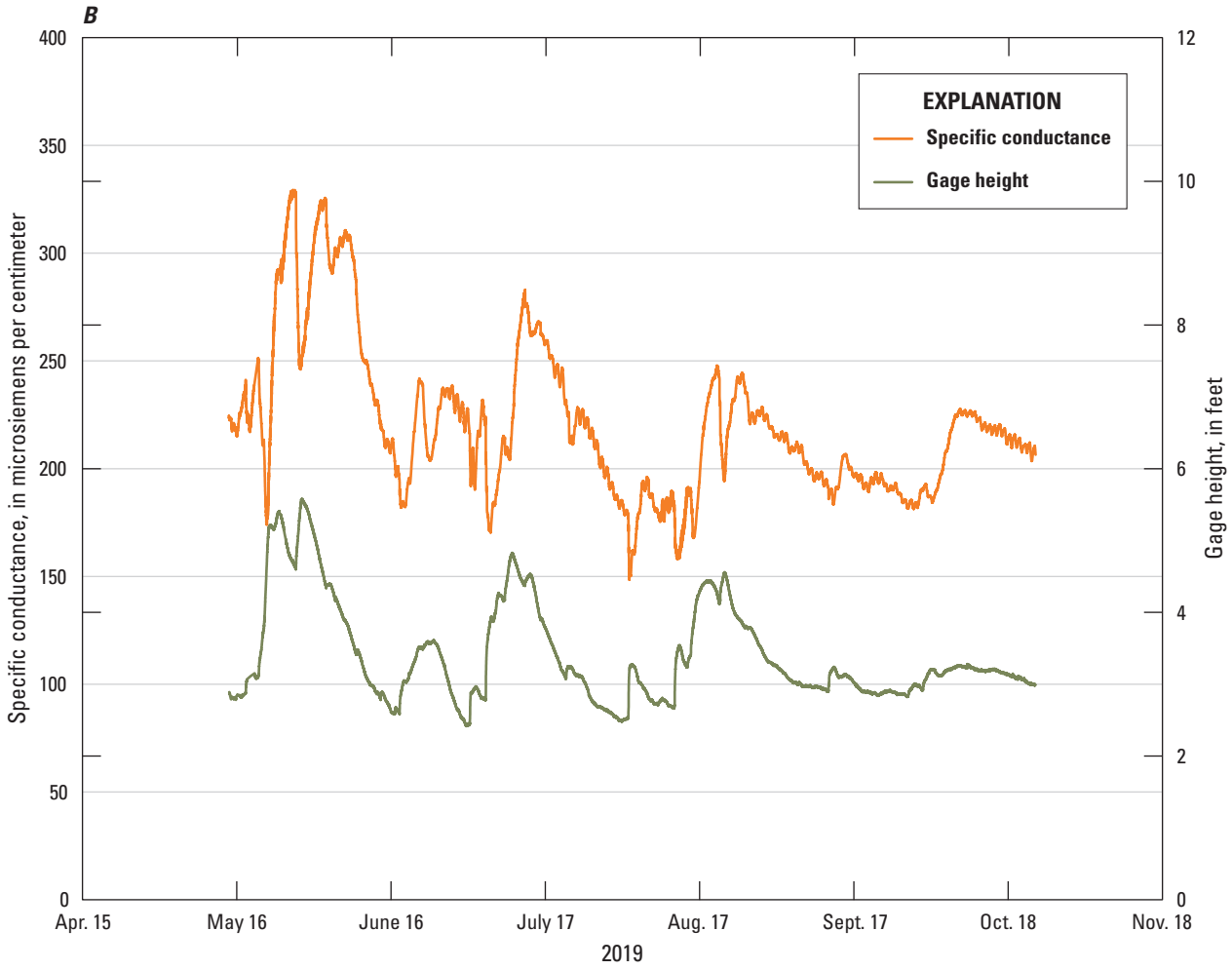

Figure 12.—Continued

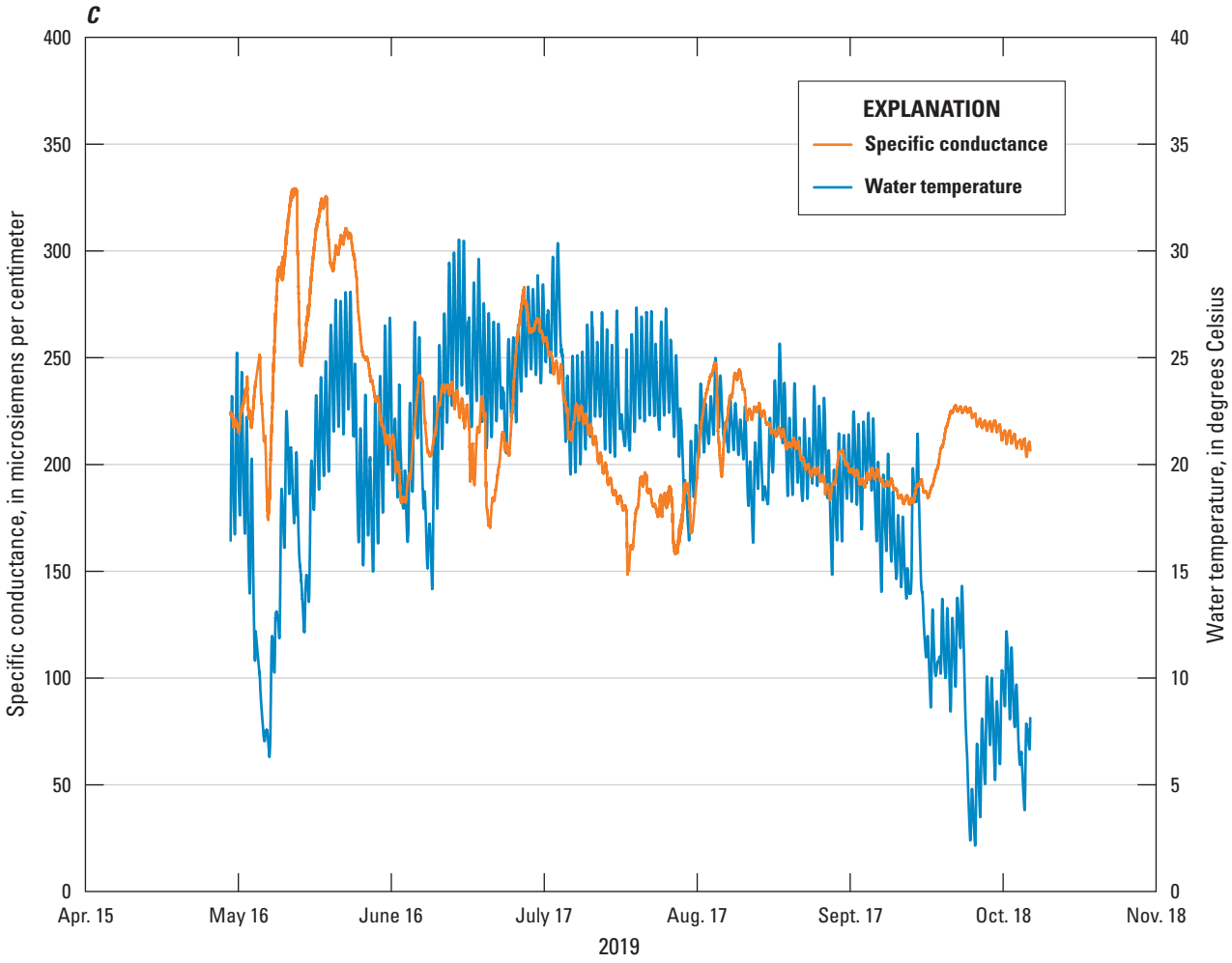

Figure 12.—Continued

Reach-Scale Streamflow Comparisons

Within the study area, historical discrete discharge measurements and streamflow records are limited. In this study, discrete discharge measurements collected on the Upper South Loup River and North Fork South Loup River near the Hoagland monitoring site in 2015 and 2019 are reported (figs. 4 and 12*A*; table 5). The Arnold streamgage and the South Loup River at Pressey streamgage sites were established in 2010 and 2017, respectively. Although discrete discharge measurements and streamflow records do not extend far enough back in time to adequately capture the full range of climatic variability in the study area, some meaningful comparisons can still be made.

Assuming that precipitation for a given year is reasonably distributed across the study area (that is, one drainage is not consistently receiving more precipitation than the other), comparison of the discharge records provides information on streamflow source of the different reaches and response to changing precipitation. To understand the relative change in streamflow at each site in response to relatively dry and wet years, thereby providing information about the relative resilience of streamflow to changing climate, streamflow records from 2015 (drier, but slightly above the long-term normal with 26.6 in. of annual precipitation) and 2019 (a wetter year with 33.4 in. of precipitation)—both measured near Stapleton (National Centers for Environmental Information, 2021)—are compared. For context, the average annual precipitation from 2000 to 2020 near Stapleton is 23.5 in. (fig. 8; National Centers for Environmental Information, 2021), meaning the differences reported here are likely an underestimate of the magnitude of streamflow response to precipitation conditions, specifically in historically dry years, but the results still provide information on the relative response of each drainage. To facilitate comparisons and understand the difference in streamflow source between sites, streamflow is normalized to drainage area, as determined from the National Hydrologic Database Plus surface water basins (Buto and Anderson, 2020), and reported on a discharge per area (cubic feet per second per square mile) basis. For daily streamflow data, the relative daily deviation from the period of record mean streamflow is reported to examine the relative stability of streamflow. A more stable streamflow during relatively wet and dry years, as well as in response to specific large precipitation events, is indicative of capture of groundwater flow paths from relatively larger storage volumes, which corresponds to less sensitivity of streamflow to short-term precipitation variability.

The discrete measured discharge of the Upper South Loup River and the North Fork South Loup River in 2015 was 3.26 and 7.14 ft^3/s, respectively (table 5). Drainage area normalized streamflow for the two sites was 0.014 and 0.31 ft^3/s per square mile, respectively. Measurements collected in August 2015 were assumed to represent base-flow conditions for a year with slightly above normal precipitation. If the measurements collected on July 11, 2019, are excluded, a clear short-term response to precipitation events (fig. 8), the 2019 mean measured discharge of the Upper South Loup River and the North Fork South Loup River was 12.8 and 10.5 ft^3/s, respectively, and drainage area normalized streamflow was 0.05 and 0.46 ft^3/s per square mile, respectively. In relatively dry (2015) and wet (2019) years, the area normalized streamflow at the Upper South Loup River was consistently less than the North Fork South Loup River, indicating streamflow at the latter site is sourced from an effectively larger drainage basin. The area-normalized streamflow of the North Fork South Loup River calculated for 2015 was larger but comparable to other streams in the Sand Hills. Peterson and others (2016) published long-term average base flow for gaged streams in the Sand Hills where base flow often exceeds 90 percent of streamflow (Szilagyi and others, 2003). The area normalized streamflow for Dismal River at Dunning, Nebr. (USGS station 06776500), Middle Loup River at Dunning, Nebr. (USGS station 06775500), and North Loup River at Taylor, Nebr. (USGS station 06786000; not shown on any maps) ranged from 0.16 to 0.23 ft^3/s per square mile. Because the area normalized streamflow of the North Fork South Loup exceeds this range, it is possible that the stream is capturing regional groundwater flow from outside of the drainage area or capturing groundwater that was recharged during a wetter than normal historical time period. In either case, the high area normalized streamflow of the North Fork South Loup River implies the capture of flow from outside the surface-water basin and a relatively large amount of groundwater storage in the basin. Conversely, the relatively lower area normalized streamflow of the Upper South Loup River as compared to the North Fork South Loup and other area rivers indicates either precipitation runs off quickly and produces high streamflow not captured in the discrete measurements or groundwater recharge from the basin ultimately discharges to a different stream reach. The wetter conditions in 2019 produced increases in area normalized streamflow by 290 percent for the Upper South Loup River and 47 percent for the North Fork South Loup River. Based on these comparisons, it can be inferred that the Upper South Loup River is more reliant on recent precipitation and likely more affected by short-term drought when compared to the North Fork South Loup River.

During the period of data collection for this study (May 2019–October 2019), the daily mean streamflow measured at the Arnold streamgage ranged from 16.4 to 788 ft^3/s and at the South Loup River at Pressey streamgage ranged from 76.3 to 4,420 ft^3/s (U.S. Geological Survey, 2021b). Daily mean streamflow normalized to drainage area was on average 0.2 and 0.05 ft^3/s per square mile for Pressey and Arnold streamgages, respectively. The area normalized streamflow at Pressey is larger compared to the area normalized streamflow at the Arnold streamgage, but comparable to other streams in the Sand Hills such as the Dismal, Middle Loup, and North Loup Rivers. These comparisons indicate that recharge captured within the drainage area upstream from the Arnold streamgage ultimately

discharges to a different stream reach or stream basin. Comparison of the relative deviation of daily streamflow from the overall mean at the two streamgages (fig. 13) shows streamflow at Pressey was somewhat less variable than at the Arnold streamgage. During periods of higher flow, there is an increased relative contribution of flow upstream from the Arnold streamgage as compared to periods of low flow (fig. 13). In combination with the continuous records of gage height and specific conductance at Hoagland, indicating contributions for shallow groundwater and overland flow (fig. 12), the differences in streamflow metrics between the Pressey and Arnold streamgages indicate that streamflow in the upper reaches of the South Loup River are more dependent on recent recharge and shallow groundwater. Conversely, streamflow from the lower reaches of the South Loup River as represented by the Pressey streamgage is likely sourced from deeper or more spatially distributed groundwater sources, likely from the Pliocene-age sand and gravel deposits.

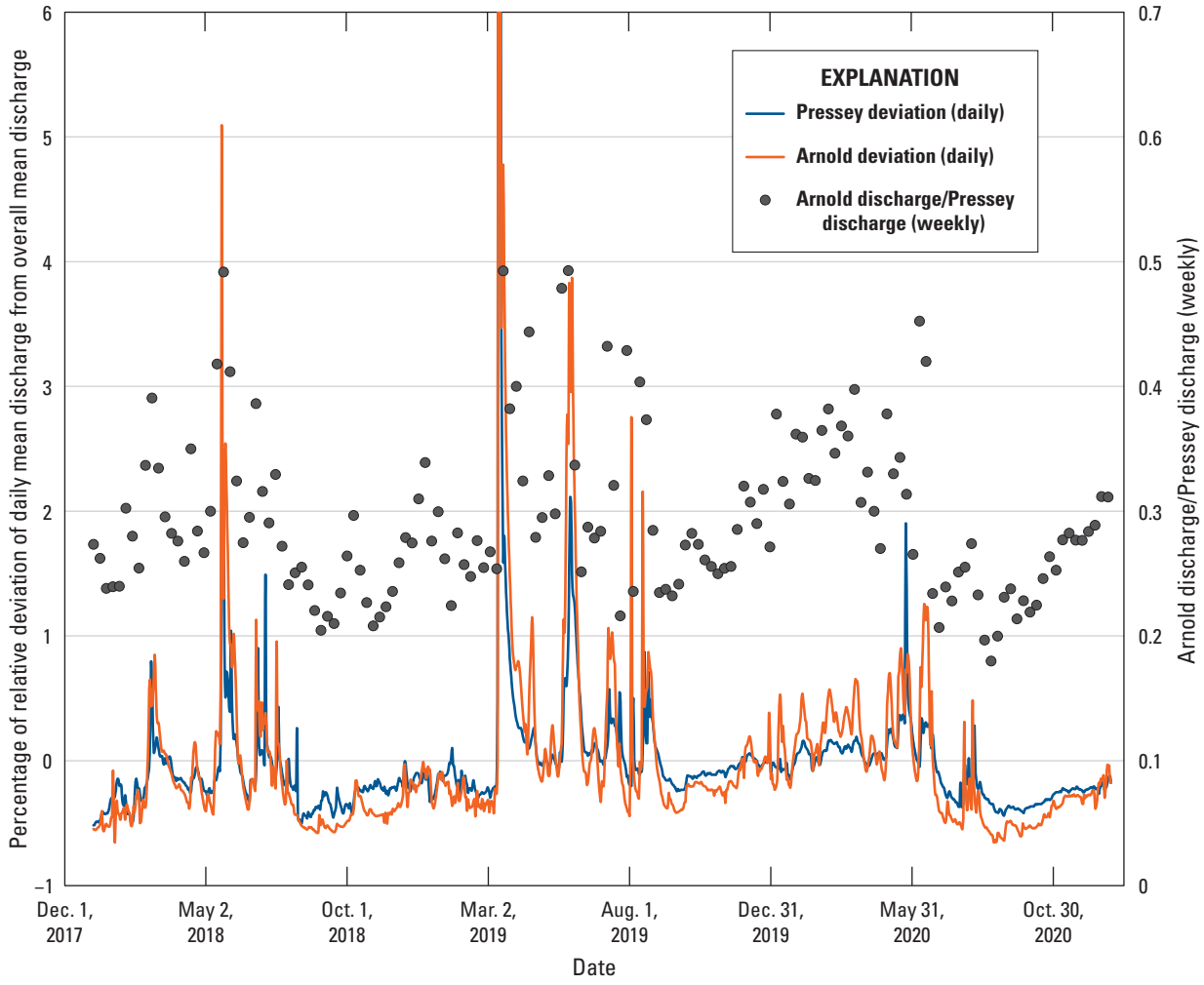

Figure 13. Comparison of daily mean streamflow deviation from average streamflow for the South Loup River at Arnold, Nebraska, streamgage (U.S. Geological Survey station 06781600) and South Loup River at Pressey WMA near Oconto, Nebr., streamgage (U.S. Geological Survey station 06781900), and the ratio of weekly mean streamflow between the two streamgages, October 2017–September 2020.

Drought Resilience of Groundwater Discharge to the Upper South Loup River

Quaternary-age deposits cover the entire study area and are the dominant source of groundwater discharge above the Arnold streamgage (Hobza and Schepers, 2018). Groundwater sampled in wells screened in Quaternary-age deposits displayed a wide range of mean ages, fraction modern, and SI values. Wells near the South Loup River, where multiple flow paths converge, had older mean ages and wider age distributions compared to wells screened immediately below the water table in groundwater recharge areas. Generally, wells with higher concentrations of chloride and TDS and higher specific conductance were indicative of younger groundwater with a narrower age distribution. Groundwater in these instances has a much larger SI and therefore is more sensitive to climatic disturbances such as short-term drought conditions. Continuously measured gage height and specific conductance data collected at the Mills Valley monitoring site indicated a highly dynamic response to precipitation events. Abrupt changes in specific conductance indicated that much of the flow that discharges from Quaternary-age springs is reliant on recent precipitation and is more sensitive to short-term drought conditions.

Downstream from the Arnold streamgage, groundwater discharge was identified within the stream channel, indicating diffuse flow through the streambed and from focused points where groundwater discharged through large, broad sheets of Pliocene-age sand and gravel (Hobza and Schepers, 2018). Groundwater sampling of the mapped springs has identified two different sample groups with different geochemical and age characteristics. A set of three springs and one well (called Western Pliocene) are located approximately 4 mi downstream from the Arnold streamgage near an area of groundwater-irrigated row crops. These samples had higher concentrations of chloride and nitrate, indicating groundwater quality in these locations is affected by agricultural activities. Generally, the age of water from these four samples was considered modern and $\delta^{18}O$ values were slightly enriched compared to other springs from Pliocene-age deposits. These four sites also showed a lower fraction of wintertime recharge when compared to other samples collected from Pliocene-age springs and wells, which indicates that a portion of the samples is recently recharged irrigation return flow. The relatively young mean age and narrow age distribution indicate that groundwater discharging near the Western Pliocene sample group is susceptible to short-term drought.

Downstream from the Western Pliocene sample group, groundwater discharging from springs in Pliocene-age deposits had much lower concentrations of nitrate, chloride, TDS, and specific conductance. The mean groundwater ages for these samples were much older, ranging from 1,900 to 2,900 years old, and were determined to be the mixture of younger and older waters. The fraction modern ranged from zero to 0.23, and the SI was an order of magnitude less than the Western Pliocene samples. Continuously measured gage height and specific conductance data collected at the Finchville monitoring site indicated little change in gage height and specific conductance during precipitation events. The relatively constant specific conductance at the Finchville monitoring site indicates that groundwater discharge from Pliocene-age sand and gravel deposits changes little in response to seasonal increases in precipitation and is likely more resilient to short-term drought conditions.

Groundwater sampled from three wells screened in the Ogallala Formation had the oldest mean ages seen in this study, ranging from 8,700 to 23,000 years, and the lowest calculated SI values in this study. Two of the three wells were located downstream from the Arnold streamgage along the margin of the South Loup River and had strong upward hydraulic gradients, indicating that groundwater from the Ogallala Formation is likely contributing to streamflow of the South Loup River. Recent groundwater modeling indicated that the Ogallala Formation contributes substantial amounts of base flow to the South Loup River upstream from the Arnold streamgage (Amanda Flynn, U.S. Geological Survey, written commun., 2021).

Summary

Streams in the Loup River Basin are sensitive to groundwater withdrawals because of the close hydrologic connection between groundwater and surface water. The Upper Loup and Lower Loup Natural Resources Districts have recently approved the South Loup Watershed Management Plan to guide the implementation of future projects intended to improve water quality and address water sustainability concerns. As part of this plan, additional hydrologic analyses were completed to evaluate the feasibility of capturing streamflow from tributaries for retiming and augmentation during low-flow periods.

In a previous study, the U.S. Geological Survey (USGS), in cooperation with the Upper Loup and Lower Loup Natural Resources Districts, and the Nebraska Environmental Trust, collected aerial thermal imagery along the South Loup River to map locations of focused groundwater discharge points, or springs. These mapped springs are important hydrologic features that sustain the flow of the South Loup River and its tributaries. Although their location has been mapped, the ability of these springs to maintain consistent flow during periods of prolonged drought has not yet been studied. In natural groundwater flow systems, the relation between climatic disturbances such as drought and groundwater discharge to streams can be complex and difficult to characterize. One approach is to use groundwater age tracers with supporting geochemical data to estimate the age of water discharging from springs and nearby wells. In this instance, groundwater age refers to the average length of time for groundwater to move from areas of recharge to areas of discharge (springs or streams). Older groundwater, with longer

transit times, can dampen the effects of a multiyear drought. Conversely, groundwater discharge sustained by springs with shorter residence times are more susceptible to short-term drought conditions, decreasing the streamflow downstream.

To assess groundwater interaction and possible effects of a multiyear drought on the streamflow of the South Loup River, the USGS in cooperation with the Upper Loup and Lower Loup Natural Resources Districts, and the Nebraska Environmental Trust, began a study examining the age and water-quality characteristics of groundwater from selected springs and monitoring wells located near the South Loup River. This report describes the age and water-quality characteristics of groundwater discharging from Pliocene-age deposits (called Pliocene-age springs) and groundwater from wells completed in Quaternary-age deposits, Pliocene-age deposits, and the Ogallala Formation. Samples from 20 springs and wells were analyzed for major ions, trace elements, nutrients, stable isotopes, dissolved gases, and selected age tracers. Age tracer and supporting geochemical data were modeled with a modified version of TracerLPM to determine the age distributions for the springs and wells sampled. Real-time water-quality, gage height, and discharge data were collected at three locations to provide additional support and context for age tracer interpretations.

Quaternary-age deposits cover the entire study area and are the dominant source of groundwater discharge above the South Loup River at Arnold, Nebraska, streamgage (USGS station 06781600). Groundwater sampled in wells screened in Quaternary-age deposits displayed a wide range of mean ages, fraction modern, and susceptibility index (SI) values. Wells near the South Loup River, where multiple flow paths converge, had older mean ages and wider age distributions compared to wells screened immediately below the water table in groundwater recharge areas. Generally, wells with higher concentrations of chloride and total dissolved solids and higher specific conductance were indicative of younger groundwater with a narrower age distribution. Groundwater in these instances had a much larger SI and therefore was more sensitive to climatic disturbances such as short-term drought conditions. Continuously measured gage height and specific conductance data collected at the South Loup River Spring 0.86 mile west of Arnold, Nebr. (USGS station 412542100125301) indicated a highly dynamic response to precipitation events. Abrupt changes in specific conductance indicated that much of the flow that discharges from Quaternary-age springs is reliant on recent precipitation and is more sensitive to short-term drought conditions.

Downstream from the South Loup River at Arnold, Nebr., streamgage (USGS station 06781600), groundwater discharge was identified within the stream channel, indicating diffuse flow through the streambed and from focused points where groundwater discharged through large, broad sheets of Pliocene-age sand and gravel. Groundwater sampling of the mapped springs has identified two different sample groups with different geochemical and age characteristics. A set of three springs and one well (called Western Pliocene) are located approximately 4 miles downstream from the South Loup River at Arnold, Nebr., streamgage (USGS station 06781600) near an area of groundwater-irrigated row crops. These samples had higher concentrations of chloride and nitrate, indicating groundwater quality in these locations is affected by agricultural activities. Generally, the age of water from these four samples was considered modern and $\delta^{18}O$ values (oxygen-18-to-oxygen-16 isotopic ratio) were slightly enriched compared to other springs from Pliocene-age deposits. These four sites also showed a lower fraction of wintertime recharge when compared to other samples collected from Pliocene-age springs and wells, which indicates that a portion of the samples is recently recharged irrigation return flow. The relatively young mean age and narrow age distribution indicate that groundwater discharging near the Western Pliocene sample group is susceptible to short-term drought.

Downstream from the Western Pliocene sample group, groundwater discharging from springs in Pliocene-age deposits had much lower concentrations of nitrate, chloride, total dissolved solids, and specific conductance. The mean groundwater ages for these samples were much older, ranging from 1,900 to 2,900 years old, and were determined to be the mixture of younger and older waters. The fraction modern ranged from zero to 0.23, and the SI was an order of magnitude less than the Western Pliocene samples. Continuously measured gage height and specific conductance data collected at the South Loup River Tributary Spring 1.3 miles Southwest of Finchville, Nebr. (USGS station 412147100055301) indicated little change in gage height and specific conductance during precipitation events. The relatively constant specific conductance indicates that groundwater discharge from Pliocene-age sand and gravel deposits changes little in response to seasonal increases in precipitation and is likely more resilient to short-term drought conditions.

Groundwater sampled from three wells screened in the Ogallala Formation were shown to have the oldest mean ages seen in this study, ranging from 8,700 to 23,000 years, and the lowest calculated SI values in this study. Two of the three wells were located downstream from the streamgage at South Loup River at Arnold, Nebr., streamgage (USGS station 06781600) along the margin of the South Loup River and had strong upward hydraulic gradients, indicating that groundwater from the Ogallala Formation is likely contributing to streamflow of the South Loup River. Recent groundwater modeling indicated that the Ogallala Formation contributes substantial amounts of base flow to the South Loup River upstream from the South Loup River at Arnold, Nebr., streamgage (USGS station 06781600).

References Cited

Aeschbach-Hertig, W., Peeters, F., Beyerle, U., and Kipfer, R., 1999, Interpretation of dissolved atmospheric noble gases in natural waters: Water Resources Research, v. 35, no. 9, p. 2779–2792.

Ahlbrandt, T.S., Swinehart, J.B., and Maroney, D.G., 1983, The dynamic Holocene dune fields of the Great Plains and Rocky Mountain basins, U.S.A, *in* Brookfield, M.E., and Ahlbrandt, T.S., eds., Eolian sediments and processes: New York, Elsevier Science Publishing Company, p. 379–406. [Also available at https://doi.org/10.1016/S0070-4571(08)70806-9.]

Barnes, P.W., and Harrison, A.T., 1982, Species distribution and community organization in a Nebraska Sandhills mixed prairie as influenced by plant/soil-water relationships: Oecologia, v. 52, no. 2, p. 192–201. [Also available at https://doi.org/10.1007/BF00363836.]

Bexfield, L.M., Jurgens, B.C., Crilley, D.M., and Christenson, S.C., 2012, Hydrogeology, water chemistry, and transport processes in the zone of contribution of a public-supply well in Albuquerque, New Mexico, 2007–9: U.S. Geological Survey Scientific Investigations Report 2011–5182, 114 p., accessed August 11, 2021, at https://pubs.usgs.gov/sir/2011/5182/.

Bleed, A.S., and Flowerday, C.A., eds., 1989, An atlas of the Sand Hills (3d ed.): Lincoln, Nebr., University of Nebraska, Conservation and Survey Division, Resource Atlas no. 5b, 260 p.

Busenberg, E., and Plummer, L.N., 2000, Dating young ground water with sulfur hexafluoride—Natural and anthropogenic sources of sulfur hexafluoride: Water Resources Research, v. 36, no. 10, p. 3011–3030. [Also available at https://doi.org/10.1029/2000WR900151.]

Buto, S.G., and Anderson, R.D., 2020, NHDPlus High Resolution (NHDPlus HR)—A hydrography framework for the Nation: U.S. Geological Survey Fact Sheet 2020–3033, 2 p., accessed May 21, 2021, at https://doi.org/10.3133/fs20203033.

Center for Advanced Land Management Information Technologies, 2007, 2005 Nebraska land use patterns: Lincoln, Nebr., University of Nebraska-Lincoln, geospatial data, accessed April 22, 2021, at https://calmit.unl.edu/2005-nebraska-statewide.

Cerling, T.E., 1984, The stable isotopic composition of modern soil carbonate and its relationship to climate: Earth and Planetary Science Letters, v. 71, no. 2, p. 229–240. [Also available at https://doi.org/10.1016/0012-821X(84)90089-X.]

Clark, I.D., and Fritz, P., 1997, Environmental isotopes in hydrogeology: New York, Lewis Publishers, 328 p.

Condra, G.E., and Reed, E.C., 1943, The geological section of Nebraska: Lincoln, Nebr., University of Nebraska-Lincoln, Conservation and Survey Division, Nebraska Geological Survey Bulletin, v. 14, p. 82.

Conservation and Survey Division, University of Nebraska-Lincoln, 2020a, Test-hole database: Lincoln, Nebr., University of Nebraska-Lincoln, Conservation and Survey Division digital data, accessed October, 21, 2020, at http://snr.unl.edu/data/geologysoils/NebraskaTestHole/.

Conservation and Survey Division, University of Nebraska-Lincoln, 2020b, Topographic regions, 2020: Lincoln, Nebr., University of Nebraska-Lincoln, Institute of Agriculture and Natural Resources, digital data, accessed October 21, 2020, at http://snr.unl.edu/csd-esic/download/geographygis/stp/toporeg_stp.zip.

Cook, P.G., and Solomon, D.K., 1995, Transport of atmospheric trace gases to the water table—Implications for groundwater with chlorofluorocarbons and dating krypton 85: Water Resources Research, v. 31, no. 2, p. 425–434. [Also available at https://doi.org/10.1029/94WR02528.]

Coplen, T.B., Brand, W.A., Gehre, M., Groning, M., Meijer, H.A.J., Toman, B., and Verkouteren, R.M., 2006, New guidelines for $\delta^{13}C$ measurements: Analytical Chemistry, accessed August 11, 2021, at https://pubs.acs.org/doi/10.1021/ac052027c.

Coplen, T.B., and Kendall, C., 2000, Stable hydrogen and oxygen isotope ratios for selected sites of the U.S. Geological Survey's NASQAN and benchmark surface-water networks: U.S. Geological Survey Open-File Report 00–160, 490 p., accessed June 23, 2020, at https://pubs.usgs.gov/of/2000/ofr00-160/.

Craig, H., 1961, Isotopic variations in meteoric waters: Science, v. 133, no. 3465, p. 1702–1703. [Also available at https://doi.org/10.1126/science.133.3465.1702.]

Cunningham, W.L., and Schalk, C.W., comps., 2011, Groundwater technical procedures of the U.S. Geological Survey: U.S. Geological Survey Techniques and Methods, book 1, chap. A1, 151 p. [Also available at https://pubs.usgs.gov/tm/1a1/.]

Darton, N.H., 1903, Preliminary report on the geology and water resources of Nebraska west of the one hundred and third meridian: U.S. Geological Survey Professional Paper 17, 69 p., 43 pls. [Also available at https://pubs.usgs.gov/pp/0017/report.pdf.]

Diffendal, R.F., Jr., 1991, Geologic map showing configuration of the bedrock surface, North Platte 1 degree x 2 degrees quadrangle, Nebraska: U.S. Geological Survey Miscellaneous Investigation Series Map I–2277, scale 1:250,000. [Also available at http://ngmdb.usgs.gov/Prodesc/proddesc_10209.htm.]

Dugan, J.T., and Zelt, R.B., 2000, Simulation and analysis of soil-water conditions in the Great Plains and adjacent areas, central United States, 1951–80: U.S. Geological Survey Water-Supply Paper 2427, 81 p. [Also available at https://pubs.usgs.gov/wsp/2427/report.pdf.]

Eberts, S.M., Böhlke, J.K., Kauffman, L.J., and Jurgens, B.C., 2012, Comparison of particle-tracking and lumped-parameter age-distribution models for evaluating vulnerability of production wells to contamination: Hydrogeology Journal, v. 20, no. 2, p. 263–282, accessed August 11, 2021, at https://doi.org/10.1007/s10040-011-0810-6.

Faure, G., 1998, Principles and applications of geochemistry (2nd ed.): Upper Saddle River, N.J., Prentice Hall, 600 p.

Fishman, M.J., ed., 1993, Methods of analysis by the U.S. Geological Survey National Water Quality Laboratory—Determination of inorganic and organic constituents in water and fluvial sediments, U.S. Geological Survey Open-File Report 93–125, 217 p. [Also available at https://doi.org/10.3133/ofr93125.]

Fishman, M.J., and Friedman, L.C., 1989, Methods for determination of inorganic substances in water and fluvial sediments: U.S. Geological Survey Techniques of Water-Resources Investigations, book 5, chap. A1, 545 p.

Flynn, A.T., and Stanton, J.S., 2018, Simulation of groundwater flow, 1895–2010, and effects of additional groundwater withdrawals on future stream base flow in the Elkhorn and Loup River Basins, central Nebraska—Phase three: U.S. Geological Survey Scientific Investigations Report 2018–5106, 65 p. [Also available at https://doi.org/10.3133/sir20185106.]

Garbarino, J.R., 1999, Methods of analysis by the U.S. Geological Survey National Water Quality Laboratory—Determination of dissolved arsenic, boron, lithium, selenium, strontium, thallium, and vanadium using inductively coupled plasma-mass spectrometry: U.S. Geological Survey Open-File Report 99–093, 31 p. [Also available at https://doi.org/10.3133/ofr9993.]

Garbarino, J.R., and Damrau, D.L., 2001, Methods of analysis by the U.S. Geological Survey National Water Quality Laboratory—Determination of organic plus inorganic mercury in filtered and unfiltered natural water with cold vapor-atomic fluorescence spectrometry: U.S. Geological Survey Water-Resources Investigations Report 01–4132, 16 p. [Also available at https://doi.org/10.3133/wri014132.]

Garbarino, J.R., Kanagy, L.K., and Cree, M.E., 2006, Determination of elements in natural-water, biota, sediment, and soil samples using collision/reaction cell inductively coupled plasma-mass spectrometry: U.S. Geological Survey Techniques and Methods, book 5, chap. B1, 88 p. [Also available at https://pubs.usgs.gov/tm/2006/tm5b1/PDF/TM5-B1.pdf.]

Gelhar, L.W., Welty, C., and Rehfeldt, K.R., 1992, A critical review of data on field-scale dispersion in aquifers: Water Resources Research, v. 28, no. 7, p. 1955–1974, accessed April 23, 2021. [Also available at https://doi.org/10.1029/92WR00607.]

Gutentag, E.D., Heimes, F.J., Krothe, N.C., Luckey, R.R., and Weeks, J.B., 1984, Geohydrology of the High Plains aquifer in parts of Colorado, Nebraska, New Mexico, Oklahoma, South Dakota, Texas, and Wyoming: U.S. Geological Survey Professional Paper 1400–B, 63 p. [Also available at https://doi.org/10.3133/pp1400B.]

Han, L.-F., and Plummer, L.N., 2016, A review of single sample-based models and other approaches for radiocarbon dating of dissolved inorganic carbon in groundwater: Earth-Science Reviews, v. 152, p. 119–142, accessed December 15, 2021, at https://doi.org/10.1016/j.earscirev.2015.11.004.

Harvey, F.E., and Welker, J.M., 2000, Stable isotope composition of precipitation in the semi-arid north-central portion of the U.S. Great Plains: Journal of Hydrology (Amsterdam), v. 238, no. 1-2, p. 90–109. [Also available at https://doi.org/10.1016/S0022-1694(00)00316-4.]

Helsel, D.R., Hirsch, R.M., Ryberg, K.R., Archfield, S.A., and Gilroy, E.J., 2020, Statistical methods in water resources: U.S. Geological Survey Techniques and Methods, book 4, chap. A3, 458 p., accessed July 13, 2020, at https://doi.org/10.3133/tm4A3. [Supersedes USGS Techniques of Water-Resources Investigations, book 4, chap. A3, version 1.1.]

Hem, J.D., 1985, Study and interpretation of the chemical characteristics of natural water: U.S. Geological Survey Water Supply Paper 2254, accessed April 16, 2021, at https://pubs.usgs.gov/wsp/wsp2254/.

Hobza, C.M., Bedrosian, P.A., and Bloss, B.R., 2012, Hydrostratigraphic interpretation of test-hole and surface geophysical data, Elkhorn and Loup River Basins, Nebraska, 2008 to 2011: U.S. Geological Survey Open-File Report 2012–1227, 95 p. [Also available at https://doi.org/10.3133/ofr20121227.]

Hobza, C.M., and Schepers, A.R., 2018, Groundwater discharge characteristics for selected streams within the Loup River Basin, Nebraska, 2014–16: U.S. Geological Survey Scientific Investigations Report 2018–5093, 50 p. [Also available at https://doi.org/10.3133/sir20185093.]

International Atomic Energy Agency and World Meteorological Organization, 2021, Global Network of Isotopes in Precipitation Database: International Atomic Energy Agency and World Meteorological Organization, accessed April 2, 2021, at https://www.iaea.org/services/networks/gnip/.

Hutson, S.S., Barber, N.L., Kenny, J.F., Linsey, K.S., Lumia, D.S., and Maupin, M.A., 2004, Estimated use of water in the United States in 2000: U.S. Geological Survey Circular 1268, 46 p. [Also available at https://doi.org/10.3133/cir1268.]

Jasechko, S., Birks, S.J., Gleeson, T., Wada, Y., Fawcett, P.J., Sharp, Z.D., McDonnell, J.J., and Welker, J.M., 2014, The pronounced seasonality of global groundwater recharge: Water Resources Research, v. 50, no. 11, p. 8845–8867, accessed April 14, 2021, at https://doi.org/10.1002/2014WR015809.

JEO Consulting Group, Inc., 2017, South Loup Watershed Management Plan: Lincoln, Nebr., JEO Consulting Group, Inc., 190 p. [Also available at https://www.llnrd.org/assets/site/SL%20Watershed%20WMP.pdf.]

Jurgens, B.C., Böhlke, J.K., and Eberts, S.M., 2012, TracerLPM (version 1)—An Excel workbook for interpreting groundwater age distributions from environmental tracer data: U.S. Geological Survey Techniques and Methods Report 4–F3, 60 p. [Also available at https://pubs.usgs.gov/tm/4-f3/.]

Jurgens, B.C., McMahon, P.B., Chapelle, F.H., and Eberts, S.M., 2009, An Excel workbook for identifying redox processes in ground water: U.S. Geological Survey Open-File Report 2009–1004, 8 p., accessed April 14, 2021, at https://pubs.usgs.gov/of/2009/1004/.

Kalin, R.M., 2000, Radiocarbon dating of groundwater systems, chap. 4 *of* Cook, P.G., and Herczeg, A.L., eds., Environmental tracers in subsurface hydrology: Boston, Kluwer Academic Publishers, p. 111–144.

Kazemi, G.A., Lehr, J.H., and Perrochet, P., 2006, Groundwater age: Hoboken, N.J., John Wiley and Sons, Inc., 325 p. [Also available at https://doi.org/10.1002/0471929514.]

Kendall, C., and Caldwell, E.A., 1998, Fundamentals of isotope geochemistry, chap. 2 *of* Kendall, C., and McDonnell, J.J., eds., Isotope tracers in catchment hydrology: Amsterdam, Elsevier, p. 51–86, accessed June 23, 2020, at https://wwwrcamnl.wr.usgs.gov/isoig/isopubs/itchch2.html.

Korus, J.T., and Joeckel, R.M., 2011, Generalized geologic and hydrostratigraphic framework of Nebraska 2011, ver. 2. Conservation and Survey Division, School of Natural Resources, Institute of Agriculture and Natural Resources, University of Nebraska-Lincoln. Geologic Maps and Charts (GMC) 38. [Also available at https://snr.unl.edu/csd/download/geology/GMC-38.pdf.]

Landwehr, J.M., and Coplen, T.B., 2006, Line-conditioned excess—A new method for characterizing stable hydrogen and oxygen isotope ratios in hydrologic systems *in* Isotopes in Environmental Studies, Aquatic Forum 2004, Proceedings: International Atomic Energy Agency, p. 132–135.

Lindsey, B.D., Jurgens, B.C., and Belitz, K., 2019, Tritium as an indicator of modern, mixed, and premodern groundwater age: U.S. Geological Survey Scientific Investigations Report 2019–5090, 18 p., accessed January 6, 2021, at https://doi.org/10.3133/sir20195090.

Loope, D.B., and Swinehart, J.B., 2000, Thinking like a dune field—Geologic history in the Nebraska Sand Hills: Great Plains Research, v. 10, p. 5–35.

Lucas, L.L., and Unterweger, M.P., 2000, Comprehensive review and critical evaluation of the half-life of tritium: Journal of Research of the National Institute of Standards and Technology, v. 105, no. 4, p. 541–549. [Also available at https://doi.org/10.6028/jres.105.043.]

McGuire, V.L., Lund, K.D., and Densmore, B.K., 2012, Saturated thickness and water in storage in the High Plains aquifer, 2009, and water-level changes and changes in water in storage in the High Plains aquifer, 1980 to 1995, 1995 to 2000, 2000 to 2005, and 2005 to 2009: U.S. Geological Survey Scientific Investigations Report 2012–5177, 28 p. [Also available at https://doi.org/10.3133/sir20125177.]

McMahon, P.B., Böhlke, J.K., and Carney, C.P., 2007, Vertical gradients in water chemistry and age in the Northern High Plains Aquifer, Nebraska, 2003: U.S. Geological Survey Scientific Investigations Report 2006–5294, accessed April 2, 2021, at https://pubs.usgs.gov/sir/2006/5294/.

McMahon, P.B., and Chapelle, F.H., 2008, Redox processes and water quality of selected principal aquifer systems: Ground Water, v. 46, no. 2, p. 259–271. [Also available at https://doi.org/10.1111/j.1745-6584.2007.00385.x.]

Michel, R.L., 1989, Tritium deposition in the continental United States, 1953–1983: U.S. Geological Survey Water-Resources Investigations Report 89–4072, 46 p. [Also available at https://doi.org/10.3133/wri894072.]

Mook, W.G., and van der Plicht, J., 1999, Reporting ^{14}C activities and concentrations: Radiocarbon, v. 41, no. 3, p. 227–239. [Also available at https://doi.org/10.1017/S0033822200057106.]

Mueller, D.K., and Helsel, D.R., 1996, Nutrients in the nation's waters—Too much of a good thing?: U.S. Geological Survey Circular 1136, 24 p. [Also available at https://pubs.usgs.gov/circ/1996/1136/report.pdf].

National Centers for Environmental Information, 2021, Data tools—1981–2010 normals: Asheville, N.C., National Centers for Environmental Information, digital data, accessed January 29, 2021, at https://www.ncdc.noaa.gov/cdo-web/datatools/normals.

Parkhurst, D.L., and Appelo, C.A.J., 1999, User's guide to PHREEQC (version 2)—A computer program for speciation, batch-reaction, one-dimensional transport, and inverse geochemical calculations: U.S. Geological Survey Water-Resources Investigations Report 99–4259, 312 p., accessed at April 2, 2021, at https://pubs.er.usgs.gov/publication/wri994259.

Peel, M.C., Finlayson, B.L., and McMahon, T.A., 2007, Updated world map of the KÖppen-Geiger climate classification: Hydrology and Earth System Sciences, v. 11, p. 1633–1644.

Peterson, S.M., Flynn, A.T., and Traylor, J.P., 2016, Groundwater-flow model of the Northern High Plains aquifer in Colorado, Kansas, Nebraska, South Dakota, and Wyoming: U.S. Geological Survey Scientific Investigations Report 2016–5153, 88 p., accessed May 2021 at https://doi.org/10.3133/sir20165153.

Peterson, S.M., Stanton, J.S., Saunders, A.T., and Bradley, J.R., 2008, Simulation of ground-water flow and effects of ground-water irrigation on base flow in the Elkhorn and Loup River Basins, Nebraska: U.S. Geological Survey Scientific Investigations Report 2008–5143, 65 p. [Also available at https://doi.org/10.3133/sir20085143.]

Phillips, D.L., and Gregg, J.W., 2001, Uncertainty in source partitioning using stable isotopes: Oecologia, v. 127, no. 2, p. 171–179, accessed April 14, 2021, at https://doi.org/10.1007/s004420000578.

Piper, A.M., 1944, A graphic procedure in the geochemical interpretation of water-analyses: Transactions - American Geophysical Union, v. 25, no. 6, p. 914–928. [Also available at https://doi.org/10.1029/TR025i006p00914.]

Révész, K., and Coplen, T.B., 2008a, Determination of the δ(2 H/1 H) of water—RSIL lab code 1574, chap. 1 *of* Révész, K., and Coplen, T.B., eds., Stable isotope-ratio methods—Methods of the Reston Stable Isotope Laboratory: U.S. Geological Survey Techniques and Methods, book 10, chap. C1, 27 p. [Also available at https://pubs.usgs.gov/tm/2007/tm10c1/.]

Révész, K., and Coplen, T.B., 2008b, Determination of the δ (18O/16O) of water—RSIL lab code 489, chap. 2 *of* Révész, K., and Coplen, T.B., eds., Stable isotope-ratio methods—Methods of the Reston Stable Isotope Laboratory: U.S. Geological Survey Techniques and Methods, book 10, chap. C2, 28 p. [Also available at https://pubs.usgs.gov/tm/2007/tm10c2/.]

Sauer, V.B., and Turnipseed, D.P., 2010, Stage measurement at gaging stations: U.S. Geological Survey Techniques and Methods, book 3, chap. A7, 45 p. [Also available at https://pubs.usgs.gov/tm/tm3-a7/.]

Solder, J.E., 2019, Dissolved gas and tracer concentrations for the High Plains aquifer, vertical flowpath study network: U.S. Geological Survey data release, accessed December 15, 2021, at https://doi.org/10.5066/P9VLFXTM.

Solder, J.E., 2021, Lumped parameter models of groundwater age, South Loup River, Nebraska: U.S. Geological Survey data release, accessed May 1, 2021, at https://doi.org/10.5066/P9L6B4XE.

Solder, J.E., Jurgens, B., Stackelberg, P.E., and Shope, C.L., 2020, Environmental tracer evidence for connection between shallow and bedrock aquifers and high intrinsic susceptibility to contamination of the conterminous U.S. glacial aquifer: Journal of Hydrology (Amsterdam), v. 583, p. 124505, accessed August 11, 2021, at https://doi.org/10.1016/j.jhydrol.2019.124505.

Souders, V.L., 2000, Geologic maps and cross sections showing configurations of bedrock surfaces, Broken Bow 1 x 2 degree quadrangle, east-central Nebraska: U.S. Geological Survey Geologic Investigations Series I–2725, scale 1:250,000.

Stackelberg, P.E., Szabo, Z., and Jurgens, B.C., 2018, Radium mobility and the age of groundwater in public-drinking-water supplies from the Cambrian-Ordovician aquifer system, north-central USA: Applied Geochemistry, v. 89, p. 34–48, accessed August 11, 2021, at https://doi.org/10.1016/j.apgeochem.2017.11.002.

Stanley, K.O., and Wayne, W.J., 1972, Epeirogenic and climatic controls of Early Pleistocene fluvial sediment dispersal in Nebraska: Geological Society of America Bulletin, v. 83, no. 12, p. 3675–3690. [Also available at https://doi.org/10.1130/0016-7606(1972)83[3675:EACCOE]2.0.CO;2.]

Stanton, J.S., Peterson, S.M., and Fienen, M.N., 2010, Simulation of groundwater flow and effects of groundwater irrigation on stream base flow in the Elkhorn and Loup River Basins, Nebraska, 1895–2055—Phase two: U.S. Geological Survey Scientific Investigations Report 2010–5149, 78 p., 1 app. [Also available at https://pubs.usgs.gov/sir/2010/5149/.]

Stanton, J.S., Qi, S.L., Ryter, D.W., Falk, S.E., Houston, N.A., Peterson, S.M., Westenbroek, S.M., and Christenson, S.C., 2011, Selected approaches to estimate water-budget components of the High Plains, 1940 through 1949 and 2000 through 2009: U.S. Geological Survey Scientific Investigations Report 2011–5183, 79 p. [Also available at https://doi.org/10.3133/sir20115183.]

Steele, G.V., Gurdak, J.J., and Hobza, C.M., 2014, Water movement through the unsaturated zone of the High Plains aquifer in the Central Platte Natural Resources District, Nebraska, 2008–12: U.S. Geological Survey Scientific Investigations Report 2014–5008, 54 p. [Also available at https://doi.org/10.3133/sir20145008.]

Steele, G.V., Sibray, S.S., and Quandt, K.A., 2007, Evaluation of ground water near Sidney, western Nebraska 2004–05: U.S. Geological Survey Scientific Investigations Report 2007–5086, 54 p. [Also available at https://doi.org/10.3133/sir20075086.]

Strauch, K.R., and Linard, J.I., 2009, Streamflow simulations and percolation estimates using the Soil and Water Assessment Tool for selected basins in North-Central Nebraska, 1940–2005: U.S. Geological Survey Scientific Investigations Report 2009–5075, 20 p. [Also available at https://doi.org/10.3133/sir20095075.]

Stuiver, M., and Polach, H.A., 1977, Discussion reporting of ^{14}C data: Radiocarbon, v. 19, no. 3, p. 355–363. [Also available at https://doi.org/10.1017/S0033822200003672.]

Struzeski, T.M., DeGiacomo, W.J., and Zayhowski, E.J., 1996, Methods of analysis by the U.S. Geological Survey National Water Quality Laboratory—Determination of dissolved aluminum and boron in water by inductively coupled plasma-atomic emission spectrometry: U.S. Geological Survey Open-File Report 96–149, 17 p. [Also available at https://doi.org/10.3133/ofr96149.]

Summerside, S.E., Dreeszen, V.H., Hartung, S.L., Khisty, M.J., and Szilagyi, J., 2001, Update and revision of regional 1x2 degree water-table configuration maps for the state of Nebraska: University of Nebraska Conservation and Survey Division Open-File Report 73, 9 p.

Swinehart, J.B., and Diffendal, R.F., Jr., 1989, Geology of the pre-dune strata, *in* Bleed, A.S., and Flowerday, C.A., eds., An atlas of the Sand Hills: Lincoln, Nebr., University of Nebraska, Conservation and Survey Division, Resource Atlas, no. 5, p. 29–42.

Swinehart, J.B., Souders, V.L., DeGraw, H.M., and Diffendal, R.F., Jr., 1985, Cenozoic paleogeography of western Nebraska, *in* Flores, R.M., and Kaplan, S.S., eds., Cenozoic paleogeography of the west-central United States: Denver, Colo., S.E.P.M. Rocky Mountain Section, Rocky Mountain Paleogeography Symposium 3, p. 209–229.

Szilagyi, J., Harvey, F.E., and Ayers, J.F., 2003, Regional estimation of base recharge to ground water using water balance and a base flow index: Ground Water, v. 41, no. 4, p. 504–513. [Also available at https://doi.org/10.1111/j.1745-6584.2003.tb02384.x.]

TE Connectivity, 2020, KPSI 355: Hampton, Va., Measurement Specialties, Inc., accessed November 16, 2020, at https://www.te.com/commerce/DocumentDelivery/DDEController?Action=srchrtrv&DocNm=KPSI_355&DocType=Data+Sheet&DocLang=English&DocFormat=pdf&PartCntxt=CAT-WLS0016.

Tesoriero, A.J., Burow, K.R., Frans, L.M., Haynes, J.V., Hobza, C.M., Lindsey, B.D., and Solder, J.E., 2019, Using age tracers and decadal sampling to discern trends in nitrate, arsenic, and uranium in groundwater beneath irrigated cropland: Environmental Science & Technology, v. 53, no. 24, p. 14152–14164.

Turnipseed, D.P., and Sauer, V.B., 2010, Discharge measurements at gaging stations: U.S. Geological Survey Techniques and Methods, book 3, chap. A8, 87 p. [Also available at https://pubs.usgs.gov/tm/tm3-a8/.]

U.S. Environmental Protection Agency, 2018, 2018 Edition of the drinking water standards and health advisories: Office of Water, U.S. Environmental Protection Agency, Fact Sheet EPA 822-F-18-001, accessed February 21, 2021, at https://www.epa.gov/sites/production/files/2018-03/documents/dwtable2018.pdf.

U.S. Geological Survey, 2004, Policy on the use of the FlowTracker for discharge measurements: U.S. Geological Survey Office of Surface Water Technical Memorandum 2004.04, accessed June 2, 2017, at https://hydroacoustics.usgs.gov/memos/OSW2004-04.pdf.

U.S. Geological Survey, 2020a, Analytical procedures for dissolved gases N2/Ar: Reston, Va., U.S. Geological Survey Groundwater Age Dating Laboratory, accessed November 17, 2020, at https://water.usgs.gov/lab/dissolved-gas/lab/analytical_procedures/.

U.S. Geological Survey, 2020b, Menlo Park Tritium Laboratory: U.S. Geological Survey website, accessed June 19, 2020, at https://water.usgs.gov/nrp/menlo-park-tritium-laboratory/.

U.S. Geological Survey, 2020c, Reston Stable Isotope Laboratory (RSIL): U.S. Geological Survey website, accessed June 19, 2020, at https://isotopes.usgs.gov/lab/methods.html.

U.S. Geological Survey, 2021a, Air curves: Reston, Va., U.S. Geological Survey Groundwater Age Dating Laboratory web page, accessed April 8, 2021, at https://water.usgs.gov/lab/software/air_curve/index.html.

U.S. Geological Survey, 2021b, USGS water data for the Nation: U.S. Geological Survey National Water Information System database, accessed March 18, 2021, at https://doi.org/10.5066/F7P55KJN.

U.S. Geological Survey, variously dated, National field manual for the collection of water-quality data: U.S. Geological Survey Techniques of Water-Resources Investigations, book 9, chaps. A1–A9, [variously paged]. [Also available at https://water.usgs.gov/owq/FieldManual/.]

Vogel, J.C., Talma, A.S., and Heaton, T.H.E., 1981, Gaseous nitrogen as evidence for denitrification in groundwater: Journal of Hydrology, v. 50, p. 191–200, accessed December 21, 2021, at https://doi.org/10.1016/0022-1694(81)90069-X.

Wagner, R.J., Boulger, R.W., Jr., Oblinger, C.J., and Smith, B.A., 2006, Guidelines and standard procedures for continuous water-quality monitors—Station operation, record computation, and data reporting: U.S. Geological Survey Techniques and Methods, book 1, chap. D3, 51 p. [Also available at https://pubs.water.usgs.gov/tm1d3.]

Wang, Y., Huntington, T.G., Osher, L.J., Wassenaar, L.I., Trumbore, S.E., Amundson, R.G., Harden, J.W., McKnight, D.M., Schiff, S.L., Aiken, G.R., Lyons, W.B., Aravena, R.O., and Baron, J.S., 1998, Carbon cycling in terrestrial environments, chap. 17 *of* Kendall, C., and McDonnell, J.J., eds., Isotope tracers in catchment hydrology: Amsterdam, Elsevier Publications, p. 577–610.

Woods Hole Oceanographic Institution, 2020, Woods Hole Oceanographic Institution Accelerator Mass Spectrometry: Woods Hole Oceanographic Institution website, accessed June 19, 2020, at https://www.whoi.edu/nosams/home.

Xylem Analytics, 2020, YSI 6-series multiparameter water quality sondes user manual: Rye Brook, N.Y., Xylem Analytics, accessed November 16, 2020, at https://www.xylem-analytics.com.au/media/pdfs/ysi-6-series-manual_001.pdf.

For more information about this publication, contact:
Director, USGS Nebraska Water Science Center
5231 South 19th Street
Lincoln, NE 68512
402–328–4100

For additional information, visit: https://www.usgs.gov/centers/ne-water

Publishing support provided by the
Rolla and Sacramento Publishing Service Centers

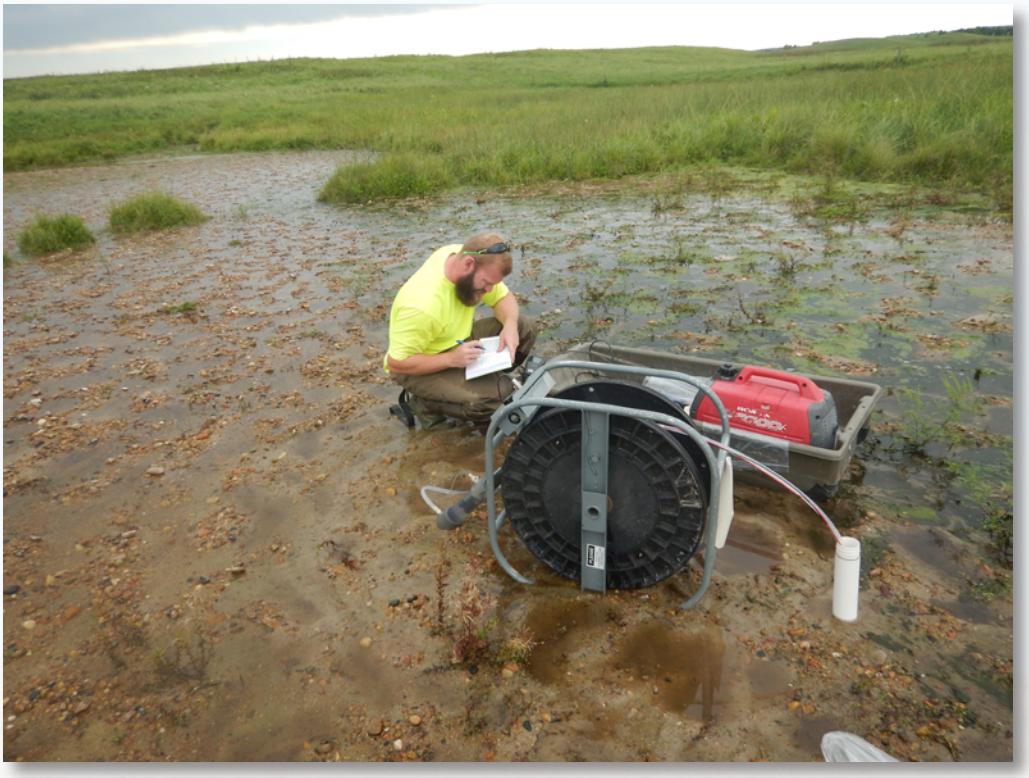

ISSN 2328-0328 (online)
https://doi.org/10.3133/sir20225042